DAVIS

NATIONAL ACADEMIES OF SCIENCE AND ENGINEERING

NATIONAL RESEARCH COUNCIL

of the

UNITED STATES OF AMERICA

UNITED STATES NATIONAL COMMITTEE

International Union of Radio Science

National Radio Science Meeting

9-13 January 1978

Sponsored by USNC/URSI
in cooperation with
Institute of Electrical and Electronics Engineers

University of Colorado at Boulder
Boulder, Colorado
U.S.A.

Price $5.00

National Radio Science Meeting
9-13 January 1978
Condensed Technical Program

SUNDAY, 8 JANUARY

2000		
USNC/URSI Meeting		Broker Inn

MONDAY, 9 JANUARY

0900-1200		
B-1	Antenna Theory	ECCR 2-28
F-1	Electromagnetic Techniques: Theoretical Models and Prediction Procedures	ECCR 0-30
H-1	Waves in Plasma	ECCR 1-46
1330-1700		
Combined Session - I		UMC Center Ballroom
1715-1900		
IEEE Wave Propagation Standards Committee Meeting		ECCR 1-42
2000-2200		
Evening Lecture (sponsored by the Denver Section, IEEE)		Auditorium, Radio Building, U.S. Dept. of Commerce

TUESDAY, 10 JANUARY

0830-1200		
Combined Session - II		UMC Center Ballroom
1330-1700		
B-2	SEM and Prony's Method	ECCR 2-28
E-1	Performing Meaningful EMI Measurements	ECCR 0-38
F-2	Atmospheric Effects	ECCR 0-30
G-1	Miscellaneous Topics	ECCR 1-42
1615		
Commission F Business Meeting		ECCR 0-30
1630		
Commission G Business Meeting		ECCR 1-42
1700		
Commission E Business Meeting		ECCR 0-38
1700-1800		
IEEE Antenna Standards Committee Meeting		ECCR 1-42
1800		
Reception		Broker Inn

WEDNESDAY, 11 JANUARY

0830-1200		
A-1	Antenna Measurements and Transients	ECCR 2-06
B-3	Guided Waves	ECCR 2-28
E-2	The Interference Environment and EMC	ECCR 0-38
F-3	Radio Oceanography	ECCR 0-30

(Continued on inside back cover)

United States National Committee

INTERNATIONAL UNION OF RADIO SCIENCE

PROGRAM AND ABSTRACTS

National Radio Science Meeting
9-13 January 1978

Sponsored by USNC/URSI in cooperation
with IEEE groups and societies:

Antennas and Propagation
Circuits and Systems
Electromagnetic Compatibility
Geoscience Electronics
Information Theory
Instrumentation and Measurement
Microwave Theory and Techniques
Nuclear and Plasma Sciences

Hosted by:

The National Oceanic and Atmospheric Administration
The National Bureau of Standards
The Institute for Telecommunication Sciences
Office of Telecommunications
The University of Colorado
The Denver Section, IEEE
and
The Denver-Boulder Chapter, IEEE/APS

Boulder, Colorado
U.S.A.

NOTE:

Programs and Abstracts of the USNC/URSI Meetings are available from:

USNC/URSI
National Academy of Sciences
2101 Constitution Avenue, N.W.
Washington, D.C. 20418

at $2 for meetings prior to 1970, $3 for 1971-75 meetings, and $5 for 1976-78 meetings.

The full papers are not published in any collected format; requests for them should be addressed to the authors who may have them published on their own initiative. Please note that these meetings are national and they are not organized by international URSI, nor are the programs available from the international Secretariat.

MEMBERSHIP

United States National Committee
INTERNATIONAL UNION OF RADIO SCIENCE

Chairman:
Dr. John V. Evans, Lincoln Laboratory, M.I.T.**
Vice Chairman:
Dr. C. Gordon Little, Environmental Research Labs, NOAA#**
Secretary:
Dr. James R. Wait, Environmental Research Labs, NOAA#**
Editor:
Dr. Thomas B.A. Senior, University of Michigan
Immediate Past Chairman:
Dr. Francis S. Johnson, University of Texas, Dallas**

Members Representing Societies, Groups and Institutes:

American Astronomical Society	Prof. Gart Westerhout
American Meteorological Society	Dr. David Atlas+
Institute of Electrical & Electronic Engineering	Dr. Ernst Weber*#
IEEE Antennas & Propagation Society	Dr. Robert C. Hansen+
IEEE Circuits & Systems Society	Dr. Mohammed S. Ghausi+
IEEE Information Theory Group	Dr. Jack K. Wolf+
Optical Society of America	Dr. Michael K. Barnoski+

Liaison Representatives from Government Agencies:

National Science Foundation	Dr. R. Marcus Price
Department of Commerce	Mr. Alan H. Shapley
National Aeronautics & Space Administration	Dr. Erwin R. Schmerling
Federal Communications Commission	Mr. Harry Fine
Office of Telecommunications Policy	Dr. John M. Kelso
Department of Defense	Mr. Emil Paroulek
Dept. of the Army	Mr. Allan W. Anderson
Dept. of the Navy	Dr. Alan H. Schooley
Dept. of the Air Force	Mr. Allan C. Schell

Ex-Officio Members:

Chairmen of the USNC-URSI Commissions:

Commission A	Dr. George E. Schafer
Commission B	Dr. Thomas A. Senior
Commission C	Dr. William F. Utlaut
Commission D	Dr. Kenneth J. Button
Commission E	Mr. George H. Hagn
Commission F	Dr. A.H. LaGrone
Commission G	Dr. Thomas E. VanZandt
Commission H	Dr. Frederick W. Crawford
Commission J	Dr. K.I. Kellermann

Officers of URSI resident in the United States:
(including Honorary Presidents)

Vice President	Prof. William E. Gordon*/**

Chairmen and Vice Chairmen of
Commissions of URSI resident
in the United States:

Chairman of Commission A	Dr. Helmut M. Altschuler
Chairman of Commission J	Prof. Gart Westerhout
Vice Chairman of Commission B	Prof. Leopold B. Felsen#
Vice Chairman of Commission E	Mr. George H. Hagn
Vice Chairman of Commission F	Prof. Alan T. Waterman, Jr.
Vice Chairman of Commission H	Dr. Frederick W. Crawford

Foreign Secretary of the U.S. National Academy of Sciences	Dr. George S. Hammond*
Chairman, Office of Physical Sciences-NRC	Dr. D. Allan Bromley
NRC Staff Officer	Richard Y. Dow
Honorary Members:	Dr. Harold H. Beverage Prof. Arthur H. Waynick#
IEEE Liaison Representatives:	K.J. Button, M.S. Ghausi, D. Heirman, D.A. Hill, E.A. Quincy J. Skilling, A. Sobti

* NAS Member
\# NAE Member
** Member of USNC-URSI Executive Committee
\+ Member-at-Large

DESCRIPTION OF

INTERNATIONAL UNION OF RADIO SCIENCE

The International Union of Radio Science is one of 17 world scientific unions organized under the International Council of Scientific Unions (ICSU). It is commonly designated as URSI (from its French name, Union Radio Scientifique Internationale). Its aims are (1) to promote the scientific study of radio communications, (2) to aid and organize radio research requiring cooperation on an international scale and to encourage the discussion and publication of the results, (3) to facilitate agreement upon common methods of measurement and the standardization of measuring instruments, and (4) to stimulate and to coordinate studies of the scientific aspects of telecommunications using electromagnetic waves, guided and unguided. The International Union itself is an organizational framework to aid in promoting these objectives. The actual technical work is largely done by the National Committees in the various countries.

The officers of the International Union are:

President:	J. Voge (France)
Immediate Past President:	Sir Granville Beynon (UK)
Vice Presidents:	W.N. Christiansen (Australia) W.E. Gordon (USA) V.V. Migulin (USSR) F.L.H.M. Stumpers (Netherlands)
Secretary General:	C.M. Minnis (Belgium)
Honorary Presidents:	B. Decaux (France) W. Dieminger (West Germany) J.A. Ratcliffe (UK) R.L. Smith-Rose (UK)

The Secretary's office and the headquarters of the organization are located at 7 Place Emile Danco, 1180 Brussels, Belgium. The Union is supported by contributions (dues) from 35 member countries. Additional funds for symposia and other scientific activities of the Union are provided by ICSU from contributions received for this purpose from UNESCO.

The International Union, as of the XVIII General Assembly held in Lima, Peru, August 1975, has nine bodies called Commissions for centralizing studies in the principal technical fields. The names of the Commissions and the chairmen follow.

A. Electromagnetic Metrology
Altschuler (USA)

B. Fields and Waves
van Bladel (Belgium)

C. Signals and Systems
Picinbono (France)

D. Physical Electronics
Smolinski (Poland)

E. Interference Environment
Likhter (USSR)

F. Wave Phenomena in Nonionized Media
Eklund (Sweden)

G. Ionospheric Radio
King (United Kingdom)

H. Waves in Plasmas
Gendrin (France)

J. Radio Astronomy
Westerhout (USA)

Every three years, the International Union holds a meeting called the General Assembly. The next General Assembly, the XIX, will be held in Helsinki, Finland in August, 1978. The Secretariat prepares and distributes the Proceedings of these General Assemblies. The International Union arranges international symposia on specific subjects pertaining to the work of one Commission or to several Commissions. The International Union also cooperates with other Unions in international symposia on subjects of joint interest.

Radio is unique among the fields of scientific work in having a specific adaptability to large-scale international research programs, for many of the phenomena that must be studied are worldwide in extent and yet are in a measure subject to control by experimenters. Exploration of space and the extension of scientific observations to the space environment is dependent on radio for its communication link and at the same time expands the scope of radio research. One of its branches, radio astronomy, involves cosmos-wide phenomena. URSI has in all this a distinct field of usefulness in furnishing a meeting ground for the numerous workers in the manifold aspects of radio research; its meetings and committee activities furnish valuable means of promoting research through exchange of ideas.

NATIONAL RADIO SCIENCE MEETING COMMITTEE MEMBERS:

Steering Committee:

S.W. Maley, Steering Committee Chairman
J.R. Wait, Technical Program Committee Chairman
R.L. Lewis, Digest Committee Chairman
E.F. Kuester, Advance Program Committee Chairman
H.A. Patterson, Registration & Facilities Committee Chairman
J.J. Tary, Evening Speaker Selection Committee Chairman
D.A. Hill, Ski Information Committee Chairman
P.L. Jensen, Publications Assistance

S.W. Maley, Chairman
H.M. Altschuler
R.C. Baird
F.S. Barnes
D.C. Chang
R.Y. Dow
W.R. Flock
R.L. Gallawa
D.A. Hill
P.L. Jensen
C.T. Johnk
R.A. Kamper
E.F. Kuester
L. Lewin
R.L. Lewis
C.G. Little
H. Patterson
E.Q. Quincy
D.B. Seidel
A.H. Shapley
A.D. Spaulding
J.J. Tary
W.F. Utlaut
T.E. VanZandt
P.F. Wacker
J.R. Wait

L. Hope, Secretary to the Committee

Technical Program Committee:

J.R. Wait, Chairman
R.C. Baird
C. Butler
D.C. Chang
D.D. Crombie
K. Davies
G. Hagn
A. Ishimaru
K.I. Kellermann
E.F. Kuester
A.H. LaGrone
R.S. Lawrence
R.H. Ott
G. Schafer
T.B.A. Senior
A. Sobti
A.D. Spaulding
W.F. Utlaut
T.E. VanZandt
P.F. Wacker

A scheduled demonstration of planar, spherical and cylindrical scanning will be presented as a part of the special session on Near-Field Antenna Measurements, URSI Commissions A and B, Session A-3, Wednesday evening, 11 January, at 2130 at the Plasma Physics Building of the National Bureau of Standards.

There will be an open house in the Plasma Physics Building of the National Bureau of Standards from 1500 to 1700, Thursday, 12 January, and from 0800 to 1700 Friday, 13 January. Planar, spherical, and cylindrical near-field scanning of antennas will be demonstrated.

MONDAY MORNING, 9 JAN., 0900-1200

Commission B Session 1

ANTENNA THEORY

Monday A.M., 9 January ECCR 2-28

Chairman: Prof. R.W. Burton, U.S. Naval

Postgraduate School, Monterey, CA 93940

B1-1
0900

ANALYSIS OF A CO-AX FED MONOPOLE:
C. M. Butler, R. D. Nevels and E. Yung,
Department of Electrical Engineering,
University of Mississippi, University,
MS 38677

The results of an investigation are presented for the problem of a coaxial waveguide terminating in a ground screen with the center conductor extending above the screen surface, forming a monopole radiator. The monopole is situated in an infinite homogeneous half space of arbitrary electrical characteristics. The waveguide is excited by a TEM incident wave, and the ground plane is assumed to be both perfectly conducting and infinite in extent. Coupled integral equations are formulated for the unknown electric current on the monopole and the unknown electric field in the aperture, fully accounting for the higher order modes occuring at the coaxial guide ground plane interface as well as the coupling between the monopole and the coax. This pair of coupled integral equation is solved numerically and results are presented for various cases of interest. Comparison is made with measured results.

Impose H_{tan} cont. at aperture

E_{tan} " by definition ?

B1-2
0915 INVESTIGATION OF THE CURRENT DISTRIBUTION ON A BASE-DRIVEN CYLINDRICAL MONOPOLE DUE TO A SUDDEN CHANGE IN ANTENNA RADIUS:

Edward K. Yung, Electrical Engineering Building, University of Illinois, Urbana, Illinois 61801
and Chalmers M. Butler, University of Mississippi, University, Mississippi 38677

An investigation of the current distribution on a base-driven cylindrical monopole due to a sudden change in antenna radius is presented. The axial current distribution on the cylindrical surface of the monopole and the radial current distribution on the annular metallic surface connecting the two coaxial antenna cylinders of different radii for a few cases of interest are obtained by the method of moments. It is observed that, when the total length of the monopole is not close to resonance and the radius of the larger cylinder is not much bigger than that of the smaller one, the current distribution on this monopole with a discontinuous cylinder radius shows little difference from that of a monopole made from a uniform-radius cylinder. On the other hand, regardless of the ratio of the cylinder radii, the current distribution on this so-called stepped-radius monopole differs substantially from that of a conventional monopole and strongly depends on the location of the discontinuity, if the total length of the antenna is close to resonance. Furthermore, the so-called edge condition dictates that the current on the bigger cylinder flow continuously around the edge onto the annular cylinder top and that its derivative be either infinite or zero at the edge. The edge condition also requires that the current at the inner corner of the cylinder top flow continuously into the smaller cylinder with a zero slope. The theoretical solution exhibits most of the above characteristics, that is, it indicates the infinite slope trend but it is difficult to realize an infinite slope in numerical analysis.

B1-3
0930 ANALYTICAL SOLUTION FOR A COAXIAL-LINE-DRIVEN MONOPOLE-CYLINDER OVER AN INFINITE GROUND PLANE:

Edward K. Yung, Electrical Engineering, University of Illinois, Urbana, Illinois 61801
and Chalmers M. Butler, University of Mississippi, University, Mississippi 38677

A method is developed for computing the current distribution on a base-driven monopole mounted on a metallic cylinder above ground and the tangential electric field at the opening of the connecting coaxial line through which the antenna is excited. This antenna configuration is hereafter denoted by monopole-cylinder. The scheme is extended to treat the sleeve monopole problem. Good agreement between the theoretical solution (current distribution and input admittance) of the monopole-cylinder and measurement is observed. Acceptable agreement is seen between theoretical current distributions on moderately thick sleeve monopoles and experimental data. The present formulation is effective to treat thick antennas whose cylinder radii are as big as a quarter wavelength. This represents a substantial extension of cylindrical antenna analysis, especially for antennas whose cylinder radii are bigger than one-tenth of a wavelength. The success of the present formulation is mainly due to the employment of the correct aperture electric field or magnetic current. The employment of the correct magnetic current implies that the tangential electric field across the annular aperture of the coaxial to line-driven antenna is considered as an unknown and is determined from equations resulting from enforcing continuity of the magnetic field across the aperture. In the vicinity of the junction where the two coaxial antenna cylinders of different radii meet, the theoretical current, including the radial current on the annular cylinder top, exhibits the characteristics predicted by the so-called edge condition. Furthermore, the study of the tangential electric field across the aperture indicates that the TEM mode of the eigenfunction expansion of the electric field in the coaxial regions does not dominate at the aperture, even in the case of an electrically small aperture. This implies that the usual magnetic frill is oversimplified.

B1-4
0950

ADMITTANCE CHARACTERISTICS OF A FINITE ARRAY OF SLOTS IN A REENTRY ENVIRONMENT

G. E. Stewart & K. E. Golden
The Ivan A. Getting Laboratories,
The Aerospace Corporation, El Segundo, CA 90250

Array antennas required to perform during reentry are subjected to extremely difficult operating conditions. These include the presence of a thick dielectric window over the array to withstand the heat, pressure, and ablation of the reentry environment as well as the overdense, lossy plasma layer. Techniques have been described in the literature for calculating the self and mutual admittances of individual elements of an array as well as the radiation patterns in the dominant mode approximation. The evaluation of these admittances for a plasma-clad dielectric window would generally involve a numerical integration over two dimensional Fourier transform space for each element pair in the array. If the window is assumed to be infinite in extent, the self-admittances of all elements are the same. The invariance of the mutual admittance under translation together with symmetry can also be used to eliminate a large number of the integrations. Even so, the number of calculations involved makes the process of evaluating the admittances impractical for all except very small arrays. Once these self and mutual admittances have been determined, the driving point admittance of each array element can be determined for any scan angle.

In this paper, the driving point admittance of an arbitrary element in such a finite planar phased array is formulated directly in terms of the field components. After Fourier transformation, the driving point admittance of any individual element can be evaluated as a single numerical integration. An array factor appears within the integrand which can be evaluated over a single unit cell and stored. Scanning the array corresponds to a simple shift of the array pattern in Fourier transform space. Similarly, the effect of the dielectric-plasma coating can be described in terms of two admittance functions $Y_{TE}(k_\perp)$ and $Y_{TM}(k_\perp)$, which appear within the integral. These functions, which depend only on the plasma/dielectric properties and the distance from the origin in k-space can be used directly to assess the possible effects of surface wave poles on the array admittance characteristics. Since they are independent of angle in k-space, they can also be readily stored and recalled.

The dynamic admittance of a finite planar array has been calculated using this technique and compared with experiment using a parallel plate structure. The effects of curvature of the array and finiteness of the window for an actual conical RV will be described.

B1-5
1040

ON TWO PARALLEL, NON-STAGGERED LOOP ANTENNAS:

Ahmed Abul-Kassem and David C. Chang
Electromagnetics Laboratory, Department of Electrical Engineering, University of Colorado, Boulder, CO 80309

The problem concerning the mutual coupling of two parallel, non-staggered thin wire loop antennas in air is not only related to the synthesis of antenna arrays consisting of circular loops, but also is important in understanding the performance of a single loop, both horizontal and vertical, over a highly conducting earth. In this paper, such a problem is analyzed by formulating two coupled integral equations for the currents on the loops. The two loops are assumed to be identical, each having a radius b and wire radius a. The separation between the planes of the two loops is ρ_o, and the shift of the two axis is z_o. The coupled integral equations are then solved by a typical Fourier series expansion method. Moment functions associated with the mutual coupling of the two loops are computed using a double Gaussian quadrature scheme and compared with the Sommerfeld integral representation which although more complicated, can be extended readily to include the case of a single loop above a finitely conducting earth. On the other hand, a thin-wire approximation is used in computing the moment functions associated with the self term (R.W.P. King and C.W. Harrison Jr., Antennas and Waves, Chapter 9, 539-597, 1969). Excitation of the two loops are assumed to be two delta function voltage generators with arbitrary locations and amplitudes. The integral equations can then be written in the form:

$$\sum_{j=1}^{2} \langle M_{ij}, I_j \rangle = V_i \delta(\phi-\phi_{si}); \quad 0 \le \phi \le 2\pi \quad \text{and} \quad i = 1,2$$

where $M_{ij} = \{(2\pi R_{ij})^{-1} \exp(ik_o R_{ij})\}$;

$$R_{11} = R_{22} = [4b^2 \sin^2(\phi-\phi') + A^2]^{\frac{1}{2}} \; ; \quad A = 2\phi \sin(\theta/2)$$

$$R_{12} = [z_o^2 + (b \sin\phi - b \sin\phi')^2 + (\rho_o + b\cos\phi' - b\cos\phi)^2]^{\frac{1}{2}}$$

$$R_{21} = (z_o^2 + (b \sin\phi' - b \sin\phi)^2 + (\rho_o + b\cos\phi - b\cos\phi')^2]^{\frac{1}{2}}$$

Here, the symbol { } denotes integration of θ around the wire and $\langle\ \rangle$ denotes integration of ϕ along the loop. V_i, ϕ_{si} are respectively the amplitude and location of sources voltage, and I_j are the total currents flowing around the corresponding loops.

It is shown that the results as obtained from the integral equations agree with the conventional magnetic dipole approach provided the loops are sufficiently small, and when the second loop is a perfect image of the first (L.E. Vogler and J.L.Noble, NBS monograph #72, 1964). For larger loops however the conventional approach cannot adequately take into account the proximity effect since the current is assumed to be uniform.

B1-6
1100

NUMERICAL GREEN'S FUNCTION FOR DIELECTRIC BODIES OF REVOLUTION AND ITS APPLICATIONS:

T. K. Wu and C. M. Butler, Electrical Engineering Department, University of Mississippi, University, Mississippi 38677

In this paper the determination of the Green's function for perfectly conducting or loaded surfaces of revolution (R. F. Harrington and J. R. Mautz, Radio Science, 7, 603-612, 1972) is extended to cover the case of homogeneous dielectric bodies of revolution, and this Green's function is employed in an integro-differential equation for the problem of a wire near such a body. The Green's function is computed from the solution of coupled surface integral equations (SIE) for the induced surface electric and magnetic currents on the dielectric body excited there by an electric current element.

It has been shown (T. B. A. Senior, Appl. Sci. Res., B-8, 418-436, 1960) that the exact electromagnetic conditions at the surface of a lossy dielectric body of large conductivity σ can be approximated by a surface impedance, relating the electric and magnetic surface currents. This approximation reduces the unknown quantities by a factor of two and enables one to derive an approximate vector integral equation (AIE) for one of the two equivalent currents. If this equation is solved by the method of moments, significant numerical efficiency over SIE is realized.

Numerical results for the Green's function are obtained from solutions of both the SIE and AIE, and they agree very well with the exact solution for the special case that the body is a sphere. The application of this numerical Green's function to the problem of a wire antenna near a dielectric body of revolution is discussed. Results for the antenna near a conducting sphere are given and compared with measured data. Also, results obtained via both SIE and AIE for the antenna near other bodies of revolution are presented.

B1-7
1120

SOME FUNDAMENTAL QUESTIONS RELATED TO THE PROBLEM OF DUAL REFLECTOR ANTENNA SYNTHESIS:

R. Mittra, University of Illinois
and
V. Galindo-Israel, Jet Propulsion Lab, California

The goal of the dual reflector antenna synthesis problem is to transform, by G.O., a given primary feed illumination incident on a subreflector into a desired amplitude and phase distribution in the projected aperture plane of the main reflector. Although an analytic approach for solving the synthesis problem for the circularly symmetric case was presented by Galindo (IEEE Ant. Symp. July 1963) and Kinber (Radio Eng. Electron Phys. 6, 1962), the resolution of the general three-dimensional problem has remained elusive. Kinber is credited with the original claim that a general solution to the three-dimensional problem does not exist. However, Kinber's paper neither presents a detailed proof, nor offers an adequate explanation as to how he derived the final result. Recently, a number of attempts for resolving the three-dimensional synthesis problem has been reported in the literature and numerical results for the main reflector and subreflector surfaces have been presented. It is natural to raise the question of validity of these solutions, particularly in light of the assertion in Kinber's paper regarding their non-existence, bearing in mind that good approximate solutions may indeed be possible in many cases. In this paper, we critically examine the above "existence" question with a view to gaining a fundamental understanding of the entire issue and pinpointing the reasons behind the nonexistence of the solution in the three-dimensional case. We argue, on the basis of a geometrical optics analysis, that the failure of the solution is attributed to the fact that the number of degrees of freedom needed to simultaneously satisfy the amplitude and phase transformation conditions are in excess of the degrees of freedom provided by the two reflector surfaces. We also illustrate the fact that an *a priori* assumption on the existence of the solution, followed by a numerical solution of the reflector surfaces using a three-dimensional version of the circularly symmetric case, eventually leads to a contradiction, since the solution derived in this manner is not self-consistent. However, this approach does lead to a good approximation if appropriate corrections are made, and this will be discussed. In addition, a simple test is developed in the paper for reliability checking the validity of any proposed numerical solution to the synthesis problem.

B1-8
1140

A TECHNIQUE FOR OBTAINING WIDE BAND TIME HARMONIC RESPONSE OF ANTENNAS AND SCATTERERS: K. Al-Badwaihy, F. El-Hefnawy, A. Kamal, A. Mustafa, Electronics and Comm. Dept., Cairo University, Egypt

Transient or wide band electromagnetic response of antennas and scatterers may be obtained from their time harmonic response at as many frequencies as is necessary. A computational algorithm is repeated at each frequency. This requires a large computer time. For finite scatterers and antennas, any field quantity $E(\bar{r},k)$ has the following Taylor expansion:

$$E(\bar{r},k) = E(\bar{r},k_o) + (k-k_o)\, E_1(\bar{r},k_o) + \tfrac{1}{2}\,(k-k_o)^2\, E_2(\bar{r},k_o) + \cdots$$

where $\bar{r}$ is the position vector, k is the wave number, and k_o is the expansion origin. The expansion converges for real values of k since E does not have poles on the real axis. In this paper it is shown that numerical determination of the coefficients E_1, E_2,... using the moment method requires very little additional effort to that of determining the first term of the expansion which is the time harmonic response at k_o. This is because these coefficients are found to satisfy integral equations with the same kernel as that of the first term of the expansion. It is thus possible to use the above expression to obtain wide band time harmonic response with a considerable reduction in computer time along with providing values of E_1 which is needed for some types of modulated signals. A general formulation for a single scatterer or antenna is given and the moment method computational algorithm for determining all the expansion coefficients is described in detail. The method is then applied to a thin antenna of length 2h. It is shown that its response up to $2h = \lambda$ can be obtained from the same computational algorithm that determines the static charge distribution on the antenna. Different expansion origins other than k=0 are tried and the obtained response is compared with previous experimental and theoretical results and agreement was found to be good.

Commission F Session 1

ELECTROMAGNETIC TECHNIQUES: THEORETICAL

MODELS AND PREDICTION PROCEDURES

Monday A.M., 9 January ECCR 0-30

Chairman: F.T. Ulaby, Center for Research, Inc.,

University of Kansas, Lawrence, KS 66045

F1-1
0900

AN EXTENDED KALMAN-BUCY FILTER FOR THE RETRIEVAL OF TEMPERATURE PROFILES AND LIQUID WATER AND WATER VAPOR COLUMNS FROM PASSIVE MICROWAVE SOUNDERS

W. H. Ledsham, P. W. Rosenkranz, and D. H. Staelin, Research Laboratory of Electronics and the Department of Electrical Engineering and Computer Science, Massachusetts Institute of Technology, Cambridge, MA 02139

The extended Kalman-Bucy filter is a powerful technique for the estimation of non-stationary random parameters in situations where the received signal is a noisy nonlinear function of those parameters. Such a filter was adapted to the problem of estimating meteorological parameters on the basis of remote sensing data from satellites. A practical 3-channel version of this filter was developed and tested for temperature and humidity retrievals obtained using the Nimbus-6 Scanning Microwave Spectrometer data. The temperature retrievals were compared with the National Meteorological Center K27 grid analysis over data rich areas (United States, Europe and Japan). When compared to a standard one-point 3-channel regression, the results were that the mean error was significantly reduced, and the rms error about the mean was reduced by a factor of 0.8-1.3; there was performance improvement at all levels below 100 mb. A causal two-look-angle retrieval also substantially reduced the mean errors, and the rms errors about the mean were reduced in this case by factors of 0.9-1.8, with performance improvement at all levels except 50 mb. Simultaneous retrievals at two look-angles yield improvement because horizontal smoothing of noise occurs and because different view angles produce different temperature weighting functions.

F1-2
0920 MICROWAVE EARTH-SPACE ATTENUATION PREDICTION PROCEDURES (FOR THE U.S.A.): E.J. Dutton, U.S. Department of Commerce, Office of Telecommunications, Institute for Telecommunications Sciences, Boulder, CO 80302

The Rice-Holmberg procedure (Rice, P.L. and N.R. Holmberg, IEEE Trans Comm. Soc., COM-21, 10, 1131-1136, 1973) and its subsequent modification for predicting rain rate distributions over a period of time (usually an average year) are examined. Some procedures for modeling earth-space rain-caused, and clear-air attenuation are discussed, after which some comparisons of data and the predictions procedures are made. Intercomparisons of different prediction techniques are also made. A sample earth-space attenuation climatology in the conterminous United States is also developed. Two small climatological "subzones," each consisting of four cities, have been developed to provide examples of the kind of attenuation variations that an earth-satellite link can expect to encounter. Results are given to indicate the climatological variability of a number of presumed earth-space paths. It is assumed that each of the data locations within a subzone is a potential earth terminal for three currently planned or operational geostationary satellites. The three satellite locations are 91° W longitude (RCA SATCOM-C Satellite), 110° W longitude (SBS-B Satellite) and 116° W longitude (CTS Satellite). It is determined within one small subzone that differences as large as 8 dB at 14 GHz are possible in the attenuation predicted for 0.01 percent of an average year when pointing at the same satellite. This implies that possible large variations in attenuation can exist even within regions of supposedly similar rainfall patterns, in addition to the already anticipated differences that can exist between zones.

F1-3
0940

THE BUMP IN THE SPECTRUM OF REFRACTIVE INDEX AND ITS EFFECTS ON RADIO WAVE SCATTERING

R. J. Hill, Wave Propagation Laboratory,
National Oceanic and Atmospheric Administration,
Boulder, CO 80302

Recent theoretical and experimental advances have produced a model of the power spectrum of quantities mixed by turbulence. This model is applicable for arbitrary diffusivity and is thereby capable of predicting the high wave-number shape of the spectra of refractivity, temperature, humidity, and the temperature-humidity cospectrum. Experiments have shown that the temperature spectrum in air has a "bump" at high wave numbers. This feature is interpreted by the theoretical model as a tendency toward a viscous-convective range at wave numbers lower than the wave numbers at which diffusion causes the spectrum to decrease rapidly. The bump is predicted to appear in the refractivity and humidity spectra and in the temperature-humidity cospectrum as well as in the temperature spectrum. The bump in the humidity spectrum is smaller than that in the temperature-humidity cospectrum which is in turn smaller than the bump in the temperature spectrum; this effect is caused by the fact that the diffusivity of water vapor in air is slightly greater than that of heat in air. The shape of the refractivity spectrum depends on the relative contributions of the temperature spectrum, humidity spectrum, and temperature-humidity cospectrum. The refractivity spectrum can have an enhanced bump if the contribution of the temperature-humidity cospectrum is negative and nearly cancels the contributions of the temperature and humidity spectra. The impact of these developments on radio wave propagation is discussed.

F1-4
1000 EM WAVE PROPAGATION IN A LATERALLY NONUNIFORM TROPOSPHERE:

Se Hyun Cho and James R. Wait, Cooperative Institute for Research In Environmental Sciences, University of Colorado/NOAA, Boulder, CO 80309

EM wave propagation in a nonuniform troposphere is studied for a cylindrical model of the earth. The refractive index of the troposphere is assumed to vary both with height and range. The formulation is facilitated by the fact that the field within a piecewise (laterally) uniform section can be represented as a discrete sum of modes that are orthogonal in the transverse plane. Using these radial wave functions, mode conversion at a junction between two laterally uniform structures is analyzed for both TE and TM waves. These results are then extended to multi-section structures.

The laterally nonuniform structures are approximated by many uniform sections that under certain conditions become an excellent representation for a gradual transition. A basic property we utilize is that the maximum coupling occurs between the most similar modes at a junction. An important case we consider is when the refractive index has essentially the same vertical variation or slope near the refractive layer and the duct itself varies along the propagation path. In such a situation, the vertical step at an elemental junction may be as large as $30\text{-}50\lambda_o$.

The possible modes for each uniform section in various multi-step models are analyzed. In each section, we show that the maximum number of the modes are determined by the effective electric height of the refractive layer. We find that the maximum number of modes becomes 10-30 for VHF and 30-100 for UHF for a duct height of 1000m. Thus the approach of using uniform multi-sections is very useful for VHF. Also, it can possibly be extended to UHF. Another important finding is that for the elevated duct, there are no significant differences between the TE and TM modes; however, some differences are expected for the surface duct as we also indicate.

At 200 MHz, a few typical profiles of refractive index are examined numerically for both the uniform and nonuniform troposphere. For the nonuniform case, the height of the refractive layer is taken to vary between 600m and 1000m over the propagation path of a few hundred kilometers. The whispering gallery type modes propagate very well although the field strength near the duct is somewhat less than that for the corresponding uniform duct. However, the field strength near the earth's surface is enhanced by a considerable amount (e.g. 20-40 dB).

F1-5
1045

A STUDY OF MODE CONVERSION IN TROPOSPHERIC DUCTS:

Rajendra K. Arora and James R. Wait, Theoretical Studies Group, Environmental Research Laboratories, NOAA, Boulder, CO 80302

It is known that electromagnetic waves can be guided along the concave side of an elevated tropospheric inversion layer with remarkably low attenuation (J.R. Wait, Electronics Letters, 4, 377-378, 1968). However, the energy coupled into such modes is extremely weak unless the excitation source is situated in the neighborhood of or above the concave boundary (J.R. Wait, Can. J. Phys., 52, 1852-1861, 1974). A mechanism has been suggested whereby energy can be transferred to these earth detached modes by mode conversion at lateral discontinuities in the path of the wave (S.H. Cho and J.R. Wait, URSI Open Commission F Symposium Proc., LaBaule, France, 37-41, 1977 and Special Issue of Radio Sci., March, 1978). The present paper contributes to further the understanding of this mode conversion phenomenon. The case where refractive index variations occur both in the vertical and horizontal directions is examined. The primary field is either TE or TM and propagates in a direction which is, in general, oblique with respect to the plane of the discontinuity. The cases of single and multiple step discontinuities as well as continuous transitions are considered. Numerical results are presented for the transmission and reflection coefficients for various modes for different types of refractive index transitions. The problem of excitation using an electric current line source is also considered and the excitation coefficients for various modes are evaluated. One of the important findings (e.g. S.H. Cho and J.R. Wait, CIRES/EM Report No. 3, 1977) is that the received VHF field strength near the earth's surface may be enhanced by as much as 40 dB due to the reconversion from whispering gallery modes to the more conventional waveguide modes. This mechanism could play a role in the tropospheric ducting data discussed recently by Pappert and Goodhart (Radio Sci., 12, 75-88, 1977).
We finally consider the relevance of the important and elegant coupled-mode approach that Bahar (Radio Sci., 11, 137-147, 1976; Can. J. Phys., 53, 1078-1096, 1975) has employed to treat such problems.

F1-6
1105 TRANSMISSION MODES IN A BRAIDED COAXIAL CABLE AND COUPLING TO THE GEOPHYSICAL ENVIRONMENT:

D.B. Seidel and J.R. Wait, Cooperative Institute for Research in Environmental Sciences, University of Colorado/NOAA, Boulder, CO 80309

Radio frequency transmission in a semi-circular tunnel containing a braided coaxial cable is considered. Such a problem models mine communication systems which are now being developed (e.g. Special Issue of Radio Science, 11, 233-418, 1976). In the general formulation, we can account for the ohmic losses in the tunnel wall as well as the possible presence of a thin lossy film layer on the outer surface of the dielectric jacket of the cable (J.R. Wait and D.A. Hill, IEEE Trans., MTT-23, 401-405, 1975). If some quasi-static approximations (J.R. Wait, IEEE Trans., AP-25, 441-443, 1977) are invoked, it is found that, in general, the propagation constants of the low-frequency transmission line modes are obtained through the solution of a cubic equation. However, for the special case when the conductivity thickness product of the lossy film layer vanishes, this cubic equation reduces to a quadratic. The spatially dispersive form of the braid transfer impedance may also be accounted for in this theory. In order to ascertain the applicability and accuracy of the quasi-static approximation, results are compared with calculations where such approximations were not used. Finally, special characteristic impedances are derived for the various modes of the equivalent multi-conductor transmission line. Such characteristic impedances are necessary for the development of a theory to describe the mode conversion that would result from the presence of axial nonuniformities on the line or in the environment.

Most of the theoretical concepts developed here may be carried over to situations where the cable is located at electrically small heights over the earth's surface.

F1-7 1125 AN EMPIRICAL MODEL FOR ANTENNA GAIN DEGRADATION DUE TO ANGLE OF ARRIVAL FLUCTUATION IN THE TROPOSPHERE:

D. M. Theobold and D. B. Hodge
ElectroScience Laboratory, The Ohio State University, Columbus, Ohio 43212

Signal levels well below those predicted by standard techniques on low elevation earth-space microwave links have been observed and reported previously. It is found in this paper that the inclusion of an additional mechanism, i.e., antenna gain degradation due to angle of arrival scintillation, is adequate for the prediction of these reduced signal levels.
Angle of arrival statistics were compiled from previous and current experiments and these results were used to establish an empirical relationship between the average angle of arrival variance and both path length for terrestrial paths and elevation angle for earth-space paths. The average realized gain was then calculated accounting for these angle of arrival fluctuations. This average gain degradation, when combined with the usual atmospheric gas absorption, adequately predicts the reduced signal levels observed at low elevation angles on earth-space paths at 2, 7.3, and 30 GHz.
This approach has been used to generate design curves for gain degradation or realizable gain as a function of antenna aperture size, frequency, and either terrestrial path length or earth-space path elevation angle.

F1-8 1145 POLARIZATION INVERSION OF 12.6 CM RADAR WAVES BY THE GALILEAN SATELLITES: EVIDENCE FOR ICY CRATERS?

S.J. Ostro and G.H. Pettengill, Department of Earth and Planetary Sciences, Massachusetts Institute of Technology, Cambridge, MA 02139

A model which postulates that significant areas of the outer three Galilean satellites of Jupiter are covered with icy, nearly hemispherical craters can explain the unexpected 12.6-cm radar polarization behavior of these bodies. As measured by Campbell et al. (Icarus, 1978, in press), the ratios μ of the echo power received in the same circular sense as transmitted, to that received in the orthogonal sense, are 1.61 ± 0.20, 1.48 ± 0.27, and 1.24 ± 0.19 for Europa, Ganymede and Callisto, respectively. All astronomical targets previously studied by radar have values of $\mu \ll 1$, i.e., the dominant circularly polarized component of echoes from the moon or inner planets has a rotational sense orthogonal to that transmitted.

In developing our model, we note that a single coherent reflection at normal incidence reverses the rotational sense of circularly polarized incident radiation ($\mu = 0$), while multiple dielectric reflections tend to produce an unpolarized echo ($\mu \to 1$). However, two intermediate reflections can produce the observed backscattering behavior, provided the angles of incidence lie between the Brewster angle and its complement. The effect is maximum when the angles equal 45°, yielding a ratio $\mu = 1.9$ for water ice. (Although silicate minerals are probably present on the satellite surfaces, water frost is the only constituent spectroscopically detected.) Randomly oriented reflecting facets, either of ice on the surface or of rocks in the interior, cannot yield the observed behavior because too few of the total possible backscattering configurations meet the above requirement. Hemispherical surface craters, on the other hand, favor "45° double-bounce" backscatter.

We have used modified geometrical optics and the Stokes formalism to model the scattering from nearly hemispherical craters whose interiors consist of plane facets many wavelengths in size. If the surface material has a refractive index ~15% larger than that of pure water ice, our model can explain the observed radar results with regard to circular and linear polarization properties, albedo, and angular scattering law.

Commission H Session 1

WAVES IN PLASMA

Monday A.M., 9 January ECCR 1-46

Chairman: K.J. Harker, Institute for

Plasma Research, Stanford University,

Stanford, CA 94305

H1-1
0900 REMOTE SENSING OF TERRESTRIAL KILOMETRIC RADIATION BY THE SPACECRAFT VOYAGERS ONE AND TWO:

The Planetary Radio Astronomy Investigator Group, c/o James W. Warwick
Department of Astro-Geophysics
University of Colorado, Boulder, CO 80309

Immediately after the launch of Voyager One (5 September 1977) and Voyager Two (20 August 1977) the Planetary Radio Astronomy (PRA) experiments aboard each spacecraft detected strong terrestrial kilometric radio emissions (TKR) of the kind associated with magnetospheric substorms and auroras. In the frequency range 100 to 300 kHz, these emissions are characteristically polarized and exhibit complex structure in frequency and polarization.

The dynamic spectra and polarization variations observed by the PRA experiments as the earth rotates can be compared with spectra from Jupiter in the decametric range. Without the structures of a satellite like Io, TKR nevertheless significantly resembles these variables in the Io-independent Jupiter source.

We have attempted to associate the observed sense of polarization with the alternating tipping of the north and south geomagnetic poles towards the spacecraft. There are complex and rapid variations of the polarization sense, which suggests that radiation emanates from both geomagnetic poles, and is received nearly simultaneously at the spacecraft.

H1-2
0925 NONLINEAR LANGMUIR WAVES:

Dwight R. Nicholson and Martin V. Goldman, Department of Astro-Geophysics, University of Colorado, Boulder, CO 80309

The behavior of intense Langmuir waves can often be described by a nonlinear set of fluid equations introduced by Zakharov in 1972 (V. E. Zakharov, Sov. Phys.-JETP 35, 908, 1972) and known as the coupled nonlinear Schrödinger equation. We solve this equation numerically, in time and in two spatial dimensions, under a variety of circumstances. For the case of electron beam-plasma interaction, as in Type III solar bursts, catastrophic soliton collapse is found to compete with quasilinear effects to limit wave energy. For the case of electromagnetic beam-plasma interaction, as in ionospheric modification by intense radio waves, catastrophic soliton collapse may also be an effective dissipation mechanism. We briefly discuss the related questions of particle acceleration by collapsing solitons, and electromagnetic radiation, near the plasma frequency and its harmonics, due to the collapsing electrostatic solitons.

H1-3 0950 A FIELD MODEL OF COUPLE-CAVITY TRAVELING WAVE TUBE (CC-TWT) AMPLIFIER INCLUDING NONLINEAR CHARACTERISTICS

A. K. Sinha, COMSAT Labs, Clarksburg, Md. 20734

A mathematical model of the CC-TWT is presented based on the physical processes involved in the system. The specified processes considered are: thermionic generation and acceleration of the electron beam, electron trapping and bunching due to wave-particle interaction, and wave regeneration and amplification. The net effect is conversion, in part, of the kinetic energy of the electrons into the electromagnetic field energy of the input signal. An expression is derived for the rate of energy exchange between an individual electron and the wave-field under resonant interaction, characterized by near equality of the electron velocity and the phase velocity of the wave. This result is then used to describe the energy variation in cavities by defining an effective Q-value of each cavity that incorporates the effect of the wave-particle interaction and coupling between cavities. The results are further generalized for an electron population of arbitrary statistical distribution constituting the beam. The interactive nonlinear evolution of the wave-field of the input signal and the electron beam as they travel along the device are described by coupled partial integro-differential equations based on Maxwell's field equations and Vlasov equation, respectively. These equations are analogous to the 'circuit equation' and the 'electronic equation', respectively, in Pierce's wave theory (J. R. Pierce, Proc. I.R.E., 35, 111-123, 1947), describing the behavior of the helix TWT. The dispersion relation resulting from the present formulation are examined for system characteristics. In particular, the solution of the field equation corresponding to the output signal is expected to provide the amplitude and phase characteristics of the device. These characteristics are useful for specification of performance for the purpose of system design of satellite communication systems employing high power, wide-band CC-TWT. A special feature of the present model is the incorporation of the frequency-dependence, or the so-called 'memory-effect' of the performance characteristics of the device.

H1-4
1045 VLF TRANSMITTER EXPERIMENTS USING SIDEBAND STRUCTURES TO SIMULATE POWER LINE HARMONIC RADIATION: C. G. Park and D. C.- D. Chang, Radioscience Laboratory, Stanford University, Stanford, Ca., 94305

The VLF transmitter at Siple, Antarctica was programmed to transmit signals consisting of several sidebands spaced 50 and 100 Hz. One objective of this experiment was to simulate wave-particle and wave-wave interactions in the magnetosphere induced by power line harmonic radiation. The results show that many power line induced effects can be simulated by radiating as little as 1 watt or less at each sideband frequency. Another objective was to study wave-wave interactions between transmitter signals and power line harmonics. The results show that non-linear wave-wave interactions can occur when one of the transmitter sidebands approaches within about 50 Hz of a power line harmonic. This is consistent with previous results which showed that the coherence bandwidth of wave-wave interactions is ~50 Hz. One unexpected result of this experiment shows that a long constant frequency input signal can produce pulsating emissions with ~0.5 sec period. Since this period is much shorter than the two-hop whistler-mode delay, it is postulated that this periodicity results from spatial bunching of particles by waves through longitudinal resonance.

H1-5 OBSERVATIONS OF f_{ne} -$2f_{pe}$ ELECTROMAGNETIC WAVES:
1110 P. Rodriguez and M.L. Kaiser, Laboratory for Extra-terrestrial Physics, Planetary Sciences Branch, Goddard Space Flight Center, Greenbelt, MD 20771

We have used the radio frequency experiments on the IMP-6 and RAE-2 satellites to study electromagnetic waves propagating at frequencies of f_{pe} and $2f_{pe}$, where f_{pe} is the electron plasma frequency at the source region. These waves are of interest because they are a local (i.e., terrestrial) example of the mode conversion and nonlinear wave interaction postulated for Type II solar radio bursts. IMP-6 orbits the earth while RAE-2 orbits the moon thus allowing as much as 90 R_E separation for simultaneous observation of the waves. The characteristic f_{pe} -$2f_{pe}$dynamic spectrum (see figure below) is detected almost continuously for all local times about the earth, without measurable spin modulation, suggesting a large spatial extent for the source region. Preliminary analysis indicates that the magnetosheath and/or bow shock is the source region, with some evidence that suprathermal electron beams are associated with the generation of the noise. The characteristic two-peacked spectrum of these waves has also been detected in the magnetotail of the earth, for which local electron densities are typically too low to correspond to the f_{pe} peak in the spectrum but correspond to magnetosheath densities. We conclude that the earth's bow shock provides plasma wave interactions analogous to those probably occurring in Type II solar burst shock waves.

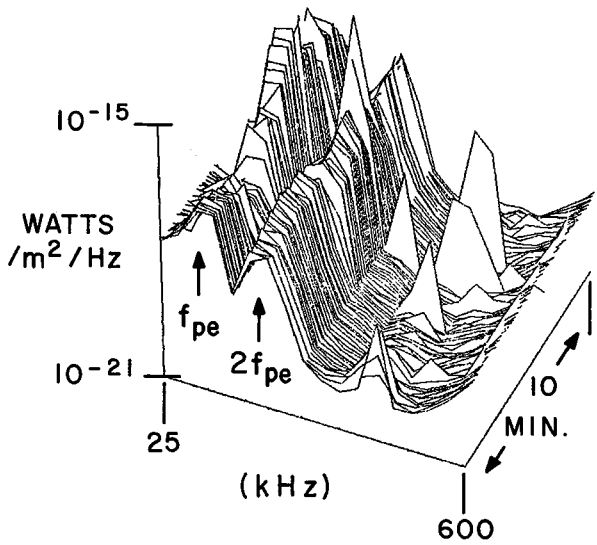

H1-6
1135 DIGITAL BISPECTRAL ANALYSIS OF PLASMA FLUCTUATION DATA ASSOCIATED WITH NON-LINEAR WAVE-WAVE INTERACTIONS.

Y. C. Kim and E. J. Powers, Department of Electrical Engineering, The University of Texas at Austin, Austin, TX 78712

It is well known that for nonlinear wave-wave interaction the wave frequencies (ω_1, ω_2, ω_3) and wave numbers (k_1, k_2, k_3) must satisfy the following selection rules or resonance conditions: $\omega_1 + \omega_2 = \omega_3$ and $k_1 + k_2 = k_3$. In analyzing fluctuation data associated with self-excited wave phenomena, one often encounters a situation where waves are present at ω_1, ω_2 and ω_3 and which satisfy the above selection rules on ω and k. At first glance, this appears to be a case of non-linear wave-wave interaction. However, if ω_3 is also a normal mode of the system, there is the possibility that it is a spontaneously excited independent mode. The question then arises of how to discriminate between the two cases. The answer lies in examining the phase coherence between the three waves. If the three waves are independently excited, then the phases of each wave will be statistically independent of the others, resulting in zero phase coherence between the waves. On the other hand, if ω_3 is due to nonlinear wave-wave interaction between the waves present at ω_1 and ω_2, then there will exist a phase consistency between them. Obviously, "linear" spectral analysis techniques are of limited value in analyzing fluctuation data characterized by nonlinear wave-wave interactions. It is the purpose of this paper to demonstrate that digital implementation of a higher-order spectrum known as the bispectrum permits one to distinguish between spontaneously excited modes and coupled modes by measuring the degree of phase coherence between modes. In addition, digital bispectral analysis may be utilized to determine the complex amplitude of the wave-wave interaction coefficient.

COMBINED SESSION I

Monday P.M., 9 January UMC Center Ballroom

Chairman: Dr. J.R. Wait, CIRES, NOAA,

University of Colorado, Boulder, CO 80309

CS1-1
1330

CURRENT TECHNICAL ISSUES IN COMPUTER COMMUNICATIONS:

Mischa Schwartz, Department of Electrical Engineering and Computer Science, Columbia University, New York, N.Y., 10027

The field of Computer Communication Networks has expanded dramatically in the past few years. A host of research topics has been spawned as a result of this activity. These include work in such diverse areas as queueing models of networks, topological design of networks, random access, techniques, and protocol design. In this tutorial talk we focus on the areas of adaptive routing, congestion control, and integrated line-and-message switching. We describe some of our own work in these areas as a point of departure.

We summarize work, using both analysis and simulation, that attempts to compare various adaptive routing techniques on the basis of message time delay and throughput. The techniques can be ranked on the basis of their use of local nodal information, local plus fixed, and local plus feedback information, collected from adjacent nodes in the network. In the congestion control work described we have carried out analyses of some current control techniques such as the British NPL isarithmic (fixed permit) approach and input buffer limiting. The combined line-and message-switching work focuses on a frame structure that adaptively assigns time slots to two classes of messages: relatively long ones that require a dedicated set of slots in successive frames once the assignment is made, and single packet messages that occupy one slot only.

CS1-2 1410 FIBER TELECOMMUNICATION RESEARCH AND APPLICATIONS

D. Gloge, Bell Laboratories,
Crawford Hill Laboratory,
Holmdel, New Jersey 07733

Advantages over coaxial cable and metallic wire systems are rapidly bringing fiber-optic systems out of the laboratory and into competition with conventional systems in telecommunications, data processing and a variety of military applications. Trial systems with fiber cables and repeaters carrying voice, data and video signals have been installed in standard telephone ducts in the United States. Similar tests are being conducted or planned in Europe and Japan. Overall results are extremely encouraging.

At the same time current research work continues to push towards the achievement of lower fiber loss, larger transmission bandwidth, greater reliability and longer device life. Signal attenuation of a fraction of a dB/km and length-bandwidth products up to 1.8 GHz-km have been reported. Device research is looking at new ternary and quaternary material systems to provide sources and detectors in the wavelength region of lower loss and dispersion.

Efforts of integrating fibers and fiber arrays with monolithic device configurations are preparing the way towards low-cost optical data bus systems. The future of such fiber applications in large data processors looks bright, but here as in telecommunications the "bottom line" is ultimately determined by cost in competition with conventional designs.

CS1-3 1540 CURRENT RESEARCH ACTIVITIES ON THE BIOLOGICAL EFFECTS OF ELECTROMAGNETIC WAVES:

C. C. Johnson, Department of Bioengineering, University of Utah, Salt Lake City, UT 84112

Spurred on by concern over the possible biological hazards of electromagnetic radiation, a sizeable research program has been sustained over the last several years in the investigation of biological effects of electromagnetic waves. Major contributions have come from interdisciplinary teams, where biological, behaviorial, and medical expertise is combined with engineers trained in microwave hardware and electromagnetic field theory.

In the United States there have been major contributions in the last three years in: (1) the development of a non-metallic temperature sensor for use in tissues such that non-perturbing tissue temperature measurements can be made during irradiation, (2) the development of field survey meters with appropriate dynamic range, frequency response, and omnidirectional characteristics, and (3) the application of basic electromagnetic field theory to models of man and experimental animals.

Major advances in non-metallic thermometry have included the use a liquid crystal sensing tip, illuminated by a gallium arsenide LED with fiberoptic conducting bundles. The liquid crystal sensor is characterized by instabilities which are troublesome and require calibration, thus Faraday rotation devices and semiconductor band-gap materials are being developed as sensors. A high resistance lead thermistor system has also been developed which shows considerable promise.

The theoretical work has been directed towards the investigation of the electromagnetic power absorption patterns in model total absorption, and scattering as a function of frequency and orientation of the biological model with respect to the electromagnetic wave field vectors. It has been discovered theoretically and verified experimentally that the greatest absorption in man occurs near 70 MHz for plane wave irradiation in free space, with the electric vector of the plane wave aligned with the long axis of the body. It is interesting to note that over an order of magnitude of difference in total absorbed power at a given frequency and incident power density can occur, depending on the orientation of the body with respect to the wave field vectors.

The current international research status in bioeffects has just been summarized at the 1978 International Symposium on the Biological Effects of Electromagnetic Waves held at Airlie House, Virginia, October-November, 1977. This conference covered a variety of biological topics including macromolecular and cellular effects, mutagenic and developmental effects, behavioral effects, sensory effects, central nervous system effects, hyperthermia and ELF effects. Engineering topics included dosimetry, thermometry, exposure systems, field survey meters, and standards. A brief summary of the highlights of this international conference will be presented.

CS1-4
1620

WHITHER THE U.S. NATIONAL COMMITTEE OF URSI?

J.V. Evans, Lincoln Laboratory, M.I.T.,
Lexington, MA 02173

The International Union of Radio Science (URSI) was formed after the First World War in response to the need to pursue radio propagation research on a global basis. This logically led to an interest in the physics of the earth's ionosphere which was fostered under the leadership of Sir Edward Appleton. Concern with natural phenomena grew after the Second World War when advances in radar and radio techniques paved the way for new branches of radio science such as radio astronomy and high power radar studies of the lower atmosphere and ionosphere. The question of what was the proper role for URSI among the various scientific unions was raised in the early 1960's and has been pushed to the fore by Henry Booker since then. In 1972 at Warsaw, Poland the URSI Council rejected a proposal that it merge with the International Association of Geomagnetism and Aeronomy (IAGA) to form a new scientific union dealing with solar-terrestrial physics, and the search for a central scientific discipline was rejoined. In 1975 at Lima, Peru URSI voted to make Telecommunications Science its central theme while maintaining responsibility for the technology of remote sensing. The Commission structure of the Union was revised to reflect this new direction, and later that year the USNC changed the commission structure within the United States to match that of the International Union. At this same meeting the USNC voted to change its own structure to secure tighter coupling to U.S. groups and societies active in radio science. The paper reviews these planned changes, the efforts that have been made to implement them, and how they may affect the future of the U.S. National Committee. The talk will also attempt to summarize recent discussions concerning the possible formation of a new scientific society for radio science that grew out of a review of the operations of the USNC undertaken by the Assembly and Mathematical and Physical Sciences (AMPS) within the National Academy of Sciences.

EVENING LECTURE*

Monday Eve., 9 January Radio Bldg., U.S. Dept. of Commerce

2000 DEPARTMENT OF DEFENSE UTILIZATION OF THE ELECTROMAGNETIC SPECTRUM AND GUIDED MEDIA: Gerald P. Dinneen, Deputy Director of Defense Research and Engineering, Washington, D.C. 20301

Utilization of the radio frequency spectrum in the Department of Defense is reviewed through illustrative examples of current communications, command and control, and sensor systems. Trends in future use are projected by review of research and development efforts in systems which must function under crowded and hostile environmental conditions. Future use of guided media such as fiber optics is also examined.

*Sponsored by the Denver Section of the IEEE.

COMBINED SESSION II

Tuesday A.M., 10 January UMC Center Ballroom

Chairman: Prof. S.W. Maley, Dept. of Electrical Engineering,

University of Colorado, Boulder, CO 80309

CS2-1
0830 ELECTROMAGNETICS IN GEOPHYSICS:
R. J. Lytle, Engineering Research Division, Lawrence Livermore Laboratory, Livermore, CA 94550

Electromagnetics has been and is now being used for a wealth of applications above the surface of the earth. It is also now being applied to a wide range of applications beneath the earth's surface. In particular, it is being used in the areas of exploration geophysics, engineering geophysics, and tectonophysics. Applications include (among others): determining the moisture content in a snowfield, predicting the occurrence of landslides, retorting oil shale in situ, monitoring the progression of the burn front and resultant cavity size for in situ coal gasification, determining the orientation of fractures in a hot dry rock geothermal reservoir, earthquake prediction, archaelogical exploration, mineral exploration in the sea and in the solid earth, hydrology studies, monitoring the temperature profile within the earth, detection of clandestine activities such as tunnels, locating and assessing the extent of a geothermal reservoir, and probing from a borehole to assess the geotechnical properties of the localized regions (e.g., determining the porosity of rock about a borehole and distinguishing between oil and water).

An overview of the different applications will be given. Also discussed will be several promising geophysical properties and exploration/interpretation techniques. These would include: electromagnetic emission by quartz bearing rocks, an empirical relationship between fluid permeability and electrical resistivity, magnetic resistivity, electrical self-potential, and pulse propagation interpretation using Prony's method. Time permitting, a presentation will be given of the state-of-the-art in the inverse problem and a list of data interpretation computer codes that are generally available from various investigators.

CS2-2 0900 HF RADAR--AN IMPORTANT NEW TOOL FOR COASTAL OCEANOGRAPHY: D. E. Barrick, Wave Propagation Laboratory, National Oceanic and Atmospheric Administration, Boulder, CO 80302

NOAA--as well as other governmental and industrial groups--is becoming increasingly involved in the conduct and management of operations in coastal waters off the United States. Some of the expanding activities which can impact the fragile coastal ecosystem include: (i) offshore petroleum drilling and recovery; (ii) mining on the continental shelf; (iii) offshore deep-water ports to service oil supertankers; (iv) industrial and nuclear plant siting near the coasts. Predicting bountiful catch areas is increasingly important to the fishing industry; the transport of many types of fish eggs and nutrients in coastal waters by the highly capricious surface currents weighs heavily in such predictions. Coastal erosion, caused by the interaction of certain wave fields with coastal and bottom topographic structures, produces damage exceeding a billion dollars a year. Finally, coastal waters are being used increasingly for recreational purposes. Coastal current fields and wave directional spectra produce perhaps the greatest impact on all of these activities; hence their effective observation is becoming increasingly important to the U.S.

A small, transportable prototype HF radar system has been constructed and demonstrated which maps near-surface currents in coastal areas. Employing first-order Bragg scatter from 6-m ocean waves, the radar deduces the current velocity from the Doppler shift of the signal with respect to its expected position. The azimuth angle to the scatter area is extracted from the complex voltages measured simultaneously at four receiving antennas. The system has been demonstrated in two coastal areas, one having a strong geostrophic current flow and the other dominated by a strong tidal flow which reverses every six hours. The maximum range of this system is about 70 km. Preliminary comparisons with drifter buoys show standard deviations between the two sets of measurements of 27 cm/s.

The same radar system is now being modified and tested for measurement of the waveheight directional spectrum. In this case, a different receiving antenna system is being used: two orthogonally oriented loops along with a coaxial monopole. This antenna change is necessitated by the nature of the echo used for the inversion process; the second-order portion is employed here, which is produced by the interaction of two sets of ocean waves. The antenna system thus forms a broad beam which is electronically scanned in angle within the receiver software. The resulting nonlinear integral equation is inverted to obtain the first several directional moments of the waveheight spectrum at desired wave frequencies. This use of the system is still undergoing theoretical and experimental investigation.

CS2-3 RF RADIATION FROM LIGHTNING:
0930 D. M. Le Vine, Code 953
NASA/Goddard Space Flight Center
Greenbelt, Maryland 20771

Radiation from lightning in the RF band from 3-300 MHz has been examined during experiments at the Kennedy Space Center (Florida) during the Thunderstorm Research International Project. Radiation in this frequency range is of interest for its potential as a vehicle for monitoring severe storms and for studying the lightning itself. Simulatneous RF measurements have been made at frequencies of about 3, 30, 139 and 295 MHz together with records of fast and slow field changes. Continuous analogue recordings have been made with a system having 300 kHz of bandwidth. Also, digital records have been made of selected events (principally return strokes) to permit detailed study of the RF radiation associated with these features of the flash.

The data reveal a distinct (temporal) pattern in the RF radiation which is essentially independent of frequency, but does depend on the type of lightning flash: Cloud-to-ground flashes are characterized by an abrupt beginning associated with the stepped leader, whereas cloud-to-cloud flashes begin with a much slower train of noise pulses which is more typical of the end of both types of flash.

Return strokes have been singled out for detailed experimental and analytical study as part of an effort to gain insight into mechanisms producing the RF radiation. This work has been encouraged by experiments performed at KSC during the summer of 1976 which documented a delay between the onset of the return stroke and the development of RF radiation. Subsequent modelling using a transmission line model for the current in the channel suggests tortuosity as an important factor in this delay. Tortuosity also has a significant effect on electric field waveforms radiated from return strokes and on the power spectrum of the fields radiated from lightning. The effects of tortuosity are to obscure information about the current pulse propagating along the return stroke channel, and to increase the high frequency (RF) portion of the spectrum.

CS2-4 INTERCONTINENTAL RADIO ASTRONOMY
1030 K. I. Kellermann, National Radio Astronomy Observatory, Green Bank, W. Va. 24944

Very Long Baseline Interferometer Observations are being made using intercontinental arrays of up to seven antennas. Recent improvements in instrumentation and in techniques of image restoration include the partial use of the interferometer phase data and the direct real time connection, via satellite link, of antennas separated by transcontinental distances. A variety of astrophysical investigations are in progress in laboratories and observatories throughout the world including the study of compact radio galaxies and quasars, interstellar molecular masers, and stellar radio sources. Terrestrial applications include the investigation of plate tectonics and global time synchronization.
The study of quasars and the nuclei of galaxies with resolutions better than one thousandth of an arc second has disclosed remarkably complex structure; in some cases sources contain components which appear to be separating at velocities well in excess of the speed of light. Although a variety of explanations have been offered for this unexpected phenomena, none are entirely satisfactory.
Current developments include the development of a new high sensitivity record-playback system with data rates up to 200 Megabits per sec and the construction of new antenna elements to provide true multi frequency imaging of celestial radio sources with sub milli-arcsec resolution.

CS2-5 THE EXTENSION OF DIRECT FREQUENCY MEASUREMENTS TO
1100 197 THz (1.5μm). THE CURRENT STATUS OF THE SPEED OF LIGHT AND THE POSSIBLE REDEFINITION OF THE METER.
K. M. Evenson, D. A. Jennings, F. R. Petersen, and J. S. Wells, Precision Laser Metrology Section, National Bureau of Standards, Boulder, Colorado 80302

The CO_2 and He-Ne lasers stabilized respectively with CO_2 and CH_4 are now accepted as frequency and wavelength standards at 9 to 12, and 3.39 μm. This is due to their excellent frequency stability and accuracy, and the direct measurement of their frequencies. The measurement of both the frequency and wavelength of the CH_4 device yielded a hundred fold increase in the accuracy of the speed of light. This paper reports the extension of direct frequency measurements to the 197 THz (1.5 μm) cw line of a He-Ne laser, and reviews the current status of laser stabilization and speed of light measurements.

CS2-6
1130 THE OPERATIONAL AND ECONOMIC ARGUMENTS FOR SINGLE-MODE OPTICAL WAVEGUIDES FOR LONG-HAUL APPLICATIONS: R. L. Gallawa, Office of Telecommunications, Institute for Telecommunication Sciences, Boulder, CO 80302

The refinements now emerging in graded index multimode fibers renders them strong contenders for use in long-haul, high bit rate optical waveguide systems. Indeed, most developmental effort today seems to be concentrated on exploiting the desirable characteristics of such graded index fibers. In the process, we seen to be ignoring the fact that the single-mode fiber is, in many respects, much more desirable than the graded index multimode fiber. This will be especially true in the case of long-haul systems such as the submarine cable applications, where it is essential that the number of repeaters be kept to a minimum to improve reliability.

This paper will review the key advantages and disadvantages of the single-mode waveguide over the multimode graded index waveguide. It will be demonstrated that with a reasonable choice of the key operational parameters, the single-mode fiber will provide considerable advantage both operationally and economically. The key disadvantage is in the connector requirements. With reasonable tolerances on the graded index fiber parameters (profile parameter and size), it will suffer disadvantages in an operational and economical sense. It is felt by the author that tolerances than can reasonably be expected will render the performance of the graded index fiber interior to that of the single-mode fiber when all engineering considerations are in. Attention will be given to both the economic and the operational considerations.

TUESDAY AFTERNOON, 10 JAN., 1330-1700

Commission B Session 2

SEM AND PRONY'S METHOD

Tuesday P.M., 10 January ECCR 2-28

Chairman: Prof. R. Mittra, Electromagnetics Laboratory, University of Illinois, Urbana, IL 61801

B2-1
1330 S E M ANALYSIS OF A HOLLOW SPHERICAL SHELL OF "SCREENED" COMPOSITE MATERIAL: K. F. Casey, Department of Electrical Engineering, Kansas State University, Manhattan, Kansas 66506

As a first step toward understanding the transient behavior of hollow bodies made of advanced composite materials, the SEM analysis of a hollow spherical shell of low-loss advanced composite with an embedded bonded wire-mesh screen is carried out. The composite material and the screen are characterized by an equivalent sheet impedance operator.
It is found that, as expected, the characteristic resonances of the body are of two types: "exterior" resonances corresponding to those of a perfectly conducting sphere and "interior" resonances corresponding to the cavity modes of a hollow perfectly conducting sphere. Analytical and numerical results are presented to illustrate the behavior of the pole locations and the associated residues as the parameters of the screen and shell are varied. The poles associated with the q=1 (TE_r) resonances all move to the left in the s-plane as the screen impedance is increased; similar behavior is exhibited by most of the poles associated with the q=2 (TM_r) resonances. The remainder (two for each value of n) move to the right in the complex s-plane, residing finally on the imaginary axis at points which correspond to waves bound to the reactive spherical surface. Numerical results are also presented to illustrate the surface current density and surface charge density response functions for a step-function plane wave excitation of the sphere.

B2-2
1350 A SIMPLE WAY OF CALCULATING TRANSIENT FIELDS OF LOADED LINEAR ANTENNAS: K.J. Langenberg, K.D. Rech, Fachrichtung Elektrotechnik, Universität des Saarlandes, D-6600 Saarbrücken, Fed. Rep. Germany

A recently published (L. Marin, T.K. Liu, Radio Sci. 11, 149-155, 1976) simple way of solving transient thin wire problems, i.e. a singularity expansion using approximate poles, modes and coupling coefficients, turns out to be very useful concerning the following aspects:

1. It works even better than stated by the authors, since their comparison of first- and second-order approximated Hallén poles with exact numerical data is not correct.
2. A straightforward extension to the transient radiation fields yields simple analytical expressions for the near- and far-field modes, even for finite rise time of the applied voltage.
3. If the thin-wire antenna is fed by a step-function voltage, the analytical expressions for the transient antenna current reduces to a Fourier series if the antenna radius tends to zero; this series corresponds to the periodic rectangular function which is obtained on the base of the lossless and homogeneous transmission line representation of the antenna. This gives nice insight in the meaning of SEM-representations.
4. The Fourier series representation fails if the antenna is center-loaded with a non-zero generator impedance. The concept of a frequency averaged antenna impedance (R.W.P. King, C.H. Harrison, Antennas and Waves, M.I.T. Press, 1969) cannot be applied to determine approximate SEM-poles. Hence we investigate the exact numerical SEM-data for ohmic generator impedances. We find, that the natural modes are nearly unaffected by the generator resistance whereas the negative real part of the first layer poles increases, dependent on the pole number and the antenna radius; their imaginary parts as well as the complex second layer poles are nearly unaffected. This sheds some light on the physical reliability of the higher order layers.
5. These investigations suggest the extension of Marin and Liu's simplified SEM-version to non-zero generator impedances, yielding approximate solutions of a wide variety of more complicated problems, such as transient fields of systems of transmission line connected linear antennas.

B2-3
1410 ON THE EXTRACTION OF THE SEM QUANTITIES FOR A THIN WIRE FROM ITS TRANSIENT RESPONSE: L. Wilson Pearson, D. Randall Roberson, Department of Electrical Engineering, University of Kentucky, Lexington, KY 40506

The results of a numerical experiment in the Prony method extraction of the SEM description of a thin wire is described. Several workers have previously obtained certain of the SEM quantities, in particular, the poles, from limited transient response data. In the present paper, the poles, modes and normalization constants related to the first ten first-layer resonances of a thin wire are derived from transient response data at a multiplicity of observation points along the wire. The transient data are produced by a time-domain numerical solution to the wire problem by way of the Livermore TWTD computer code. Agreement with other available solutions is observed to be excellent for low noise levels for both the poles and the natural modes. Potential sensitivities of the normalization constant computation are discussed. Representative results are presented to demonstrate the sensitivity of the extracted information to noise-corrupted transient data. Methods for processing the data which take advantage of the intrinsic spatial redundancies in order to minimize the effects of noise are discussed.

Code ⇒ TD response ⇒ Prony

B2-4
1430

ON THE TIME DOMAIN REPRESENTATION OF ~~CURRENTS~~ BY THE SEM: D. R. Wilton, Department of Electrical Engineering, University of Mississippi, University, MS 38677

Resolvent Kernel ($\bar{H}^{-1}$)

The so-called "question of the entire function" in SEM can be reduced to considerations for the LHP or RHP closure of the Bromwich contour in the Laplace inversion integral. (By Cauchy's theorem, closure in the RHP yields no response while closure in the LHP yields, by the residue theorem, the familiar damped exponential series.) The question is one of how causality manifests itself in the representation. To answer this, it is necessary to discern the s-plane asymptotic behavior of the resolvent kernel. This is apparently an extremely difficult task, especially since the result most likely depends on both observation and source coordinates.

In this paper we interpret the meaning of the postulated Class I and Class II coupling coefficients introduced by Baum and the Class X coefficient introduced by Mittra and Pearson in terms of the asymptotic behavior of the resolvent kernel. Evidence is presented to suggest that both Class II and Class X forms are valid but that Class I is valid only if used with a significant modification. Furthermore, a new class, Class Ω, is introduced which is more "liberal" than Classes II and X, but more "conservative" than Class I. Additional evidence indicates that Class Ω may be connected with the asymptotic behavior of the resolvent in the LHP and that Class II is connected with the corresponding RHP behavior, while Class X is based purely on physical considerations. While these observations are both preliminary and tentative, they do seem to shed light on SEM time domain representations and may eventually lead to more rigorous results.

?, Abromovich?
Closure of Contour

B2-5 1530 APPLICATION OF PRONY'S METHOD TO RADIATION-PATTERN IMAGING*:

E. K. Miller and D. L. Lager, Lawrence Livermore Laboratory, University of California, Livermore, CA 94550

Prony's method has been applied in electromagnetics to find the SEM poles of impulsively excited objects from their transient responses. It is a procedure by which the poles and residues (or their equivalent) of a complex exponential series can be obtained from a sequence of its sampled values. While Prony's method has been used primarily for exponential signals which are functions of time, it can be applied to other physically interesting problems whose solutions are exponential in other variables.

The application discussed in this paper is that of imaging isotropic point sources from their far fields. We consider a linear array in particular and note that for this problem the poles of the pattern are the physical locations of the sources. We examine the characteristics of the extracted poles as a function of the source parameters and the sampled data. The utility of eigen-values analysis of the data is also demonstrated, especially in terms of how the aperture affects the data rank. Finally, extensions of the procedure to more general source distributions is considered.

B2-6 1540 APPLICATION OF PRONY'S METHOD TO TIME-DOMAIN REFLECTOMETER DATA AND EQUIVALENT CIRCUIT SYNTHESIS

Daniel H. Schaubert, Harry Diamond Laboratories, 2800 Powder Mill Road, Adelphi, MD 20783

The singularity expansion of time-domain reflectometer (TDR) data has been computed and used to calculate lumped-element equivalent circuits for the impedance of some typical antennas. Prony's algorithm was used to obtain the poles of the antenna's terminal voltage due to a step-like excitation. The residues, however, were calculated subject to the uniform error norm instead of the least squared error norm. Although it requires much longer to calculate, the uniform error norm approximation is often orders of magnitude better than the least squared error approximation. The physical realizability of impedance functions obtained from experimental data has been investigated. Also, the procedures necessary to synthesize the lumped-element network have been evaluated. A simple partial fraction expansion of a realizable impedance function representing an antenna was found to yield nonrealizable element values. A general network synthesis procedure, such as Brune's method is required.

B2-7
1550

SOME POLE EXTRACTION RESULTS USING ITERATIVE METHODS:

J.T. Cordaro, Department of Electrical Engineering and Computer Science, University of New Mexico, Albuquerque, NM 87131

Several investigators, including the author, have used Prony's method to extract poles from measured EMP data. When using Prony's method with experimental data, it is necessary to fit the data with extra poles to remove bias in the pole estimates. This approach works up to a point, but the number of poles that can be used is limited by the amount of data available and by the conditioning of the linear equations that are solved in implementing the method. It is common to have the mean squared error between the data and reconstructed signal decrease as the number of poles is increased. At the same time, the error between the actual and calculated system pole values decreases, but when this process is continued with too large a number of poles, the equations become ill-conditioned and the process must be terminated.

We have been experimenting with two iterative techniques that give more accurate results than Prony's method. The improvement over Prony's method comes from the fact that neither technique uses extra poles; they operate by iteratively learning the noise covariance matrix. An estimate of this covariance is used to compute the Gauss-Markov estimate of the poles. If the covariance were known exactly the pole estimates would be unbiased. It is not known but the learning process is iterated until the mean squared error converges. Our experience has been that when observation noise is present, the resulting pole estimates are more accurate than those obtained with Prony's method.

We have applied the methods to cylinder EMP response data. Poles found in the response and incident field have been calculated. From these results, it is possible to sort out the poles that correspond to natural frequencies in the cylinder.

B2-8
1600 FIRST ORDER ERROR ANALYSIS OF PRONY'S METHOD:

G.J. Scrivner, Computer Sciences Corporation, 201 LaVeta Drive, NE, Albuquerque, NM 87108

The noise sensitivity of Prony's method of extracting poles and residues directly from transient response data is reasonably well known. The matrix equation resulting from applying Prony's algorithm is perturbed by noise both with respect to the matrix elements and to the elements of the vector source term. A first order error analysis is presented which provides analytic expressions for the expected value of the solution vector. In addition, the standard deviation of the components of the solution vector is studied and a bound upon this quantity is obtained. This first order analysis highlights the importance of the eigenstructure of the Prony matrix and the nature of the perturbation in this eigenstructure due to the presence of noise in the data. With this realization, the first order Rayleigh-Schrodinger perturbation method is used to study the statistical properties of the perturbation in the eigenstructure. Most important in this respect is the perturbation of the zero eigenvalue associated with the unperturbed Prony matrix of order one higher than the number of actual poles existing in the transient response data. It is the perturbation of this eigenvalue which can often make the task of determination of the number of true poles in the data formidable. Numerical results are presented which compare the expected values of eigenvalue shifts and solution vector components to theory. Comparisons of numerically generated standard deviations associated with these parameters are compared to the theoretical bounds which have been obtained. Comparisons are found to be quite favorable in all cases examined. The importance and implications of the above results to the data analyst using Prony's method are briefly discussed.

B2-9
1610

IMPROVING PARAMETER ESTIMATES IN TRANSIENT ELECTROMAGNETIC MODELLING:

D. G. Dudley, Department of Electrical Engineering, University of Arizona
Tucson, AZ 85721

The use of Prony's method to identify the damped resonances in electromagnetic data has been shown to be a special case in the estimation of the parameters of a single-input, single-output linear system (Dudley, D. G., Radio Science, to appear). The inherent errors in the data, however, cause the evaluation of the system parameters to be biased. In addition, subsequent calculation of the poles from the parameters is mathematically ill-posed so that small bias can produce large pole errors.

The problem can be viewed as a classic linear least squares minimization in which the components of the residual vector are colored noise. Early results in time series analysis (Mann and Wald, Econometrica, 11, 173-320, 1943) have shown that the colored noise is responsible for the parameter bias.

In this paper, a generalized least square technique is adopted. The model results formally in a filter which whitens the colored noise and thereby reduces the parameter bias. Numerical results are presented in which the filtering method is applied against known analytical models corrupted with various noise forms. Some observations are made concerning the uncertainties in obtaining acceptable results and some recommendations are given concerning the advisability of definitive analysis of the experimental process which produced the electromagnetic data.

Commission E Session 1 (Invited)

PERFORMING MEANINGFUL EMI MEASUREMENTS

Tuesday P.M., 10 January ECCR 0-38

Organizer and Chairman: M.L. Crawford,

National Bureau of Standards, Boulder, CO 80302

E1-1
1330

ANTENNA FACTORS IN SHIELDED ROOMS

J. M. Roe and W. H. Coalson, Electronic Systems Department, McDonnell Douglas Astronautics Company-East, St. Louis, MO 63166

Extensive measurements of antenna to antenna coupling factors in shielded rooms have shown that the use of antenna gain as measured under free space conditions is not valid in shielded rooms. The measurements utilized standard antennas as prescribed in MIL-STD-462 and covered the frequency range of 1-10 GHz. To simulate random positions of equipment and other fixtures within the shielded room, a paddle wheel mode tuner was used with extensive computer-aided data acquistion. It was shown that for antennas with gains less than 20 dB and for antenna to antenna spacing of one or more meters one cannot distinguish among the transmit or receive properties of the various antennas tested. The antenna samples included waveguide horns, ridged horns, conical log-spirals, and simple bare wires.

When these results are applied to the calibration of radiated susceptibility or radiated emissions tests, it is found that the correction factors diverge - i.e., the inferred susceptibility of a particular test sample is less than would be calculated using the free space antenna factor but the emissions are greater. A comparison of the statistical distributions of free space antenna patterns to the pickup pattern inside a shielded room suggests that a longwire antenna is best suited for calibrating electronic equipment tests.

E1-2
1355

EMES - A LARGE, AUTOMATED, 1 MHz TO 10 GHz, EMR/EMP SIMULATOR

Neith Pollard, EMR/EMP Instrumentation Division Supervisor, Sandia Laboratories, Albuquerque, NM 87115

This paper describes the electrical characteristics and automated features of a broadband electromagnetic environments simulator (EMES) used to test weapons and weapon components. It is, of course, suitable for testing any other objects of appropriate size. The simulator consists of a three plate, rectangular cross section 50 ohm transmission line operating in TEM mode. The "working volume" in which test objects can be placed is 4 meters high, 11 meters wide and 5 meters long. The system operates over a frequency range of 1 megahertz to 10 gigahertz. A wall of rf absorber pyramids, each 4 meters long, is mounted across the receiving end of the line to suppress the generation of higher order modes and thus maintain TEM mode transmission above the 19 megahertz first resonance of the line. The outer conductor is continuous resulting in a nonradiating facility.
CW excitation of the line is from a 200 milliwatt synthesizer/amplifier system remotely controlled by a PDP 11/40 minicomputer. This output is amplified to 200 watts and fed through a coaxial-to-stripline transition into the simulator. Net power into the line is monitored by the computer and necessary gain adjustments are automatically made to maintain the programmed test conditions. The frequency is step swept over the range of interest at a rate dictated by the sensor and data acquisition response time, all under computer control.
The line is also designed to accept simulated EMP pulses up to 400 kilovolts.

E1-3
1420

THE NBS ELECTROMAGNETIC FIELD PROBE PROJECT

F. X. Ries, National Bureau of Standards,
Boulder, Colorado 80302

Electromagnetic field probes are needed to measure the EM environmental characteristics to identify the fields which can cause interactions with both electronic and biological systems. This talk will outline the electromagnetic field probe project of the National Bureau of Standards' Electromagnetic Interference and Radiation Hazards program. The present tasks objectives will be covered in an overview manner. These tasks include such areas as: 1) isotropic broadband electric field measurements from 1 MHz to 1 GHz, 2) frequency selective isotropic electric field measurements from 10 MHz to 1 GHz, 3) directive frequency selective electric field measurements from 20 MHz to 6 GHz, and 4) measurement of temperature in the presence of a electromagnetic field. Much of this work is concerned with the development of special antennas such as resistively loaded dipoles and TEM forms, and electrically short dipoles.

E1-4 1445 STANDARDS FOR THE GENERATION AND MEASUREMENT OF IMPULSIVE FIELDS AT NBS: A. R. Ondrejka and R. A. Lawton, Electromagnetics Division, National Bureau of Standards, Boulder, CO 80302

Interference due to radiated impulse-like electromagnetic energy has been a constant problem in the fields of telecommunications and electronic instrumention. Sources such as lightning or automotive ignition interfere with AM/FM radio or TV and cause mostly inconvenience, but the radiated impulses from an electric razor, for example, can cause a serious malfunction of a sensitive device as a Pacemaker with fatal results to the wearer. Good measurments of these radiated fields help in developing an understanding of the radiating and receiving impulse characteristics of antennas, either intended or accidental. This knowledge can then be used to reduce such interference. Work is in progress at NBS to generate and measure fields which resemble this type of interference. The fields generated have a simple time structure usually an impulse or short duration damped sinusoid and are measured in the time domain. The shortest impulse presently used has a duration of 90 picoseconds and contains useable frequency components from 50 MHz up to at least 6 GHz. It is radiated from a conical transmission line located over a ground plane. Receiving antennas include a resistively loaded monopole and a specially designed TEM horn antenna, each having a useful frequency range of at least a decade. The impulsive fields are mathematically well defined on or above the ground plane and after having verified them experimentally using a "standard" receiver, can now be used to measure the receiving impulse response of any receiving antenna. The longest pulses used in our investigations have a duration of 20 μs and provide measurements at frequencies down to 1 kHz. At such low frequencies, the fields are generated in a Crawford TEM cell and measured using a short monopole antenna which is made broadband by the high impedance FET amplifier which it drives. Its useful bandwidth extends from 500 Hz to 500 MHz.
In the frequency range 50 MHz to 6 GHz, both the antennas and the measurement system (impulse generators and Automatic Pulse Measurement System) have been analyzed to determine the possible sources of error and to estimate their magnitudes. Experiments have just begun in the frequency range 500 Hz to 500 MHz and no error analysis is presently available. Work is still pending for the frequencies above 6 GHz.

E1-5 1540 ELECTROMAGNETIC SUSCEPTIBILITY MEASUREMENTS USING A MODE-STIRRED CHAMBER: O. C. Dunaway, Electromagnetic Effects Division, Naval Surface Weapons Center, Dahlgren, VA 22448

The concept of a system electromagnetic susceptibility measurement technique, derived from MIL-STD-1377 for measuring cable and enclosure shielding effectiveness, is presented. This technique is intended as a fast, inexpensive alternative to anechoic chamber measurements for use in the design and development cycle or qualification testing of electronic systems. The basic instrumentation requirements and the repeatability of measurements made with the technique are discussed. Determination of a quantity equivalent to the power density necessary to obtain the same test system response in a planewave situation is shown to be required. A test program designed to answer this problem is described and results are presented. The data analysis procedure is illustrated and test results on a representative electronic system are compared with data taken on the same system in an anechoic chamber.

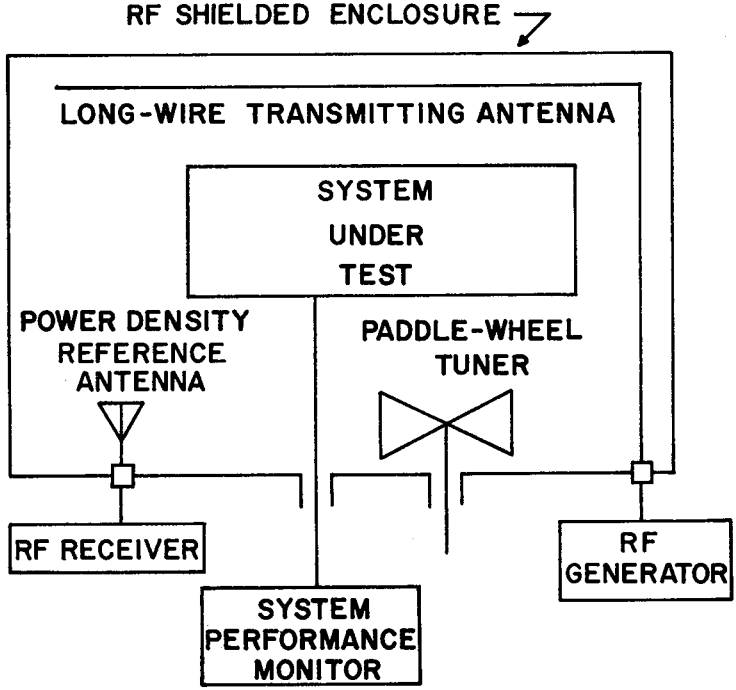

E1-6
1605

A PROPOSED ELECTROMAGNETIC TEST FACILITY FOR LARGE SYSTEMS

J. W. Adams, National Bureau of Standards
Boulder, Colorado 80302

With increasing use of electronic systems on vehicles and medical devices, as well as continued use of rack-sized communication and computer systems, there is a strong need for a reliable means of evaluating whole-system electromagnetic susceptibility and emissions.
Shielded rooms, anechoic chambers, open spaces, and TEM cells can be used under some specific conditions, but all have such severe limitations that comprehensive, effective testing is impossible.
A facility using several different concepts is proposed. An underground facility with layered, earth-and-wire overburden can provide electromagnetic isolation. Haulageways with swinging doors lined with anechoic backing material provide workable access while maintaining this isolation. A large test volume can be provided by a transmission line. Tapered sections on the ends of this transmission line should provide energy launch mechanisms. Higher order modes will be present, and even enhanced with mechanical stirring. The resulting fields must be monitored with an extensive network of isotropic probes. The field will be highly variable and must be statistically bounded. The need for rotation of the test object or the field, the power levels required for generation of desired field strength levels, and other related topics are discussed.

E1-7
1630 MEASUREMENT OF SPURIOUS SIGNALS FROM MICROWAVE OVENS

Harold C. Anderson, Applied Research Dept.
Litton Microwave Cooking, Minneapolis, Minn

Spurious signals from microwave ovens are measured in the microwave range with a hand-held antenna at a distance of three meters from the oven. A search is made in azimuth and elevation for the maximum lobe. The value measured is converted to a free space field in microvolts per meter at 1000 feet for the purpose of showing compliance with the FCC rules and to effective radiated power to show compliance with the CISPR recommendations.

The Italian National Committee proposed to the International Special Committee on Radio Interference (CISPR/A, Italy 1, London March, 1974) that a shielded room approximately two meters cubed be used for the measurements. In the room mode stirrers were to be installed consisting of two metallic vanes. One vane was to be 170 cm long by 50 cm wide and rotate at 120 rpm; the other vane was to be 170 cm long and 42 cm wide and to rotate at 150 rpm. The vanes were to be mounted on adjacent walls. After the room had been calibrated a microwave oven or other microwave generating apparatus would be placed in the chamber, the doors closed and the mode stirrers started. The total radiated power on each spurious frequency would be measured by way of an antenna in the chamber and the measuring equipment on the outside.

A chamber was built up at Litton for the purpose of evaluating the technique as an improved method for measuring spurious. Results of the research at Litton and of recent work by the Italian engineers at Naples will be reviewed.

Relating the value of the spurious signal measured in the chamber to its interference potential to a communications service is necessary if the technique is to be of value. An approach to establishing such a relationship will be suggested.

Commission F Session 2

ATMOSPHERIC EFFECTS

Tuesday P.M., 10 January ECCR 0-30

Chairman: R. Lawrence, NOAA,

Boulder, CO 80302

F2-1
1400 *PRESSURE BROADENING OF OXYGEN MICROWAVE LINES BY OTHER ATMOSPHERIC GASES*

Gary G. Gimmestad and Hans J. Liebe
Institute for Telecommunications Sciences/OT
Boulder, CO 80302

Previous laboratory measurements have yielded the strengths and widths of twenty of the self-broadened oxygen microwave lines with an error of 1 to 4 percent (Liebe, Gimmestad, and Hopponen, IEEE Trans. Antennas Propag. 25, 327 (1977)). The width measurements reported here were obtained from a systematic study of collisional influences by air molecules other than oxygen (see Figure). In theory, the width depends directly on the intermolecular potential function $V(O_2 - X)$, hence the quantum number dependence of $O_2 - X$ pairs indicates deviations from the potential form to be used for $O_2 - O_2$. The difference in O_2 and AIR widths is cast into a simple model modifying the EHF atmospheric prediction scheme reported in the reference given above.

Figure follows on page 49.

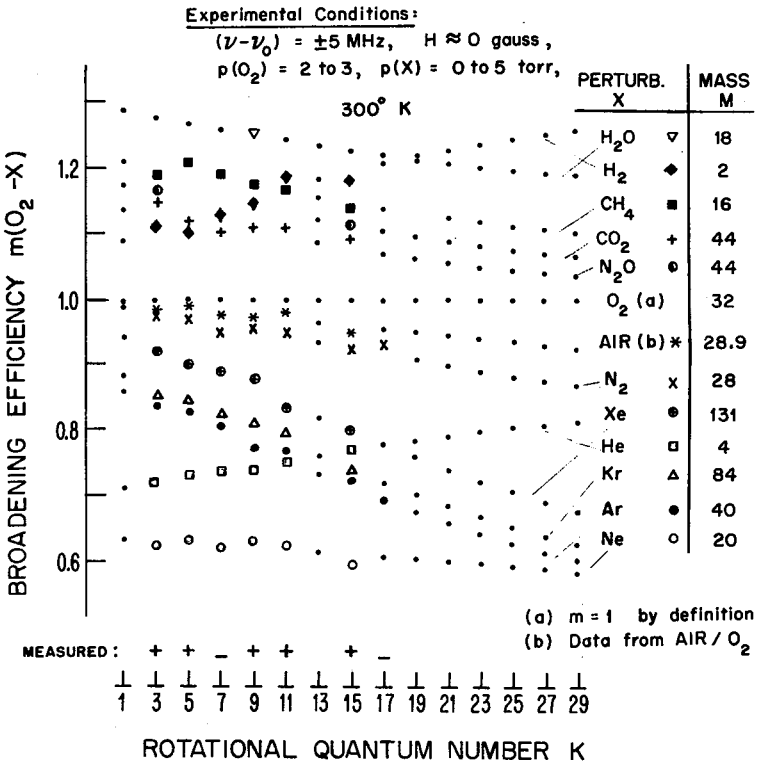

F2-2
1425

A RADIOMETEOROLOGICAL STUDY IN A TROPICAL CONTINENTAL REGION: M.S. Assis and N.R. Dhein, CETUC-PUC/RJ, Rua Marques de Sao Vicente, 209, Rio de Janeiro - 20.000 - RJ, Brasil

Experimental measurements in 6 GHz band carried out in central west region of Brasil (tropical continental climate) have shown an anomalous propagation behavior during night periods. It was inferred from signal recording analysis that the phenomenon is due to tropospheric ducts.

This work studies the meteorological conditions in this area, in order to establish a connection with duct formation. To this end surface meteorological data, radiosonde data and refractometer measurements were used. Three different aspects of the problem are investigated and discussed: (i) The correlation between duct occurrence and humidity and temperature gradients; (ii) A comparative analysis between the behavior of surface meteorological parameters and duct formation; (iii) The relation between wind and stratification. The fine scale measurements with refractometer has proved to be the most effective way to study the variation of refractive index with height. However, surface data (temperature and humidity) are also of importance for a qualitative analysis of the problem.

F2-3
1450 EVAPORATION DUCT INFLUENCES ON BEYOND THE HORIZON HIGH ALTITUDE SIGNALS: H.V. Hitney, R.A. Pappert, and C.P. Hattan, Propagation Division, Naval Ocean Systems Center, San Diego, CA 92152; and C.L. Goodhart, Megatek Corporation, San Diego, CA 92106

A case study of beyond the horizon propagation previously examined in terms of an earth detached duct produced by an elevated layer at 2000 ft. will be re-examined in terms of ducting produced by evaporation ducts (duct heights $\lesssim$ 100 ft.). The case study applies to a frequency of 3087.7 MHz, a transmitter altitude of 68 ft. and a receiver altitude of 3000 ft. Results indicate that relatively shallow surface ducts of the type examined can significantly affect signal level beyond the horizon at elevations which are an order of magnitude or more greater than the duct height and could conceibably account in large measure for the disparities previously reported. Coupling between an evaporation duct and an earth detached duct will also be discussed.

F2-4
1515 THE INFLUENCE OF OROGRAPHIC FEATURES ON LINE-OF-SIGHT FADING: C. Fengler, Department of Electrical Engineering, McGill University, Montreal, Que. H3A 2A7

The conditions at which fading on line-of-sight links occurs are summarized. Further discussion is restricted to paths with sufficient ground clearance and the corresponding refractive index profiles are considered in association with meteorological elements. The results are applied to selected areas of the North American continent. The seasonal probability of the occurrence of strong line-of-sight fading is derived from geographical and orographical factors.

Commission G Session 1

MISCELLANEOUS TOPICS

Tuesday P.M., 10 January ECCR 1-42

Chairman: Dr. Kenneth Davies, NOAA, R 43

Boulder, CO 80302

G1-1
1330 A MATRIX METHOD OF EVALUATING THE REFLECTION COEFFICIENT OF ANISOTROPIC AND INHOMOGENEOUS IONOSPHERE PROFILES:

D. Llanwyn Jones, Wheatstone Physics Laboratory, University of London, King's College, Strand, London WC2R 2LS, England.

A method of determining the electromagnetic wave reflection coefficient of a horizontally stratified ionospheric plasma is described. The method may be applied to any continuous ionospheric profile of electron density, ion density, and collisional frequency. The effect of the Earth's magnetic field is fully included, no approximations being made. In common with techniques proposed by other authors the continuous ionospheric profile is divided into a sufficiently large number of horizontal slabs, each of which is considered to be homogeneous. The inter-slab reflection coefficient is evaluated using a 4x4 matrix technique and these reflection coefficients are then propagated downwards through the profile using an iterative formula involving 2x2 matrices which, in the isotropic case with the Earth's magnetic field put equal to zero, reduces to the known iterative solution for this situation.
The method is completely free of the 'numerical swamping' which affects some 4x4 matrix solutions and some numerical integration schemes. It requires no storage of the matrices appropriate to the individual strata and allows for the inclusion of the effects of heavy ions in the lowest regions of the ionosphere in a particularly simple way. Finally, a comparison will be made with results calculated using only 4x4 matrices.

G1-2
1355 ABSORPTION AND RESONANCE PHENOMENA OF ELF RADIO WAVES IN THE EARTH-IONOSPHERE WAVEGUIDE:

Richard A. Pappert, EM Propagation Division, Code 532
Naval Ocean Systems Center, San Diego, CA 92152

Full wave calculations of normal modes associated with ELF propagation in the earth-ionosphere waveguide (Seafarer frequencies will be stressed) often exhibit a low altitude absorption peak at about 55 km during the day and around 70 km during the night as well as a high altitude absorption at about 115 km for both day and night. Theoretical analysis suggests that the low altitude line shape should be essentially Lorentzian, whereas the high altitude absorption line shape should be approximately Gaussian. Comparison of the location of the full wave absorption peaks as well as their line shapes with theoretical predictions will be made. Full wave solutions also indicate an attenuation rate resonance associated with nighttime sporadic E layering. Origin of the resonance will be clarified by examining a simple model ionosphere.

G1-3
1420 REAL-TIME DATA ACQUISITION AND INTERPRETATION CAPABILITIES OF A COMPUTER-INTERACTIVE DIGITAL IONOSONDE.

J.W. Wright, Space Environment Laboratory, NOAA
Environmental Research Laboratories, Boulder,
CO 80302

Recently a wider variety of operating programs have been added to the software system of the 'Dynasonde'. Alternate data acquisition modes are available to control the choices and compromises among alternate frequency-time patterns, choices of receiving antenna, sampling rates, etc. Self-calibration methods reduce system effects on virtual height and phase measurements. Real-time echo recognition and noise-rejection methods yield economies of data retention, and facilitate direct analysis to geophysical parameters. Deletion of protected frequencies, automatic optimization of sounding frequency range, and acquisition of maximum information per transmitted pulse are software-defined. Features of a real-time, dynamic, digital display within the system include high-resolution ionograms, polarization discrimination, 'skymap' and 'gonionogram' displays, and methods for summarizing large volumes of data.

G1-4 PULSE DISPERSION IN THE IONOSPHERE
1445

Adolf K. Paul, Space Environment Laboratory, NOAA Environmental Research Laboratories, Boulder, Colorado 80302

The travel time of a radio pulse reflected from the ionosphere can be measured in two different ways. In the classical approach a certain characteristics of the pulse shape is selected and the time difference between the appearances of this characteristic in the transmitted pulse and the reflected echo is measured. The other approach is based on the principle of the stationary phase and the travel time can be derived from the phase change over a small frequency increment. The Dynasonde provides the information to compare the two methods. Systematic differences were found in areas where the travel time (virtual height) varies rapidly with frequency. A computer simulation of the pulse propagation through highly dispersive parts of the ionosphere reveals that virtual heights derived from the "leading edge" of the echo can be too low by 10 km or more, while the error in the virtual height derived from the phase variation over an 8 kHz frequency increment is much smaller by approximately a factor 50.

G1-5
1510 UNUSUAL SCALE HEIGHT DISTRIBUTION NEAR F-REGION MAXIMUM SUGGESTED BY INCOHERENT SCATTER AND TEC MEASUREMENTS: D.B. Odom, T.I.S. Boak, III, Raytheon Company, Wayland, Mass. 01778 and J.A. Klobuchar, AFGL (PHP), Hanscom AFB, Mass. 01731

Accurate mapping of the ionospheric structure is increasingly important for high-precision, ground-based radars and satellite navigation systems. A statistical model, developed to describe the global ionospheric structure, was compared with one year of incoherent scatter measurements from Millstone Hill, Mass. This model accurately predicted the F-layer maximum density and height, but the total electron content predictions were systematically low.

A subsequent comparison with ATS6 data suggested that the Chapman-like distribution used by the model was not actually present. Instead, the ATS6 data indicated a "flattening" of the F-layer in the region above the height of maximum density (hmF2). This required a revision of the model to have different scale heights above and below hmF2. When this revised model was compared with the Millstone Hill measurements, the discrepancy between the predicted and observed total electron content disappeared. To check the statistical validity of this result, Faraday rotation measurements taken by the ATS3 satellite were compared with the model. The results of this comparison with the ATS3 data and the unusual nature of the topside F2 layer structure suggested by these measurements are discussed.

G1-6 1535 OBSERVATIONS OF THERMAL SELF-FOCUSING IN THE IONOSPHERE

L.M. Duncan, Department of Space Physics and Astronomy, Rice University, Houston, Texas 77001
R.A. Behnke, National Astronomy and Ionosphere Center, P.O. Box 995, Arecibo, Puerto Rico 00612

During a recent ionospheric modification heating experiment at the Arecibo Observatory intense high-frequency electromagnetic radiation incident on the overdense ionosphere was observed to undergo thermal self-focusing, producing large field-aligned striations. The observations were made using incoherent backscatter radar measurements of electron plasma wave enhancements. These enhancements are produced by parametric instabilities, coupling the electromagnetic pump wave into electrostatic plasma oscillations. The strength of the enhanced plasma waves directly depends on the local intensity of the pump electric field. In addition, because of frequency and wave number matching conditions for both the parametric wave-plasma interaction and the incoherent backscatter process, these enhanced waves are detected at only one particular altitude. As a result, systematic measurements of the enhanced plasma line while sweeping the narrow backscatter radar beam across the interaction region yield a two-dimensional cross-section characteristic of the local electric field intensity. The electric field maps thus generated show self-focusing spatial striations and large-scale structuring of the illuminated plasma. Because the direction and rate of radar movement are experimentally controlled, the cross-sectional dimensions of the striations are easily measured. Alternatively, if the radar is fixed, the striations follow a slow natural (E x B) drift through the beam, allowing a detailed study of the small-scale structure within individual striations. Once the size is known, striation velocities can be calculated from these drift observations. The striation measurements are shown to be in agreement with thermal self-focusing theoretical predictions.

G1-7
1600 BROADBAND HF RADIO NOISE IN THE TOPSIDE IONOSPHERE:

C.M. Rush, Air Force Geophysics Laboratory, Hanscom AFB, MA 01731; D. Nelson, Aerospace Corp.; E. Ziemba, Analytical Systems Engineering Corp.; A.L. Snyder, Air Force Geophysics Laboratory; V.G. Patterson, Air Force Global Weather Central; T.F. Tascione, Air Force Global Weather Central

A broad-band high frequency receiver is operating on board a recently launched Defense Meteorological Satellite that has been placed in a roughly circular orbit at 840 Km. This receiver was designed to permit inference of the sub-satellite value of the F2 region critical frequency assuming that the signals reaching the receiver are propagated directly from the surface of the earth through the ionosphere. The receiver itself sweeps the frequencies 1.2 to 13.9 MHz in 100 KHz steps every 32 seconds, has a dynamic range of 60 db, and provides as output the log of the field strength.
The variation of the intensity of the received data as a function of frequency, latitude and longitude will be described. Particular emphasis will be placed on the differences in the form of the data when the satellite is over land as compared to over the oceans. In addition, techniques that have been developed to determine foF2 from the satellite records will be described and the accuracy of the determinations briefly described.

WEDNESDAY MORNING, 11 JAN., 0830-1200

Commission A Session 1

ANTENNA MEASUREMENTS AND TRANSIENTS

Wednesday A.M., 11 January ECCR 2-06

Chairman: C. Stubenrauch, National Bureau of Standards, Boulder, CO 80302

A1-1 0830 EARTH TERMINAL ANTENNA MEASUREMENTS FOR COMPATIBILITY STUDIES

R. G. FitzGerrell, U.S. Department of Commerce, Office of Telecommunications, Institute for Telecommunication Sciences, Boulder, CO 80302

The objective of this study was to determine the sidelobe power-gain performance of a 6.1-m diameter G/T-26 satellite earth station antenna using airborne transmitting antennas as sources of test site illumination. The test antenna was centered on a heavy duty turntable and rotated while the helicopter traversed a flight path designed to produce nearly uniform coverage of the hemisphere relative to the test antenna. A relative gain method of measurement was employed with a single receiver switched rapidly between a reference gain antenna and the test antenna. Since the reference antenna was mounted on the optical tracking system used to obtain helicopter elevation and azimuth angles relative to the test site, it was always pointed at the test signal source. A linearly polarized standard gain horn was used as the reference antenna, and its gain was reduced 3 dB to account for the polarization loss for the measurement of the circularly polarized test antennas. Each separate measurement resulted in 60,000 to 90,000 received signal amplitude data points stored on magnetic tape along with the angular positions of the turntable and optical tracker for each point. Data tapes were processed on the data system minicomputer after a set of measurements were completed. Measured data are presented in the CCIR format for proper left-hand circular polarization and cross polarization. This statistical data format, as discussed elsewhere (R. G. FitzGerrell and L. L. Haidle, Microwaves, Vol. 15, No. 7, 59-60, 1976), shows power gain versus ϕ, the angle off the axis of the main lobe, resulting in a spatial distribution of the sidelobe levels relative to the main lobe.

A1-2
0900

MICROWAVE DETECTORS FOR THE MASSES

J. A. Landt, Los Alamos Scientific Laboratory, Los Alamos, NM 87545

Increasing public concern about safe microwave power levels and leakage from microwave ovens has resulted in the development of low cost, easily constructed, yet sensitive microwave detectors. A typical detector responds to a power density of ½ mW/cm^2 at 2450 MHz. These devices have also served as valuable troubleshooting aides in the development of a passive electronic identification system employing microwave energy (A. R. Koelle, et al, Proc. IEEE, 63, 1260-1261, 1975). The topic of this paper is the numerical analysis of several different types of these detectors. The electromagnetic calculations were performed using a computer program based on a time-domain electric-field integral equation. This computer program also contains a time domain nodal analysis of the circuitry attached to the antenna. This approach permits rapid evaluation of detector performance by performing the analysis of the circuitry coincidentally with the analysis of the antenna. The time stepping procedure used here is well suited for non-linear as well as linear circuit elements. Approximate solutions were obtained using lumped element antenna models in conjunction with a time domain circuit analysis program. These results were compared with the more accurate solutions discussed above. These comparisons show good agreement in some cases and very poor agreement in other cases. The quality of the agreement appears to depend on the detail of the lumped element antenna model. It was found that the required model detail is sometimes difficult to determine without comparison to the complete solution.

A1-3
1000 THE REACTIVE AND FAR-FIELD BOUNDARIES FOR ARBITRARY ANTENNAS DERIVED FROM THEIR QUALITY FACTOR

Arthur D. Yaghjian, National Bureau of Standards
Boulder, Colorado 80302

In measuring antennas on near-field ranges it is often necessary to estimate the distance from the antenna beyond which the reactive fields are insignificant, and the far-field distance beyond which the angular field distribution does not undergo significant changes. The near-field reactive region is commonly taken to extend a fraction of a wavelength λ from the antenna, and the far-field region is commonly taken to exist beyond the "Rayleigh distance" of $2D^2/\lambda$, where D is the maximum overall dimension of the antenna. Both criteria, however, are rules of thumb which do not apply in general. The criterion of the reactive region extending a fraction of a wavelength comes from the results for dipoles and other analytically solvable antennas, and from experimental evidence. The Rayleigh distance criterion is derived for electrically large antennas under the assumption of smoothly behaved current distributions. It is not difficult to find antennas (for example, electrically small or **super-gain** antennas) for which both criteria are invalid. Thus a more rigorous derivation is given for the boundaries defining the reactive and far-field regions of arbitrary antennas. The approach utilizes both the plane and spherical wave description of antennas to derive the reactive and far field distances in terms of the overall dimension and quality factor for an arbitrary antenna. For a low quality factor, the distances reduce to the usual fractional wavelength for the reactive region, and to a generalized Rayleigh distance which applies to antennas of arbitrary electrical size.

A1-4
1030 RAPID DETECTION OF CHARGE AND SURFACE CURRENT DISTRIBUTIONS ON RADIATING AND SCATTERING STRUCTURES: R. W. Burton and J. D. Selim, Department of Electrical Engineering, Naval Postgraduate School, Monterey, CA 93940

The detection and accurate measurement of charge and surface current distributions are slow, tedious, and expensive procedures. A technique for the rapid measurement of the magnitude of these distributions by an infrared scanner is presented. By utilizing the small but significant I^2R heating effect of antennas and scatterers with appropriate coatings, thermal distributions are measured. These distributions are quantized into various color levels by a Thermavision and are presented on a color TV-type monitor. Measurements of surface currents on flat-plate scatterers at various angles to an incident electromagnetic wave are described. Distributions of charge density on transmitting and scattering electrically thin monopoles and crossed dipoles are compared with comprehensive measurements and theory (see, for example, R. W. Burton and R. W. P. King, IEEE Trans. Antennas Propagat., AP-23, 657-664, 1975). Technological issues such as power levels required, surface coatings, and limitations are discussed.

A1-5
1100 THE MEASUREMENT OF THE SCATTERED FIELDS FROM A METAL LOOP AND A STRAIGHT WIRE PLACED ABOVE THE GROUND: L. C. Shen, Department of Electrical Engineering, University of Houston, Houston, TX 77004; and R. W. P. King, Rajeev Bansal, and H. M. Lee, Gordon McKay Laboratory, Harvard University, Cambridge, MA 02138

The experimental setup and techniques for measuring the fields scattered from a metal circular loop and a straight wire placed above the ground are described. Measured back-scattering, forward-scattering, and other bistatic scattering fields are presented as functions of loop size, incident angle, and distance above the ground. The frequency used in the experiment was 1.5 GHz. Resonant and nonresonant loops and straight wire a half-wavelength long were used. The experiment was performed on an open ground with the scatterer placed less than a third of a wavelength above the ground. The relative complex permittivity of the ground ranged from 5 + i0.6 to 13 + i2.2 or k_g/k_0 = 2.2 + i0.1 to 3.6 + i0.3, respectively.

Commission B Session 3

GUIDED WAVES

Wednesday A.M., 11 January ECCR 2-28

Chairman: Prof. K.F. Casey, Department of Electrical Engineering, Kansas State University, Manhattan, KS 66506

B3-1
0830 **Backscatter-Attenuation and Frequency Domain-Bandwidth Measurements in Optical Fibers**

B. Danielson, G. Day, and D. Franzen
Electromagnetics Division, 276.01
National Bureau of Standards
Boulder, Colorado 80302

Optical fiber attenuation has been measured by observing the Rayleigh backscatter from pulses propagating through a fiber. Backscatter returns give the attenuation as a function of length in a non-destructive manner. We have implemented this technique using polarization selection rather than tapered couplers or gated photomultipliers. (Barnoski, M., Applied Optics, 15 p. 2112; Personick, S., B.S.T.J., 56 p. 355.) Backscatter information has been obtained at various wavelengths using switched, cw sources as well as a pulsed, first positive N_2 laser. A comparison is given between attenuation measured by backscatter and by the more conventional method of cutting the fiber. Results will also be presented on attenuation losses induced by fiber bends which are readily observed in backscatter returns.

Optical fiber bandwidth has been measured directly in the frequency domain. We have developed $LiTaO_3$ electro-optic modulators which allow for the sine-wave modulation of light to 1 GHz. The present system can sweep from 1 MHz to 1 GHz. The response of an optical fiber to the above range of modulation frequencies will be given.

B3-2 0850 FUNDAMENTAL MODES OF DIELECTRIC FIBERS OF ARBITRARY CROSS SECTION:

Edward F. Kuester, Electromagnetics Laboratory, Department of Electrical Engineering, University of Colorado, Boulder, CO 80309

Open dielectric waveguides of many different cross-sectional shapes have been fabricated or proposed for use in optical communications. However, only those with circular boundaries can be analyzed in closed form, and others which are of interest either because of desirable propagation properties or as a result of particular fabrication techniques must be analyzed numerically or by analytical approximation.

A technique is presented which utilizes a variational formulation of an integral equation over the waveguide cross-section. For fundamental modes, the electric fields in the cross-section can be approximated very simply as either constant, or more accurately by a polynomial of second degree in the cross-sectional coordinates. If the constant field approximation is used, the variational expression yields a closed-form approximate eigenvalue equation for the propagation constants of the fundamental modes. The transcendental functions entering into this equation can be expressed as convergent series in the ratio of the rod diameter to the penetration depth of the mode into the outer medium (itself a known function of the unknown propagation constant). The coefficients of these series are dimensionless and depend only on the shape of the rod, and not its diameter or any of the other parameters which enter into the dispersion equation. Thus in contrast to other integral equation methods, numerical integrations over the cross-section need only be done once for a particular shape of guide, and the results stored as coefficients to be used for generating dispersion curves as desired. Not only does the present method involve a minimum of numerical integration and manipulation of large matrices, but it is actually more accurate the closer we come to cutoff, where most approaches breakdown.

Results will be presented for several guide shapes for which comparisons are available. Also recovered is a general formula giving the analytical behavior of the propagation constants for fundamental modes on guides of arbitrary cross-section near cutoff.

B3-3
0910

EFFECTIVE DIELECTRIC PARAMETERS FOR ANALYSIS OF QUASI-SEPARABLE WAVEGUIDES

R. Menendez, R. Mittra, P. Yang, N. Deo
Electromagnetics Laboratory, University of Illinois, Urbana, Illinois 61801

The basic difficulty in obtaining the propagation characteristics of dielectric waveguides lies in dealing with non-separable structures. Since a fully rigorous solution of Maxwell's equations for such geometries is time-consuming, a reliable approximate method is desirable. Simple rectangular rod guides have been analyzed (E.A.J.Marcatili, Bell Syst. Tech. J., 48, 2071-2102, 1969) by tacitly assuming the separability of the solutions in the two transverse dimensions. The solutions of the two uncoupled slab dielectric guides are then combined to yield an approximate propagation constant for the rod guide. Results from this technique can be quite satisfactory within certain limits. A more general approach, which couples the two slab problems, and can handle more challenging geometries, centers around the concept of an effective dielectric permittivity (W. McLevige, et. al., IEEE Trans. Microwave Theory Tech., 23, 787-794, 1975). The present authors find, however, that this approach must be further generalized to correctly incorporate polarization effects. We show that two effective dielectric parameters are necessary: an effective permittivity and an effective permeability. Depending upon the orientation of the dominent E and H vectors, it is proper to use either the effective permittivity or the effective permeability to couple the two slab problems. This approach allows the vector nature of the fields to be incorporated in the solutions. When applied to geometries which are separable, this approach reduces to the exact solution. A variety of different dielectric waveguide configurations, e.g., simple rod, inverted strip, and strip-loaded insular guides have been analyzed by this technique, and the results compared with measured data. Results obtained by coupling the two transverse solutions via either effective parameter offer an improvement over the simple uncoupled approach. Furthermore, comparing the solutions obtained from the two effective parameters provides a simple test of the reliability of the overall solution. Effective dielectric parameters offer a simple approximate method of obtaining the propagation characteristics of dielectric guiding structures, and, as such, can be useful tools in the design of more complicated integrated devices such as directional filters, couplers, etc.

B3-4
0930

ANALYTICAL THEORY OF DISPERSION IN MICROSTRIP:

David C. Chang and Edward F. Kuester
Electromagnetics Laboratory, Department of Electrical Engineering, University of Colorado, Boulder, CO 80309

Microstrip waveguiding structures have assumed an increasingly important role in the design of communication systems with the rapid advances in microwave integrated circuit technology. Although many numerical and experimental investigations on striplines have been carried out, a basic, comprehensive understanding of the underlying physical mechanisms which influence the behavior of the fundamental mode of such a structure still seems to be lacking. This is true in particular as regards the frequency dependence of the propagation constant of the mode. It is the aim of this paper to clarify the various processes responsible for this dispersion which have only been embedded implicitly in the results of previous treatments.

As is well known, at very low frequencies the propagation constant of the fundamental or quasi-TEM mode can be obtained from the values L and C of inductance and capacitance per unit length for the static problem. When normalized to the propagation constant of free space, we designate this propagation constant as α_s. We investigate the special case of a narrow microstrip (strip width less than substrate thickness) and obtain an approximate dispersion equation for this case in closed form. For zero frequency, the static value α_s is recovered. As frequency increases, correction terms of two kinds appear in the equation. The first kind is a straightforward one essentially reflecting the frequency dependence of the line parameters L and C. The other correction is intimately related to the existence of a TM_0 surface wave which can propagate in any direction along the slab in the absence of the strip. Ordinarily, this term in the dispersion equation will be small, but when the propagation constant α of the stripline mode comes close to that of the surface wave, α_p, it can become the largest term in the dispersion equation, because of the inverse square root nature of this term.

If α_s is sufficiently large (which will be the case for large enough substrate permittivity), α_p (which must start at the value 1 for zero frequency) will not come close enough to α to influence it until very high frequencies. On the other hand, if α_s is close to 1 (i.e., the substrate permittivity is close to that of the air), then most of the dispersion will be due to the influence of the TM_0 surface wave, and significant spreading of the fields along the substrate will occur. This is in contrast to the typical picture of the quasi-TEM mode, and can have serious implications for the tendency of the mode to radiate at irregularities in the line.

B3-5
1020 ON THE SPECTRAL DOMAIN FORMULATION FOR MICROSTRIP LINE STRUCTURE: Tatsuo Itoh, Department of Electrical Engineering, University of Kentucky, Lexington, KY 40506

Microstrip lines and other similar printed circuit structures have been in use for microwave and millimeter-wave integrated circuits. Traditional methods for analyzing such structures are based on the quasi-TEM theory in which the dominant mode is assumed to be a slight perturbation of the well-known TEM field (H.E. Steinhelfer, IEEE Trans., MTT-16, 439-444, 1968). Full-wave analyses have also been published by a number of workers (T. Itoh and R. Mittra, IEEE Trans., MTT-21, 496-498, 1973). Recently, in their work on the wire-above-ground problem, Kuester and Chang pointed out potential importance of surface waves in microstrip-type geometry (1977 International Microwave Symposium).
This paper first reconfirms that the spectral domain technique results in the complete full-wave solution of microstrip problems. We show graphically the relation of surface waves to the quasi-TEM solution. It is then pointed out that a number of quantities of interest associated with microstrip junctions, such as the surface wave excitation and Q of microstrip resonators, can be obtained from the spectral domain formulation.

B3-6
1040

A FREQUENCY DEPENDENT DYADIC GREEN'S FUNCTION IN THE SPACE DOMAIN FOR MICROSTRIP STRUCTURES: Y.L. Chow and I.N. El-Behery, Department of Electrical Engineering, University of Waterloo, Waterloo, Ontario, N2L 3G1, Canada

A spatial dyadic Green's function $\overline{\overline{G}}$ can be used in the integral equation

$$\vec{E}_{tan}(\vec{r}) = \int_s \overline{\overline{G}}(\vec{r} - \vec{r})\, \vec{J}(\vec{r})\, dS$$

to solve for the current $\vec{J}$ on a conducting surface S. Frequency dependent solutions of such type have been difficult for the microstrip structures as their dyadic Green's function in the space domain was not available. This paper gives an approach that enables us to compute efficiently the desired Green's function in both 2-D and 3-D. The approach is to selectively replace the static charge images of Silvester's Green's function (Proc. IEE, 115, 43-48, 1968) by oscillating charges and current sources. The selection is done in such a way that the tangential boundary conditions and the wave equations in the dielectric and the free spaces are satisfied over the microstrip structure. Within the required area, the resulted dyadic Green's function in 2-D is found to check very well with that Fourier-transformed from the dyadic Green's function in the spectral domain by Denlinger (IEEE-MTT, 18, 30-38, 1971). An example of the Green's function element G_{xx} is given below.

The computing time needed for each element of the dyadic Green's function is short, not much longer than that needed for the static Green's function of Silvester. As the integral equation involves only tangential components of $\vec{E}$ and $\vec{J}$, the dyadic Green's function is a 2 x 2 matrix. Only three elements in the matrix are needed to be computed as it can be proved that the cross-elements are equal, both in 2-D and 3-D. The proof, the computing time, the details of the approach and a numerical example in calculating the propagation constant of a microstrip line are presented in the paper.

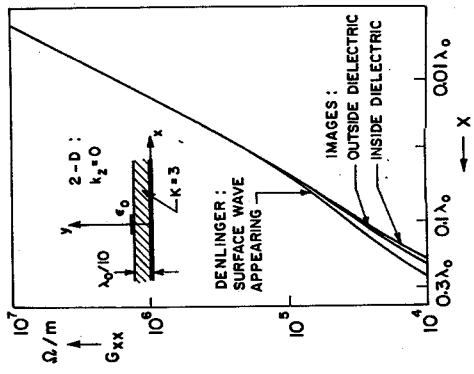

B3-7
1100

CHARACTERISTIC IMPEDANCE OF A RECTANGULAR TRANSMISSION LINE WITH OFFSET INNER CONDUCTOR:

J.C. Tippet and D.C. Chang, Electromagnetics Laboratory, Department of Electrical Engineering, University of Colorado, Boulder, CO 80309

The cross-section of the rectangular transmission line analyzed in this paper is shown below. The zero thickness inner conductor is arbitrarily situated but is parallel to the x-axis. Both conductors are perfectly conducting, and the medium between the two conductors is a homogeneous dielectric.

This type of transmission line has found use in EMI measurement systems as a transducer for coupling EM energy from a device under test into the TEM mode of the transmission line. The inner conductor is often offset in order to accommodate larger test devices. The transmission line usually connects through a tapered section to ordinary coax. Thus, in order to minimize the impedance mismatch, the transmission line must be designed to have a nominal characteristic impedance. This provided the motivation for our analysis.

This problem is formulated using an integral equation--Green's function formulation. The kernel of the resulting integral equation is split into its singular and nonsingular parts. The nonsingular part is then expanded in terms of Chebyshev polynomials, and the integral equation is inverted using the singular integral equation technique.

The solution is given in terms of complete elliptic integrals. An approximation which involves keeping only a finite number of terms in the expansion for the nonsingular part of the kernel results in a simple yet very accurate formula for the capacitance. The higher-order terms decay as $e^{-m\pi(b-h)/a}$ so that only a few of them need be retained. Keeping only one term provides a surprisingly accurate result for a wide range of practical geometries (error $<.5\%$ for $b/a \geq .5$, $h = 0$, $w_1/w_2 = 1$).

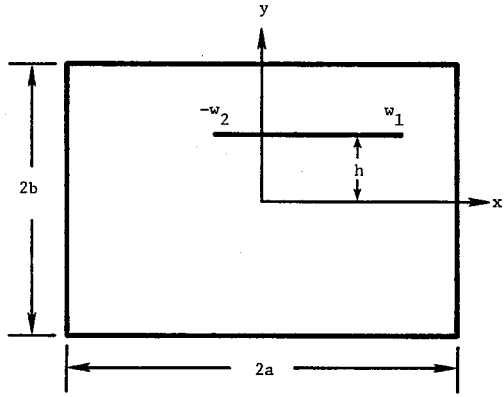

B3-8
1120 LEAKY MODES IN FINITE-WIDTH, PARALLEL-PLATE WAVEGUIDE:

A. Rushdi, R. Menendez, R. Mittra and S. W. Lee
Electromagnetics Laboratory, University of Illinois, Urbana, Illinois 61801

The parallel-plate, finite-width waveguide is often used as an EMP simulator [Baum, C.E., SS Note 21, June 1966]. The fields excited in such a waveguide can be expressed as a superposition of the TEM mode, higher-order TE and TM leaky modes, and a continuous spectrum. In this paper, we only concern ourselves with the problem of computing the leaky modes in finite-width waveguides, since when added to the TEM mode, they often constitute the dominant portion of the field launched into the region between the plates. The wave vector for the n^{th} mode may be written as $\bar{k} = k_{xn}\,\hat{x} + (n\pi/2h)\,\hat{y} + k_z\,\hat{z}$, where k_z and k_{xn} are both complex for leaky modes. The wave numbers k_{xn} and k_z belong to the third and first quadrants respectively, so that the fields decay as $z \to \infty$ but grow exponentially in the x-direction, a characteristic that is typical of leaky modes. Considering an EM wave incident from the side opening at $x = 0$, the reflection coefficient S_{nm} is obtained with the aid of an auxiliary two-dimensional problem (Mittra and Lee, Analytical Techniques in the Theory of Guided Waves, McMillan, 1971), under the approximation that the interaction between the two openings is negligible. The transverse resonance condition leads to the vector eigenvalue equation $([R] - [I]\,\bar{A}) = \bar{0}$, where $[I]$ is the identity matrix, $[R] = [R_{nm}] = [S_{nm} \exp(i(k_{xn}+k_{xm})w)]$ and $\bar{A}$ is the mode vector. The paper discusses some search procedures for extracting the complex roots k_z of the corresponding determinantal equation and presents some representative results. Next, the eigenvalue equation is solved for the mode vector $\bar{A}$ and the corresponding transverse field distributions are plotted for several modes. Special emphasis is given to the TE_{z0} modes which dominate the other leaky modes when the plate width is large.

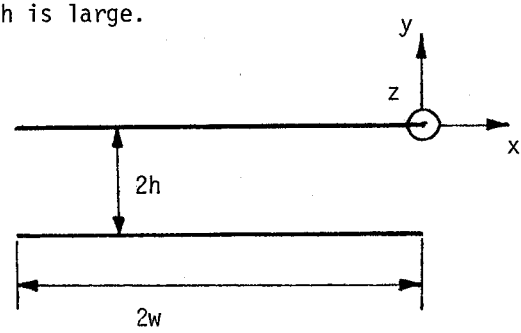

Geometry of the Problem

B3-9
1140

SOURCE EXCITATION OF AN OPEN, PARALLEL-PLATE WAVEGUIDE:

V. Krichevsky and R. Mittra
Electrical Engineering, University of Illinois,
Urbana, Illinois 61801 U.S.A.

The parallel-plate simulator is an important device for EMP testing and has been investigated by a number of authors. However, all of the previous analyses of this open waveguide problem have been limited to the investigation of leaky modes, and the source excitation problem has not been discussed in the literature. In this paper, we consider the problem of an open, finite-width, parallel-plate waveguide which is excited by a y-directed current source (see Fig. 1). The source current is assumed to be confined at $x=x_0$, have a $\sin(n\pi\, y/2H)$, or $\cos(n\pi\, y/2H)$ variation in the y-direction and an $\exp(i\beta z)$ behavior along the longitudinal (z) direction. Such an excitation can be interpreted as one spectral component of a transversely confined source, and the solution to the longitudinally confined source problem can be subsequently constructed by an appropriate superposition of the spectral solutions derived in the paper. Using a vector potential approach and a Fourier transform analysis, we have reduced the original problem to that of solving two coupled integral equations, which are resolved via the Wiener-Hopf technique.

We examine the important question of the excitation or the non-excitation of the TEM mode and derive the condition of complex resonance in open, finite-width waveguides. The resonance condition is given by $T = R \cdot f \exp(i2kL) = \pm 1$, where R is the wave reflection coefficient at the open end of the waveguide and $f = 1 + \exp(-i\,\pi/4)\,\pi^{-1/2} Hk/\sqrt{kL}$. For $(Hk)^2\pi^{-1} \lesssim (kL)^{-1} \ll 1$, the function f can be approximately replaced by unity, leading to a simplified resonance condition which then becomes identical to the leaky mode eigenvalue equation obtained by previous authors.

The complex resonances may be identified with the leaky modes in the guide that are potentially useful for the representation of source-excited fields in open waveguides. We further show that the resonance condition given above is valid strictly under the condition that only the TEM-mode can propagate in the guide and it becomes necessary to deal with a more general matrix equation for the case where more than one propagating mode can be supported

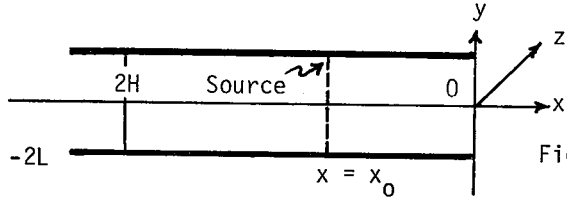

Fig. 1

Commission E Session 2

THE INTERFERENCE ENVIRONMENT AND EMC

Wednesday A.M., 11 January ECCR 0-38

Chairman: A.D. Spaulding, Office of Telecommunications, Institute for Telecommunication Sciences, Boulder, CO 80302

E2-1
0830 HIGHLIGHTS OF THE 2ND SYMPOSIUM AND TECHNICAL EXHIBITION ON ELECTROMAGNETIC COMPATIBILITY, MONTREUX, SWITZERLAND (28-30 JUNE 1977): G.H. Hagn, SRI International (formerly Stanford Research Institute), 1611 N. Kent, Arlington, VA 22209

Approximately 375 scientists and engineers from over 20 countries attended the 21 technical sessions and 4 workshops of this international meeting on Electromagnetic Compatibility (EMC) cosponsored by URSI. This paper will summarize the technical highlights. An excellent 576-page symposium proceedings, "Electromagnetic Compatibility 1977," is available from the IEEE as 77CH 1224-5EMC.

E2-2
0855 AN AUTOMATED TECHNIQUE FOR CALCULATING INTERFERENCE FROM AIRBORNE TRANSMITTERS TO TERRESTRIAL RECEIVERS: E.J. Haakinson, Office of Telecommunications, Institute for Telecommunication Sciences, Boulder, CO 80302

An automated technique, embodied in a computer program, has been developed with the ability to automatically compute and plot interference contours around existing microwave systems when new airborne systems are proposed or planned. The frequency manager or spectrum analyst can utilize the program technique to vary the airborne system parameters and examine the size and influence of the interference contours on the eletromagnetic environment.
The computer program implements a procedure for determining the level of interference generated in a terrestrial microwave terminal (or system of microwave terminals) by an airborne telecommunication system. The output of this procedure is a set of contours defining those aircraft positions which produce a constant signal-to-interference (S/I) ratio to the terrestrial systems being analyzed. The S/I contours are plotted on a map with U.S. state boundaries. The user supplies the basic aircraft data while the terrestrial receiver(s) data are obtained from a computer accessible data base.
Examples of the techniques output and a recent application will be shown and discussed.

E2-3
0920

ORBIT UTILIZATION AND THE "SMALL" EARTH STATION ANTENNA: William A. Kissick, Spectrum Utilization Division, Institute for Telecommunication Sciences, Office of Telecommunications, Boulder, CO 80302

The effects of some different earth station antenna patterns on the spacing of satellites in the geostationary orbit are calculated using the methods of Appendix 29 to the International (ITU) Radio Regulations. Both simple analytic and measured antenna patterns are used to represent the earth terminals. The problem of a standard of reference is discussed. The orbital spacing required between the satellites of two co-channel systems is determined for several scenerios of earth station locations. The results indicate that spacings two to three times greater are required when a "small" earth terminal antenna is employed in one of the systems.

E2-4
0945

AN IMPROVED APPROACH TO MAN-MADE-NOISE MEASUREMENT TECHNIQUES:
F. H. Tabor, IIT Research Institute, ECAC, North Severn, Annapolis, MD 21402

Past analyses of receiver noise responses have revealed a non-predictable response to certain kinds of noise. It was suspected that certain types of noise were not susceptible to classification as either *white Gaussian* or *impulsive*, but that some intermediate classification or range of classifications was called for. An Exploratory Research task was undertaken to develop other-than-traditional techniques for measuring man-made noise, and to apply those techniques in the measurement of noise radiated by several commonly found man-made sources.

It was found that sources whose noise spectra have impulsive origins do indeed result in receiver behavior that is sometimes uncharacteristic of "impulsive" noise. The behavior changes at or near a bandwidth whose frequency is equal to the impulse repetition frequency.

The measurement technique developed consists of displaying the noise power spectra in incremented bandwidths on a spectrum analyzer. Comparison of the change in power level to the change in bandwidth results in a mathematical model useful in predicting response at any receiver bandwidth. Ten different sources were measured, and the bandwidth factors have been included in this paper.

E2-5
1035 LIGHTNING RETURN STROKE AND ITS RADIO EMISSION: J.B. Smyth and D.C. Smyth, Smyth Research Associates, San Diego, CA 92123

An exact solution of Maxwell's equations is used to describe the return stroke and the associated radio emission (J.B. Smyth and D.C. Smyth, Radio Science, 11, 977-984, 1976). When the leader develops to the earth's surface the associated electromagnetic field propagating down the arc filament produces a reflected wave which is guided upward along the conducting channel. The intensity of the electric field of the reflected wave is approximately equal to the intensity of the electric field of the incident wave but of opposite direction. The solution shows how electric displacement is transformed into electrical conduction current and transferred between the atmosphere and the earth. It is further shown that the source of the radio emissions is this transformation.

E2-6
1100

NOISE POWER DUE TO DIGITAL ERRORS IN A PCM TELEPHONE CHANNEL:

Hiroshi Akima, Institute for Telecommunication Sciences, Office of Telecommunications, U.S. Department of Commerce, 325 Broadway, Boulder, CO 80302

Errors in digital transmission in a pulse-code-modulation (PCM) telephone channel result in additional noise power at the receiver output. The noise power in a telephone channel is usually represented in terms of psophometrically weighted noise power at a zero relative level point, while the quality of a digital signal is represented in terms of bit error rate (BER). In this paper, the relation between the noise power and the BER is calculated for three types of assumed signal distributions (i.e., Laplacian, sinusoidal, and uniform) for a wide range of signal levels, for both the A-law and μ-law compandings with several companding parameter values for each, for the 7-bit and 8-bit quantizings, and for two coding schemes (i.e., the straightforward coding and the absolute-value coding with a sign bit).

When each bit error occurs independently and the BER is small (say, 10^{-3} or less), the noise power is proportional to the BER. The noise power is relatively insensitive to the number of bits for a sample in quantizing, to the type of the signal distribution, and to the companding law. The noise power varies widely depending on the signal level, the companding parameter value, and the coding scheme, but this is mostly in the range of low signal levels (say, -30 dB relative to the saturation level or lower).

The calculated results indicate that, in a practical range of the signal level and for the second coding scheme (i.e., the absolute-value coding with a sign bit), the noise power does not exceed 10 000 and 50 000 pW0p if the BER equals 10^{-5} and 5×10^{-5}, respectively, where pW stands for picowatt ($= 10^{-12}$ W), 0 for a zero relative level point, and the last p for psophometrically weighted. Since these noise power values are used by the CCIR in its Recommendation 353-2 for specifying allowable noise power for systems in the fixed satellite service for frequency division multiplex telephony, it is recommended that the corresponding BER values be adopted as allowable BER's for systems in the fixed satellite service for PCM telephony.

E2-7
1125

MICROPROCESSORS AND EM SPECTRUM RECORDING:
Tom Harr, EMCAD Group, Institute for Telecommunication Sciences, Office of Telecommunications, Department of Commerce, Boulder, CO 80302

Microprocessors (sometines referred to as miniature computers on a chip) and their applications are being found more and more in everyday usage, so it is only logical that they will be used for the control of Electromagnetic Spectrum monitoring and recording. In the application described in this paper the performance of a routine, manual, time consuming (and sometimes inaccurate) method of receiving and recording over-the-air EM signals is accomplished. These signals are then analyzed for their spectral characteristics or they can be analyzed for propagation loss purposes.

A microprocessor device functions as the controlling element for some commonly used RF test equipment, and also controls the recording data on digital magnetic tape as well as performing limited data analysis. The measurement system itself consists of four (or three) small instruments. This small size and portability of the system is one of its most useful features. For spectrum measurements, the system consists of a spectrum analyzer, a three axis display unit, a digital tape recorder and the control unit. For propagation loss or signal level measurements a field intensity meter is substituted for the spectrum analyzer and the three axis display unit.

The system operation and system performance features will be discussed in this talk. Two actual measurement situations (which were conducted by the U.S. Army Communications Electronics-Engineering Installation Agency) will be discussed, and some limited results will be presented.

E2-8
1150

URBAN CONGESTION AND SOLAR CYCLE EFFECTS ON CB RADIO RANGE

Leslie A. Berry, U.S. Department of Commerce, Office of Telecommunications, Institute for Telecommunication Sciences, Boulder, CO 80302

The proliferation of Citizen's Band radio has occurred during a period of low solar activity when sky-wave propagation of 27 MHz signals was unlikely. Lucas (New York Times, July 11, 1976) pointed out that ionospherically propagated interference might significantly decrease the local range of CB radios near the peak of a solar cycle. On the other hand, increasing local congestion has already decreased this range in urban areas. The combined effects of noise, local co-channel interference, and sky-wave interference on radio range have been computed as functions of solar activity, fraction of the population transmitting on a channel, and area population for reasonable statistical distributions of transmitter and receiver characteristics. The model and the input data used in the calculation will be described.

The conclusions are the following: If the ionospheric critical frequency, foF2, is about the same during the next solar cycle as it has been during the four cycles it has been measured; and if CB Radio use remains at its current levels or increases; then for about eight daylight hours per day for eight months of each of the three years near the peak of the cycle, the operational range of CB users in cities with about 100,000 population or less will be reduced by more than half by skip interference. The range of users in sparsely populated rural areas may be only one-sixth of their present range. About one-third of the population of the U.S. lives in such small cities and rural areas. In metropolitan areas with one million or more residents, local interference limits the operational range of CB so much that increased sky-wave interference will probably not be significant. About half of the population of the U.S. lives in such cities.

Commission F Session 3

RADIO OCEANOGRAPHY

Wednesday A.M., 11 January ECCR 0-30

Chairman: W.C. Keller, Naval Research Laboratory, Washington, D.C. 20375

F3-1
0830

EFFECT OF LARGE-SCALE OCEAN SURFACE FEATURES ON RADAR ALTIMETER RETURNS:
Leonard Fedor, Wave Propagation Laboratory, National Oceanic Atmospheric Administration, Boulder, CO 80302

Ocean surface features on the order of several kilometers in size are shown to have pronounced effects on the detected signals of a satellite-borne radar altimeter. Examination of data obtained from the GEOS-3 radar altimeter suggests the possibility that 1) the radar returns exhibit the effects of focusing by large-scale features, and 2) plots of the estimated sea-surface height indicates a preference for ocean wavelength scale sizes on the order of 4 km – the nominal size of the radar footprint. A modified equation for the observed radar cross section is given which verifies that the above observations are possible. A discussion is given on its resultant effects on estimates of the sea-surface height and on estimates of significant waveheight.

F3-2
0855

MEASUREMENT OF OCEAN WAVEHEIGHTS USING GEOS-3 ALTIMETER:
C. L. Rufenach, NOAA Environmental Research Laboratories, Wave Propagation Laboratory, Boulder, CO 80302, and W. R. Alpers, Institute of Geophysics, University of Hamburg and Max-Planck-Institute of Meteorology, Hamburg, Germany

Radar Altimeter signals from the low-orbiting satellite GEOS-3 were analyzed for two selected orbits when high seas were known to exist. These high-sea conditions are associated with: (1) the Hurricane "Caroline" in the Gulf of Mexico, and (2) a North Atlantic storm.
The measured values of significant wave height $H_{1/3}$, are in reasonable agreement with surface measurements provided the altimeter data are properly edited. Analysis of the North Atlantic storm show that standard deviation in $H_{1/3}$, is 0.6 m or less and the waveheight is overestimated for $H_{1/3}$, $\lesssim$ 4 m. Furthermore, statistical analysis of the average pulse slope implies random fluctuations in $H_{1/3}$ such that 75% of the values are within $\pm$ 1 m for a spatial resolution of 70 km.

F3-3
0920

THE WAVE MODULATION DOPPLER SPECTROMETER

D.E. Weissman, Dept. of Engineering and Computer Sciences, Hofstra University Hempstead, New York 11550

J.W. Johnson, N.A.S.A. Langley Research Center, Hampton, Virginia 23665

A measurement technique has been developed that can determine the dominant water wavelength from distinct features that are present in the backscatter signal spectrum when a microwave radar is operated in a scatterometer-type configuration. These features are associated with variations in the microwave reflectivity (incoherent) along the water waves, and so can be used to infer the dominant wavelength of the surface spectrum. This effect is caused by the relative motion between the water waves and the nadir-looking radar, and the fact that while the instantaneous doppler frequency at the receiver returned by any elementary group of scatterers on a water wave is monotonically changing, the difference in the doppler frequency between any two scatterers stays approximately constant as these waves travel through the narrow radar beam. Therefore periodic variations along the surface of the cross section/unit area lead to periodic enhancements in the power spectral density of the envelope fluctuations in the returned signal.

A laboratory radar (microwave, CW) illuminated several wavelengths of wind generated waves in a wavetank. The envelope fluctuations of the backscattered signal was subjected to a time series analysis with the power spectral density and autocorrelation function being computed. A very distinctive spike is seen in the measured autocorrelation as a result of the periodic radar cross section variations within the fan beam illumination.

A theoretical formulation based on a simple surface model interprets the most dominant features in the autocorrelation, and uses the value of delay at which the spike occurs to infer a value for the surface wavelength that is in excellent agreement with known surface conditions.

Theoretical and measured results will be presented which demonstrate the dependence of the autocorrelation function on the surface and the radar system parameters such as altitude and electromagnetic wavelength.

F3-4
0945

MULTI-FREQUENCY HF-RADAR SEA SCATTER MEASUREMENTS

D.B. Trizna, John C. Moore,
U.S. Naval Research Laboratory
Washington, D.C. 20375

Simultaneous sea clutter measurements at ten radar frequencies and ten look angles covering 80 degrees of azimuth were made using an HF radar on San Clemente Island, CA. These data were collected in conjunction with several other remote sensing instruments, including those to be incorporated in SEASAT, in a time frame from Feb. 15 to Mar. 31, 1977. Results of a preliminary analysis of some of the HF data are reported upon. Varions types of sea conditions were encountered, including apparent narrow band swell (in frequency and direction), broad band swell from a storm in the North Pacific, and local wind driven waves. Calibrated measurements of the first order Bragg lines in the Doppler spectrum, versus radar frequency and look angle, were used to infer estimates of the directional sea surface wave spectrum.

F3-5
1035 CORRELATION OF GEOS-3 MEASURED $\sigma^\circ(0^\circ)$ VALUES WITH HINDCAST SURFACE WIND SPEED ESTIMATES

G. S. Brown, Applied Science Associates, 105 East Chatham, Apex, NC 27502

There is, within the microwave remote sensing community, an intense desire to determine how the surface scattering cross section per unit area, σ°, varies with ocean surface conditions. This desire stems from the fact that some experimental evidence tends to indicate a unique relationship between σ° and surface wind speed and, therefore, that a measurement of σ° could determine the surface wind. Unfortunately, there are other data which indicate that σ° cannot be used to infer wind speed to any degree of accuracy. In neither case are the data sets extensive enough to give strong credibility to either hypothesis. The GEOS-3 radar altimeter has been operating for over two years now and has obtained measurements of $\sigma^\circ(0^\circ)$ for many different surface conditions. In the case of GEOS-3, the only "surface truth" data compatible with the $\sigma^\circ(0^\circ)$ data base are the hindcast estimates of surface wind speed produced by the Special Projects Branch of the National Weather Surface of Suitland, Maryland. This paper presents preliminary results of attempts to correlate $\sigma^\circ(0^\circ)$ and the SPB estimates of surface wind speed. First of all, there is a great deal of scatter in the data which cannot be isolated to either a nonunique relation between $\sigma^\circ(0^\circ)$ and wind speed or incorrect wind speed estimates. However, there is a trend in the preliminary data which tends to indicate that the $\sigma^\circ(0^\circ)$-wind speed relation is swell dependent. For surface winds in excess of 7m/s, a surface with swell tends to give rise to a larger $\sigma^\circ(0^\circ)$, than a surface with no swell, by roughly 2 dB. If a logarithmic relation between wind speed and $\sigma^\circ(0^\circ)$ is assumed, and the unknown parameters are determined by a least squares fit to the wind speed vs. $\sigma^\circ(0^\circ)$ data, very good agreement with the Cox and Munk mean square slope measurements and a Gaussian slope density is obtained for the case of swell. For no swell, the least squares fit produces good agreement with Wu's (J. Wu, J. Geophy. Res., 82, 1359-1362, 1977) wave tank measurements of mean square slope in the case of no preexisting waves on the surface. A discussion of how a radar altimeter might be used to determine the presence of swell will also be presented.

F3-6
1100 MEASUREMENT OF OCEAN ANISOTROPIC RADAR SCATTERING CHARACTERISTICS AT K_u-BAND: W.L. Jones and L.C. Schroeder, Langley Research Center, National Aeronautics and Space Administration, Hampton, VA 23665; J.L. Mitchell, Vought Aerospace Corp., Hampton, VA 23665

Radar backscatter signatures of the ocean have been measured at 13.9 GHz using an aircraft scatterometer (AAFE RADSCAT). During the experiment, a pencil beam antenna provided a conical scan of the ocean's surface thereby measuring the azimuthal scattering characteristic. The form of the characteristic is predominantly cosinusoidal second harmonic of radar azimuth relative to the sea surface wind direction, but there is also a significant third harmonic component which results from the upwind/downwind assymmetry. The strongest return is upwind with the crosswind observations being equal and a minimum. The degree of modulation, determined by the upwind to crosswind ratio, increases with incidence angle and decreases with windspeed.

Results are presented for two aircraft missions: North Sea (JONSWAP) Sept., 1975 and Atlantic Ocean Jan., 1976. The normalized radar cross section was measured for both vertical and horizontal polarizations at incidence angles of 20^{o}, 40^{o} and 65^{o} and over a range of windspeeds of 4 m/s to 20 m/s. These data extend previous results presented by the authors (W.L. Jones, L.C. Schroeder, and J.L. Mitchell, IEEE Trans. Antennas Propagat/IEEE J. Oceanic Eng., Jan. 1977).

F3-7
1125

OCEAN SURFACE ROUGHNESS AS DERIVED FROM MICROWAVE SUN GLITTER MEASUREMENTS:

C. T. Swift,† and H-J. C. Blume, NASA Langley Research Center, Hampton, VA 23665

A precision S-band radiometer was operationally developed by NASA in 1972 to demonstrate the capability of all-weather passive microwave sensors to remotely measure ocean temperature to within 1°K absolute. To this end, over 140 flight hours of data were collected utilizing the Wallops C-54 aircraft as a platform for the instrument. In the process of collecting this data base, several experiments were conducted to assess the effects of sunlight scattering from the ocean and into the receiver. As a by-product of this effort, data were collected as a function of sun elevation angle. Azimuthal angles were achieved by rolling the aircraft and banking to collect data over several multiples of 2π.

An analytical model was developed, and the results compare favorably with the experimental data. The analysis is extended to the SEASAT Scanning Multi-Channel Microwave Radiometer (SMMR) geometry, and working graphs are presented for the user to assess the degrading effects of the sun scatter. The ramifications of measuring roughness from the glitter pattern are also discussed.

† On leave at the NOAA Wave Propagation Laboratory, Boulder, CO 80302.

F3-8
1150

MICROWAVE RADIOMETER MEASUREMENTS OF SALINITY AND TEMPERATURE IN ESTUARIAL WATERS:

C. T. Swift,† H-J. C. Blume, B. M. Kendall, and J. C. Fedors, NASA Langley Research Center, Hampton, VA 23665

During a 3-1/2 hour period on August 24, 1976, the salinity and temperature of the lower Chesapeake Bay were inferred by passive microwave sensors installed on a NASA/WALLOPS C-54 aircraft. From these data, lines of constant salinity (isohalines) and temperature (isotherms) were developed. The chart of isohalines reveal the fundamental dynamics of the lower Bay. For example, the saline concentration reveals the effects of the Coriolis force and the mixing/circulation of fresh water into the Atlantic Ocean. The chart of isotherms was much less spectacular because of the relatively low thermal contrast characteristics of the Bay during later summer. Preliminary results were presented at the IVCRM in Hamburg, and the Proceedings are forthcoming. This paper "wraps-up" the project, focussing on quantitative comparisons with ground truth, the spatial variability of ground truth, and the user reaction to the remotely sensed data.

† On leave at the NOAA Wave Propagation Laboratory, Boulder, CO 80302

Commission G Session 2

IONOSPHERIC IRREGULARITIES AND DRIFTS-I

(In Memory of Wolfgang Pfister)

Wednesday A.M., 11 January ECCR 1-42

Chairman: Dr. Jules Aarons, PHP, AFGL,

Hanscom AFB, MA 01731

G2-1
0830 HISTORY AND CURRENT STATUS OF SCATTERING AND DIFFRACTION BY THE IONOSPHERE: S.A. Bowhill, Dept. of Electrical Engineering, Univ. of Illinois, Urbana, IL 61801

G2-2
0855 A DIFFRACTION APPROACH TO VHF SCINTILLATION.
M.L.Heron, Physics Department, James Cook University of North Queensland, Townsville, Australia. 4811

The relationship between irregularity structures and VHF scintillation remains enigmatic despite an increasing number of theoretical and experimental approaches. The work of Bowhill (J.Res. NBS 65D, 275, 1961) who used a thin irregularity layer with a Gaussian autocorrelation has been extended to a thick but weakly scattering layer by Booker (J.A.T.P. 37, 1089, 1975). Several people have pointed out that Gaussian statistics often do not describe the phenomena very well and a power law spectrum can be assumed in a model. (Rufenach, C.L., Radio Science, 10, 155, 1975). Another mechanism for producing amplitude fluctuations is that of diffraction about isolated dense irregularities (Heron, M.L. J.A.T.P., 38, 1027, 1976 and Davies,K. and Whitehead, D. J.A.T.P., 39, 383, 1977). A simple extension of these results suggests that an apparently random and extensive patch of scintillation could be caused by a few dense, strongly scattering irregularities. The questions of thick or thin screen, weak or strong scattering and those of the statistics remain without conclusive answers and this is probably due to the presence of all the various combinations at various times.
This paper contains a brief review showing some examples of the mechanisms mentioned above and then outlines a method of analysis of phase and amplitude records which has the potential of providing parameters of the scattering layer for each experimental record. The amplitude and phase data at the ground are treated as though they describe an aperture and the Fresnel-Kirchoff integration formula is applied to find the diffraction pattern at a range of altitudes. The calculation for the parameters of a thin screen model is to be illustrated.

G2-3
0920

A THEORETICAL MODEL FOR IONOSPHERIC SCINTILLATION CAUSED BY WEAK IRREGULARITIES OF IONIZATION DENSITY:

Henry G. Booker and Doris C. Miller,
SRI International, Menlo Park, CA 94025

A theory of ionospheric scintillation is developed on the basis of long isotropic field-aligned irregularities possessing an inverse power-law spectrum extending from an outer scale [wave length/(2 π)] linked to the scale-height of the atmosphere down to an inner scale of the order of the ionic gyroradius. Spectral indices p from 0 to 6 are considered mathematically, and from 1 to 4 numerically. For $p < 3$ it is important to take account not only of the outer scale but also of the inner scale if the spectrum is to represent a stated mean square fluctuation of ionization density. Frequencies from 100 Mhz to 10 Ghz are considered, particularly for equatorial regions.

Collapsing the entire plasma envelope to a single phase-changing screen is found to be unsatisfactory unless different heights are used for phase and amplitude scintillations, both heights differing from the height of maximum fluctuation in ionization density. Calculations are based on a distribution of phase-changing screens throughout the plasmasphere. Even disregarding traveling ionospheric disturbances, large phase fluctuations are encountered exceeding 100 radians at 100 Mhz under evening conditions, and exceeding 1 radian at 3 Ghz under presunrise conditions. For VHF transmission from a stationary satellite, saturated amplitude fluctuations can occur at an altitude of 1000 km even before the F region is encountered. But explanation of the observed large amplitude fluctuations at 4-6 Ghz requires strong fluctuations of ionization density near the maximum of the F region, leading to several primary rays of approximately equal importance joining the satellite to the earth terminal and consequently to multipath interference. In striking contrast is the necessity to keep ionization fluctuations well under 1% by day to avoid creating amplitude fluctuations that are too strong. Theoretical scintillation spectra are derived applicable for stationary satellites.

Ionospheric scintillation, spread F and traveling ionospheric disturbances are pictured as related phenomena driven by acoustic gravity waves in the neutral atmosphere.

G2-4
0945

A THEORETICAL MODEL FOR EQUATORIAL IONOSPHERIC SPREAD F ECHOES IN THE HF AND VHF BANDS:

Henry G. Booker, University of California, San Diego, La Jolla, CA 92093
Jerry A. Ferguson, Naval Ocean Systems Center, San Diego, CA 92152

A theory of spread F echoes is presented particularly suitable for equatorial regions, especially under presunrise conditions. In the HF band the theory is based on a spectrum of irregularities of ionization density extending from an outer scale [wavelength/(2 π)] linked to the scale-height of the atmosphere down to an inner scale of the order of the ionic gyroradius. The irregularities are assumed to be aligned along the earth's magnetic field and to have lengths of the order of the outer scale. Inverse power-law spectral indices from 0 to 6 are considered mathematically, and from 1 to 4 numerically. Spectral indices between 1 and 3 fit observations of presunrise equatorial spread F satisfactorily. An essential feature of the fit arises from the assumed cut-off in the turbulence spectrum at the ionic gyroradius. It is also assumed, however, that a weak extension of the spectrum, probably in the form of an angular spectrum of compressional plasma waves, exists from the ionic gyroradius down to the electronic gyroradius, and on this basis a theory is presented of spread F echoes in the VHF band. Strong spread F is pictured as arising primarily from an instability, not in the ionospheric plasma, but in the neutral atmosphere; the instability is associated with acoustic gravity waves.

G2-5
1010 ON THE CO-EXISTENCE OF KM- AND M- SIZED IRREGULARITIES IN THE NIGHTTIME EQUATORIAL IONOSPHERE:

Santimay Basu, Emmanuel College, Boston, MA 02115; Sunanda Basu and Jules Aarons, Air Force Geophysics Laboratory, Hanscom AFB, MA 01731; J.P. McClure, University of Texas at Dallas, Richardson, Texas 74080; and M.D. Cousins, Stanford Research Institute, Menlo Park, CA 94025

Nighttime multifrequency scintillation and 50 MHz radar backscatter observations simultaneously performed over a nearly common ionospheric volume at the dip equator in Peru during March, 1977 were used to study the relationship between the large scale irregularities ($\sim$ 0.1 to 1 km) giving rise to scintillations and small scale irregularities (3m) causing 50 MHz backscatter. It is shown that during the generation phase of equatorial irregularities in the late evening hours, the km - and m - sized irregularities co-exist whereas in the later phase, approximately an hour after the onset, the m - sized irregularities decay but the large scale ones continue to retain their high spectral intensities. During the generation phase it is also possible to have a dramatic increase in scintillations when the elevation angle to the satellite happens to coincide with the tilt of the plume structure on backscatter maps. Using multistation scintillation observations from a host of geostationary satellites as well as from the Wideband satellite, it is shown that eastward drifting irregularity structures detected around midnight cause intense scintillations at UHF as well as moderate scintillations at L-band but generally fail to give rise to appreciable backscatter. Thus, contrary to expectations, it is possible to have L-band scintillations without any plume structure on backscatter maps. This indicates that during the later phase a cut-off of the spectral intensity probably occurs at wavelengths shorter than 100 m.

G2-6 AMPLITUDE AND PHASE SCINTILLATION AT HIGH LATITUDES
1035 C. L. Rino, Radio Physics Laboratory
SRI International, Menlo Park, California 94025

Amplitude and phase scintillation measurements have been routinely made at Poker Flat, Alaska (near Fairbanks) since May 1976 using the Wideband Satellite (P76-5) which is in a 1000-km sun-synchronous circular orbit inclined at 100^{o}. Phase-coherent beacon signals are transmitted at S-band, L-band, UHF, and VHF, with the S-band signal being used in the receiver as a phase reference to synchronously demodulate all the other signals.

Enhanced levels of phase scintillation are always observed within the region of diffuse auroral precipitation. In the region of the high-latitude plasma trough, the phase scintillation is substantially weaker. Very large phase-scintillation enhancements are associated with discrete arcs. The corresponding amplitude-scintillation level is generally small. Surges and active auroral forms produce enhanced levels of amplitude scintillation. In all cases, the phase scintillation has the power-law form Tf^{-p}, with p highly variable but typically near 2.5 on the average.

A prominent feature in about 80% of the high-latitude passes is a localized but pronounced scintillation enhancement. When the propagation path is within the region of the diffuse aurora, the enhancement can be entirely explained as a geometrical effect due to field-aligned, sheet-like irregularities with an east-west orientation. In a number of cases, however, a pronounced scintillation enhancement occurs at or very near the equatorward edge of the diffuse aurora. For these latter events, the scintillation appears to be associated with enhanced F-region ionization produced by soft-particle fluxes.

G2-7 IONOSPHERIC IRREGULARITY ANISOTROPY AND DRIFTS AT HIGH
1100 LATITUDES

R. C. Livingston and C. L. Rino
Radio Physics Laboratory, SRI International
Menlo Park, California 94025

Spaced-receiver measurements are being routinely collected in the auroral zone at Poker Flat, Alaska as part of the Wideband satellite transmission experiment. The complex signal at 413 MHz is received at each of the three remote antennas, 300 m west, 600 m east, and 900 m south of the main station. A method has been derived from which the anisotropy parameters and true drift velocity of the medium-scale (about 1 to 10 km) ionospheric irregularities can be implied. Comparison of the Poker Flat data with theoretical calculations based on a generalized irregularity model has shown consistent evidence for sheet-like (10:10:1) irregularities in the nighttime auroral ionosphere. A number of these comparisons will be discussed for a variety of geomagnetically disturbed conditions.

G2-8 WIDEBAND SATELLITE STUDY OF HIGH-LATITUDE TOTAL
1125 ELECTRON CONTENT

M. D. Cousins and O. de la Beaujardiere
Radio Physics Laboratory, SRI International,
Menlo Park, California 94025

Measurements of high-latitude total electron content (TEC) have been made regularly using the Wideband Satellite since June 1976. Our interpretation of these data is presented. The propagation path extends from the satellite to the receiving station at Poker Flat, Alaska. Routine experiments coordinated with the Chatanika radar provide electron density profiles, electric fields, currents, and differential electron energy spectra. These measurements support our interpretation of the TEC data.

Each pass of the satellite produces a scanning measurement of TEC through the auroral zone--a TEC signature. A study of the entire data set reveals commonly occurring TEC signatures and establishes their relation to high-latitude phenomena. For example, the trough is regularly identified in the TEC data. The location and details of this and other features have been studied and are presented. TEC observations of the diffuse aurora, discrete arcs, and the polar cap are also characterized.

Commission J Session 1

INTERFEROMETRY AND APERTURE SYNTHESIS - I

Wednesday A.M., 11 January ECCR 1-40

Chairman: A.E.E. Rogers, Northeast Radio Observatory Corporation, Haystack Observatory, Westford, MA 01886

J1-1 0830 THE M.I.T. APERTURE SYNTHESIS INTERFEROMETER SYSTEM: A. Parrish, T. Giuffrida, B. Allen, A. Haschick, M.I.T.; G. Papadopulos, Univ. of Patras, Patras, Greece, and B. F. Burke, M.I.T., Cambridge, MA 02139.

The M.I.T. Aperture Synthesis Interferometer, consisting of one moveable and two fixed 5.5 meter antennas, is now complete and operating with a maximum available spacing of 22600 wavelengths at 1.35 cm. The equipment includes mixer radiometers with various DSB noise temperatures between 500 and 700 K. The radiometers use phase-locked Gunn oscillators and servo length-controlled reference frequency cables. The 75 MHz wide IF bandwidths are processed by digital delay units and correlators. A minicomputer, which performs user interface, antenna pointing, delay compensation, and fringe fitting completes the system. Initial data indicates that the interferometer meets the design objective of a relatively simple system capable of obtaining phase stable data over a wide range of spacings.

J1-2
0855

THE MIT RADIO INTERFEROMETER ON-LINE DATA PROCESSING SYSTEM:

T.S.Giuffrida, B.J.Rossin, R.L.Fiedler, A.Parrish, and B.F.Burke, Department of Physics, Room 26-344, Massachusetts Institute of Technology, Cambridge, MA 02139

Since reliability and simplicity were desired in the MIT Interferometer, a digital on-line data system was constructed. The I.F. from each radiometer is sampled at a rate of 150 MHz and converted into two bit numbers. To avoid using 150 MHz throughout the system, eight parallel data streams are used. Everything but the sampler can then be clocked at 18.75 MHz; thus only the sampler is ECL, the remainder is TTL.

An instrumental delay is needed to compensate for the geometric delay between the antennas but analog delay systems often introduce phase delay uncertainties. The digital system eliminates this problem, and provides accurate delays easily. The correlator is a multiply circuit which consists of five gates for each of the parallel streams.

After the correlations have been accumulated for one eighth of a second, a minicomputer reads in a 32 bit number. The computer is used to set the digital delays, and perform a least squares fit to the accumulations. The fit is done every 28.125 seconds and provides a fringe amplitude and phase. These amplitudes and phases are then written on tape, for later analysis on a large computer. Stable and reliable operation of the system has been demonstrated.

J1-3 0920 CURRENT CAPABILITIES AND OBSERVATIONS AT THE VLA

A.R. Thompson and B.G. Clark, National Radio Astronomy Observatory, VLA Project, Socorro, NM 87801

The VLA, located near Socorro, New Mexico, is now being used for observations of astronomical objects, although the primary activity on the instrument is still the ongoing construction program. Observations are being carried out both to test the instrument and to carry out astronomical programs. The instrument is valuable for astronomical observations particularly because of its very high sensitivity at 6 cm wavelength.
A sketch of current capabilities will be given and some results of the instrument test programs.
The National Radio Astronomy Observatory is operated by Associated Universities, Inc. under contract with the National Science Foundation.

J1-4 0945 EARLY VLA MAPS OF 4 PLANETARY NEBULAE:

R.M. Hjellming, B. Balick, and C. Bignell, National Radio Astronomy Observatory, Socorro, NM 87801

The planetary nebulae NGC 40, IC3568, NGC 7354, and NGC 7027 were mapped at λ6 cm using the aperture synthesis technique and 6 or 7 antennas of the Very Large Array (VLA) currently under construction in New Mexico. The observations were made in May-July, 1977 with a linear array along a 5.2 km section of the south-west arm which is oriented 35° from an E-W line. The resulting synthesized beams had 3" half power widths, with some elongation for the lower declination objects. The maps for NGC 7027, NGC 7354, and NGC 40 are comparable in quality with the best published maps. The map of IC3568 considerably improves our knowledge of the radio structure of this unusually symmetric planetary nebula.

J1-5 1045 ASTROMETRY VIA CONNECTED ELEMENT INTERFEROMETRY:
K.J. Johnston, E.O. Hulburt Center for Space Research, Naval Research Laboratory, Washington, D.C. 20375, and C.M. Wade, National Radio Astronomy Observatory, Charlottesville, Virginia 22903

The use of connected element radio interferometers for astrometry will be reviewed. Emphasis will be given to the accuracy presently achievable in source position, baselines, earth rotation, and polar motion.

J1-6 1110 Recent Astrometric Observations on Intercontinental Baselines
E.J. Cohen, J.L. Fanselow, G.H. Purcell, Jr., D.H. Rogstad, and J.B. Thomas, Advanced VLBI Systems Group, Jet Propulsion Laboratory, Pasadena, CA 91103.

Since December, 1976, stations of the Deep Space Network in Australia, California, and Spain have conducted a series of astrometric observations involving about fifty extragalactic radio sources. Most of the observations were made simultaneously at X- and S-band to permit calibration of ionospheric propagation effects. Within each band we typically observed four time-multiplexed frequency channels, each 2 MHz wide, having a total spanned bandwidth of 20 MHz. The data were recorded on the Mark II recording system, correlated at the Caltech-J.P.L. correlator, and further reduced by conventional bandwidth synthesis methods.
Preliminary analysis of individual observing sessions indicates baselines consistent with previous measurements, with formal errors on single components as small as 30 cm. At the same time the formal errors on source coordinates were between 0".006 and 0".04 in favorable cases. However, we find discrepancies between some of these source positions and other published results.

J1-7
1135

ASTRONOMY VIA LONG BASELINE INTERFEROMETRY:

C. A. Knight, H. F. Hinteregger, A.E.E. Rogers, A.R. Whitney, Northeast Radio Observatory Corporation, Haystack Observatory, Westford, MA 01886; J.J. Wittels, W.D. Cotton, C.C. Counselman, I.I. Shapiro, Department of Earth and Planetary Sciences, MIT, Cambridge, MA 02139; T.A. Clark, J.W. Ryan, C. Ma, Goddard Space Flight Center, Greenbelt, MD 20771; D.S. Robertson, National Geodetic Survey, Rockville, MD 20852

Repeated measurements of radio source coordinates by VLBI using the Mark-I system demonstrate a repeatability at ∿0".01 for most sources. Absolute coordinates determined by VLBI compare satisfactorily with independent determinations by other methods. Differential coordinate measurements between close pairs of sources are made with repeatability at ∿0".001. Implementation of the "Mark-III" VLBI system will permit a significant improvement in measurement accuracy.

J1-8 1200 VLBI BASELINE MEASUREMENTS TO A TRANSPORTABLE ANTENNA WITH DECIMETER ACCURACY: A. E. Niell, P. F. MacDoran, D. D. Morabito, K. M. Ong, and G. M. Resch, JPL, and J. F. Dracup, NGS

The Project ARIES (Astronomical Radio Interferometric Earth Surveying) 9 m transportable antenna has been used as one element of a Very Long Baseline Interferometer System for accurate vector baseline measurements to the Caltech Owens Valley Radio Observatory 40 m telescope and to the 64 m station of the NASA Deep Space Network at Goldstone, California. To demonstrate baseline measurement accuracy by comparison with conventional geodetic techniques the ARIES antenna was located first at Palos Verdes and then across Santa Monica Bay at Malibu, California. The vector baselines were then determined from each site to the OVRO antenna. The 42 km Palos Verdes/Malibu baseline was obtained by differencing the two vectors. The length and azimuth of the PV/MAL baseline was then measured by the National Geodetic Survey using conventional geodetic techniques. The values obtained by the two techniques differ by 6 $\pm$ 10 cm in length and 10 $\pm$ 20 cm in azimuth. Between 1974 August and 1977 August the ARIES antenna occupied a site at JPL near Pasadena, California on four separate occasions. The baseline to the 64 m DSN antenna was measured one or more times during each occupation. These experiments have all been correlated on the Caltech/JPL VLBI Processor and the results will be discussed.

Commission B Session 4

ANTENNAS

Wednesday P.M., 11 January ECCR 2-26

Chairman: Dr. D.H. Schaubert, Harry

Diamond Laboratories, Adelphi, MD 20783

B4-1
1330 IMPEDANCE AND RADIATION CHARACTERISTICS OF THE MJS-77 PLANETARY RADIO ASTRONOMY ANTENNA:

Dr. Edward P. Sayre, Department Systems & Computer Engineering, Boston University, Boston, Massachusetts

The radiation and impedance characteristics of the Planetary Radio Astronomy (PRA) antenna experiment to imposed electromagnetic fields have been examined. The PRA antennas are orthogonal monopoles of ten meter nominal length mounted on the Mariner Jupiter Saturn (MJS-77) spacecraft body behind the hi-gain parabolic antenna.

The method of analysis used was the Method of Moments. A wire grid model of the MJS-77 spacecraft was used to simulate all significant spacecraft components, including spacecraft body, hi-gain antenna and magnetometer boom. Using this model, computation of the effective length and input impedance and radiation characteristics of each monopole is carried out in the presence of the spacecraft.

Examination of the dimensions of the spacecraft body show it to be electrically small at the frequencies considered. Consequently, the PRA monopole patterns deviate from those predicted were the antennas mounted on a large ground plane. Computations show that the presence of the spacecraft causes an out-of-plane tipping of the dipole moment of each antenna and unexpected cross-polarized effects. The direction of the actual dipole moment of each antenna is given from which the effective position is derived. Impedance calculations show that the presence of the spacecraft causes an increase of input capacitance but little change in radiation resistance. Effective height is constant over the range of 20KHz to 2.5MHz considered.

B4-2 NEW CLASS OF REFLECTOR ANTENNAS
1350 V.J. Vokurka, Department of Electrical Engineering, Eindhoven University of Technology, Eindhoven, Netherlands.

These new devices have been developed according to the requirements of the ideal, physically realizable reflector antenna. Instead of optimizing the radiation behaviour of reflectors which are derived from systems of revolution, we have laid down the following conditions for our "ideal" reflector antenna:

(a) it should be of the beam-waveguide type,
(b) there should be no (theoretical) restrictions with regard to cross-polarisation limits,
(c) no constraints on shaping,
(d) independent control of the aperture distribution in both principal planes.

Focusing system satisfying these requirements consists of sets of confocal cylindrical surfaces as shown schematically in the picture below. Such a configuration is suitable for use in combination with spherical or "plane"-wave sources. The near-field radiation characteristics of corrugated horns prove to be suitable for this purpose. Since there is no blockage the diffraction effects can be easily minimized. Both symmetrical and asymmetrical far-field patterns can be created, which implies that these antennas are suitable for a large number of applications. Excellent radiation performance has also been found experimentally. For instance, it has been shown that an antenna of this type with an aperture dimension of about 25λ satisfies the FCC side-lobe envelope. The cross-polarisation is found to be less than -35dB in any plane through the beam axis. Due to the cylindrical structure, manufacture is expected to be simpler than that of reflectors of revolution.

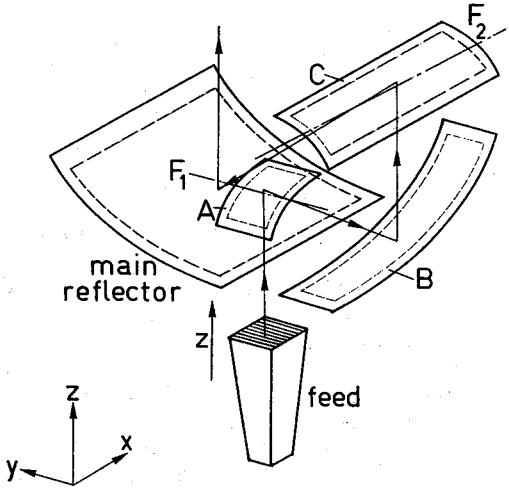

B4-3
1410

TRANSIENTS IN RESISTIVELY LOADED "TEM" HORNS

Motohisa Kanda, National Bureau of Standards,
Boulder, Colorado 80302

Recent study related to EMP phenomena has focused strong attention on the subject of transients EM fields. Antenna structures which are able to preserve time-domain waveform of EMP need to be inherently broadband and non-dispersive. One such antenna which has been successfully fabricated is a dipole with continuously tapered resistive loading [M. Kanda, 1977 AP-S International Symposium Digest, 230-233].
In another effort to attain increased directivity or increased antenna gain, a "TEM" horn with continuously tapered resistive loading has been considered as a broadband and non-dispersive antenna with low VSWR. With proper continuously tapered resistive loading, the reflection coefficient of a 30 cm long resistively loaded "TEM" horn stays below 0.5 for the frequency range from 100 MHz to 8 GHz as shown in the figure. For a comparison the reflection coefficients of a 30 cm long conducting TEM horn and a 1 m long Cornell TEM horn are also shown. The antenna transfer function of a resistively loaded "TEM" horn is flat to ± 3 dB for the frequency range from 20 MHz to 6 GHz.
The one-dimensional theoretical analysis for a resistively loaded "TEM" horn using the method of moments has been performed in the frequency domain. The final use of FFT techniques then allows the determination of transient radiated EM fields for a known input pulse waveform. Comparison between theory and time domain measurements is also given.

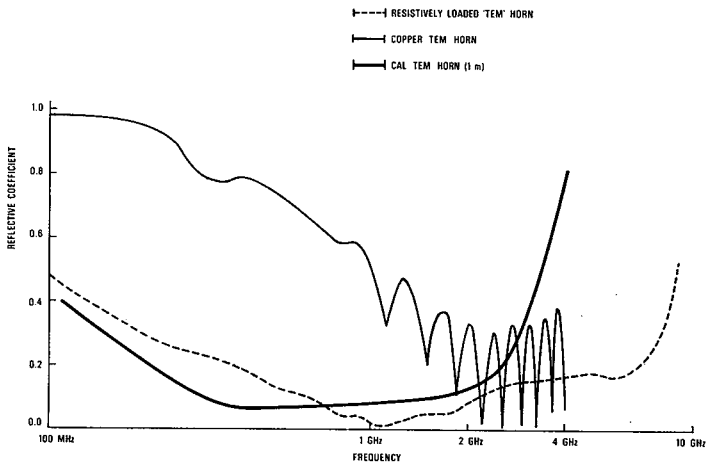

B4-4
1430

MULTIPATH PERFORMANCE OF FLUSH MOUNTED AIRCRAFT ANTENNAS:

V. P. CABLE
Department of Electrical and Computer Engineering, California State University, Northridge, CA 91330

This report presents the results of a preliminary investigation on the performance of airborne phased arrays in an aircraft/satellite multipath environment. A simplified model is developed which predicts the multipath performance of flush (conformal) arrays mounted on the upper part of the main aircraft fuselage. The diffracted multipath energy is reflected off the earth's surface and compared to the energy in the direct path as a function of satellite position (zenith to horizon). These first results indicate improved performance (reduced level of multipath) for larger arrays, but that improvement is also a function of placement of the array. When a specific requirement for "rejecting" multipath is set, say 20 dB down, optimum array placement is to the side of the aircraft (45° off zenith). Here, the conventional phased array also has its best scan capability (zenith to horizon). However, if a 40 dB threshold for rejecting multipath is needed, the optimum position appears to be at the top (zenith). The conventional array in this case has a somewhat limited scan coverage, but a hybrid (slow wave mode) is mentioned as a possible solution to expanding this coverage to the horizon. (R. J. Mailloux, Microwave Journal.) Possible methods for reduction of multipath contributions for this hybrid array are discussed.

B4-5
1520

ELECTROSTATICALLY CONTROLLED THIN-FILM ANTENNA

J. H. Lang, D. H. Staelin, and J. R. Melcher,
Research Laboratory of Electronics and the Department of Electrical Engineering and Computer Science, Massachusetts Institute of Technology, Cambridge, MA 02139

One limit to the maximum size of antennas in space is the minimum feasible mass per unit area. Densities of several grams per square meter may be approached by using a thin film or mesh antenna reflector surface. Such a flexible reflecting surface can be precisely controlled by electrostatic forces arising from charge distributions continuously and rapidly manipulated by a scanning electron beam or other means. Continual optical measurements of reflector shape can provide the data necessary for effective control. Launch of such deployable parabolic antennas up to $\sim$ 1 km diameter from a single NASA Space Shuttle appears to be feasible.
The present analysis is for a configuration comprising two roughly parallel thin films. One film is the perfectly conducting elastic reflector surface of the antenna, and the other is located a short distance behind it and is composed of $\gtrsim 10^4$ conducting elements insulated so that each can hold an independent charge. This charge can be made more negative by impacting the desired segment with an electron beam of the appropriate energy, and made more positive by employing a beam that can penetrate the segment and emerge on the far side together with secondary electrons, all of which are captured by the conducting film.
The conducting film is tensioned by a rigid rim, and is deflected toward the desired parabolic shape by a bias field provided by the approximately parallel semi-rigid segmented surface located nearby. The separation between surfaces would normally be a few times larger than the rms tolerance to which the segmented surface can be held. By solving the electric and mechanical equations of motion for such a system it was found that $\sim$ 50 spatial modes were unstable for one reasonable set of antenna parameters, and that the growth time constants for these modes were all greater than several seconds. It was found that they could all be stabilized for a 1-km diameter antenna using a small computer, a 100-measurements per second laser system, and electron beam powers of $\lesssim$ 2 kw. Problems introduced by A.C. and D.C. surface position noise, and by the interplanetary environment at synchronous orbit altitudes all appear surmountable.

B4-6
1540

AN ANALYSIS TECHNIQUE OF REFLECTOR ICING

W. A. Davis, Air Force Institute of Technology
AFIT/ENG, Wright-Patterson AFB, Ohio 45433

In recent years, the effects of icing on reflector antenna systems used in precision approach radars has become an ever increasing problem of interest. This paper presents a simple technique that may be used for the analysis of the icing on such reflector systems. For simplicity, the ice is assumed to have a uniform vertical thickness over the upper side of exposed surfaces.

Beginning with a uniform phase front in the beam direction for the un-iced reflector, one can trace rays back to the reflector using geometrical optics to determine the angle of incidence at each point on the reflector. The phase and amplitude of the rays for the iced reflector are computed by local plane wave analysis and used to calculate the far field in the manner of physical optics. This technique gives downward beam shifts of up to 30 milliradians for some typical reflectors. This technique modifies the array aperture function. The full pattern can be obtained from the convolution of the computed pattern with the pattern of the orginal system.

B4-7
1600

DIFFRACTION BY A DIELECTRIC LOADED SECTORAL HORN WITH CYLINDRICAL APERTURE:

R.A. Nair, A.K. Kamul and S.C. Gupta, Department of Electronics and Communication Engineering, University of Roorkee, Roorkee -247672, India

Results of the analytical and experimental study of the radiation properties of dielectric loaded H-plane sectoral horn with cylindrical aperture are presented. The horn fields are determined in terms of cylindrical wave functions and the characteristic equation for the propagation phase constant k_r is derived. The radiation characteristics of the system are derived by the aperture field method based on the vector diffraction formula. The radiation pattern is found to have increased directivity and reduced sidelobe levels probable with dielectric loading.

To establish the analytical results, experiments were carried out using a H-plane sectoral horn ($\alpha_o = 22^o$, R = 18 cm), with circular aperture centered along the apex loaded with 0.1 mm thick mica sheets on the parallel walls. The experimental results were found to be in reasonable agreement with theoretical results. It is concluded that dielectric coated H-plane sectoral horns with cylindrical apertures have radiation patterns with significantly increased directivity and reduced probable sidelobe levels. Since the theory is in satisfactory agreement with experiments, the dielectric coated H-plane horn with cylindrical aperture can be used either as a convenient source of highly directive electromagnetic radiation or as a feed for paraboloidal reflection antennas.

B4-8 1620 RADIATION PATTERNS OF CORRUGATED CONICAL HORNS EMPLOYING SLOPE DIFFRACTION: M.S. Narasimhan, Center for Systems and Devices, Indian Institute of Technology, Madras-600 036, India.

This paper describes a technique of calculating the principal plane radiation patterns of corrugated conical horns supporting balanced hybrid modes, through a slope wave diffraction formulation. Slope wave diffraction has been employed earlier to study diffraction of cylindrical waves by a straight edge. In order to deal with geometric diffraction of spherical waves by the curved edge of a corrugated conical horn (with non-vanishing H_r in the H-plane and non-vanishing E_r in the E-plane), this analysis is modified with the help of the theory presented by Koyoumjian and Phathak and an expression is derived for the non-axial diffracted far-field in terms of slope wave diffraction coefficient with a knowledge of field expansion for the HE_{11} mode within a corrugated conical horn. The on axis diffracted far-fields are calculated from the equivalent electric and magnetic currents lying along the circular edge of the horn using a procedure described by Ryan and Peters. In order to verify the validity of the analysis presented, radiation patterns of wide flare corrugated conical horns supporting the balance HE_{11} mode have been calculated and compared with the measured patterns and an excellent agreement is noticed between the two.

Commission B Session 5

SCATTERING: INVERSE AND DIRECT

Wednesday P.M., 11 January ECCR 2-28

Chairman: Dr. J.K. Schindler, RADC/USAF,

Hanscom AFB, MA 01731

B5-1
1330 A UNIQUENESS PROOF FOR THE BOJARSKI EXACT INVERSE SCATTERING THEORY, AND ITS CONSEQUENCES FOR THE HOLOGRAPHIC RADIO CAMERA

W. Ross Stone, Megatek Corporation, 1055 Shafter Street, San Diego, CA 92106; and Department of Applied Physics and Information Sciences, University of California, San Diego.

By recording the complex field values received on the ground from a transionospheric satellite transmission, the Holographic Radio Camera (W.R. Stone, J. Atmos. Terr. Phys.,38,583-92, 1976) reconstructs the three dimensional distribution of the field and of the (complex) refractive index in the ionosphere. This is a classical inverse scattering problem: Given the boundary values, determine the source term in the wave equation. The uniqueness of this determination is of fundamental importance. Recently, a mathematically rigorous proof of the uniqueness of Bojarski's exact solution to this inverse scattering problem has been presented (N. Bleistein and J.K. Cohen, J. Math. Phys., 18, 194-201, 1977).

This paper presents a new and much simpler proof of the uniqueness of Bojarski's solution in general, and of the uniqueness of the reconstruction of the refractive index obtained with the Holographic Radio Camera in particular. The physical significance of the conditions on the boundary values which must be met to achieve uniqueness is clearly shown. The result is shown to involve a physical relationship of equal importance to the relationship between the boundary values and the fields in the uniqueness of the direct scattering problem (i.e., the uniqueness of the solution for the fields in the wave equation). A second result also becomes evident from this proof. It is commonly stated that a holographic reconstruction yields the fields which existed in "object space" between the source and the recording aperture. It is shown that this is only true to within an approximation. Furthermore, the approximation involved is precisely such that once made, the information relating the field values to the refractive index is lost.

B5-2
1350

PROFILE RECONSTRUCTION FOR REFLECTION COEFFICIENTS WITH DISCRETE AND CONTINUOUS SPECTRA:

A. K. Jordan, Naval Research Laboratory, Washington, D. C. 20375, and Saeyoung Ahn*, Locus, Inc., Washington, D. C. 20022

The profile of permittivity of an inhomogeneous dielectric region is reconstructed from the analytic representation of the reflection coefficient. The present communication extends our reconstruction method to include reflection coefficients with discrete spectra in addition to the continuous spectra that have been considered previously (Ahn and Jordan, IEEE Trans. Ant. & Prop., AP-24, 879-882; 1976). Reflection coefficients with discrete spectra are encountered when the scattering region possesses characteristic modes. Reflection from an inhomogeneous half-space with permittivity $\epsilon(x)$ is considered. The reflection coefficient, $r(k)$, where k is the wave number, is assumed to have two poles in the lower half k-plane (these represent the continuous spectrum) and one pole on the positive imaginary axis (this represents the discrete spectrum). The profile reconstruction method is an application of the Gelfand-Levitan inverse scattering theory (Kay, Comm. Pure Appl. Math., 13, 371-393; 1961). The profile function, $q(x)$, obtained from this reflection coefficient is shown below. A physical interpretation of $q(x)$ is given and related to the dielectric properties of the medium. The profile function and reflection coefficient of this example are compared with the examples of continuous spectra.

*Present Address: Naval Research Laboratory

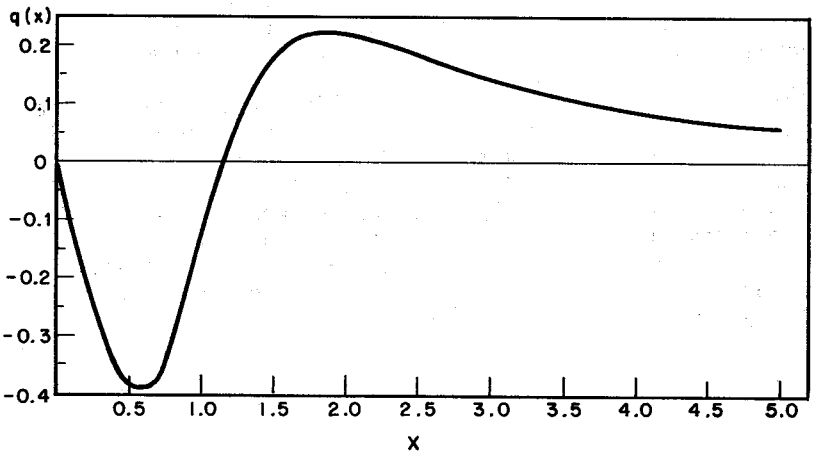

B5-3 TRANSFER FUNCTIONS OF SCATTERING POINTS:
1410

S. M. Sherman and C. N. Campopiano
RCA Government Systems Division
Moorestown, N.J. 08057

In the physical-optics method of electromagnetic scattering analysis, the echo from a radar target can be decomposed into contributions from discrete scattering points. With sufficient pulse bandwidth, the individual scattering points can be resolved in range. Even when they are not resolved, there is often an advantage in calculating their individual echo contributions and summing them (with due attention to time displacements and relative phases) rather than dealing with the entire body. This approach gives insight into the scattering mechanism and sometimes simplifies the calculations.

Each scattering point is characterized by a transfer function having magnitude and phase, as in circuit theory, defined so that the square of the magnitude equals the radar cross-section of the scattering point. The fact that the transfer function also includes a phase characteristic (over and above the phase due to distance from the radar) is often overlooked. The phase has important effects on the characteristics of echo pulses from resolved as well as unresolved scattering points. To derive the transfer function for a specified aspect, the body geometry is first expressed in the form of projected area vs. range for that aspect. Each discontinuity in this "area function" or in any of its derivatives, including the discontinuity at the leading edge of the body, produces a scattering point, which is represented as being due to an "incremental area function" originating at that point, superimposed on the continuation of the preceding area function. A Laplace transformation of the incremental area function yields the transfer function. Examples are given for various body shapes. Transfer functions are particularly simple to derive when the incremental area functions can be expressed as polynomials.

Given the incident pulse waveform and the transfer function of a scattering point, one can calculate the echo pulse waveform. Computer-generated examples are given. A simple approximate method has also been developed, which describes the changes in the pulse upon reflection in terms of a time shift (in addition to the propagation time delay), a phase shift of the carrier relative to the envelope, and a shift in instantaneous frequency.

B5-4
1430

PULSE DIFFUSION IN A DENSE DISTRIBUTION OF SCATTERERS:

Akira Ishimaru
Department of Electrical Engineering, University of Washington, Seattle, Washington 98195

Most studies on wave propagation and scattering in random media are based on various simplifying assumptions such as tenuous scatterers or weak inhomogeneities or forward scattering. If the random medium is dense, then the wave behaves in a manner similar to diffusion process, and there are just as much backscattering as forward scattering. This paper presents a theoretical and experimental study of the behavior of a short pulse in a dense distribution of scatterers. Experimental data are taken from the measurement of picosecond pulses scattered from a solution containing 2μm diameter Latex particles with the volume density of up to 10 percent. The theory is based on the integral and differential equations for the two-frequency mutual coherence function in the first order smoothing approximation. The differential equation is similar to the equation of transfer, but includes the effects of correlations at two different frequencies. Analytical solutions of this equation are not available at present. However noting that the scattering process is similar to diffusion, the original equation is approximated by a diffusion equation. This can be easily solved analytically for a variety of geometries. In particular we obtained diffusion solutions for a point source and for a plane slab problem. They are similar to the pulse propagation in a conducting medium. Theoretical calculations are compared with experimental data for the particle volume densities ranging from 10^{-4} to 10 percent. The diffusion effects are noticeable in the density range of 1 to 10 percent, and good agreements between theory and experiments are obtained.

B5-5
1520 SCATTERED FIELDS NEAR DIELECTRIC SLABS AND HOLLOW WEDGES: G. Tricoles, E.L. Rope, R.A. Hayward, General Dynamics Electronics Division, P.O. Box 81127, San Diego, CA 92138

Microwave fields near finite dielectric slabs and hollow wedges were computed by applying a moment method (J.H. Richmond, IEEE Trans., AP-13 pp 334-341, 1965). For the slab, incidence angle was varied from normal to grazing; for the wedge, which had 90^{o} angle at the vertex, incidence was axial. The wave polarization was perpendicular. Nearfield phase and intensity were also measured with a small probe antenna and a microwave interferometer. Near the slab on the wedge walls the intensity data show fringes with spacings accurately determined by a model that assumes interference behind slab-guided waves and plane, free space waves. Shallower and narrower fringes are superimposed; these result from guided waves propagating in opposite directions on the dielectric structure. The spatial distribution of the field was determined for the shadowed and directly illuminated regions as well as the region of reflection. Effects of thickness and dielectric constant are given, along with some computational aspects.

B5-6
1540 BROAD BAND RADAR CROSS SECTION REDUCTION BY BENDING OF A FLAT PLATE:

K. M. Mitzner, Aircraft Group,
Northrop Corporation, Hawthorne, CA 90250

There is a growing interest in developing simple characterizations of the way the radar cross section (RCS) of a body changes when the body is deformed. For example, Knott (IEEE Trans. Antennas Propagat., AP-24, 882-884, 1976) has studied the effect of deforming a flat plate into a cylindrical segment.

In this paper, the same problem is examined from a different point of view. We ask how much we have to bend the plate in order to reduce the RCS for backscatter normal to the original plate by at least a given amount for all wavelengths less than λ_o. We find, for example, that we can obtain a minimum reduction of approximately 9 db by bending the plate in a parabolic arc with the same endpoints as the flat plate and with the center line displaced approximately 3/8 λ_o. Because of the lobe structure of the curve of RCS reduction versus frequency, much greater deformations are needed to get significantly greater broad band reductions. Specifically, it is necessary to increase the displacement above approximately 2/3 λ_o to get any further change in the minimum reduction, and a 3 db change requires an increase in the displacement to about 1.2 λ_o. This paper also considers the penalties we pay for reducing RCS by bending, specifically the spreading out of the range of incidence angles at which the backscatter RCS is comparable to, sometimes even higher than, the backscatter RCS for normal incidence.

B5-7
1600

AN IMPROVED FORMULATION FOR EXTENDING THE GTD USING THE MOMENT METHOD:

John Sahalos and Gary A. Thiele,
ElectroScience Laboratory, The Ohio State University, Columbus, Ohio 43212

In 1975 two techniques were published which combined the method of moments and the geometrical theory of diffraction. One technique extended the moment method through the use of the GTD while the second used the moment method to solve for unknown diffraction coefficients thereby extending the GTD. We wish to consider the latter here.

One problem area that existed with the original solution (W. D. Burnside, et.al. IEEE APS, 23, 551-558, 1975) was associated with a field incident along or nearly along one wall of a wedge structure. This paper will show an improved series representation for the diffracted current that is sufficient at all incidence angles. In addition, this improved formulation is insensitive to the location of the match points in the GTD region whereas the original formulation exhibited a sensitivity to the match point locations.

The improved formulation is then applied to the problem of bistatic scattering by a triangular pyramid. The GTD-MM solution obtained is approximate and presently neglects the scattering by the four tips. Nevertheless results are obtained that compare very well with experimental data as indicated by the data in the figure. (The field due to tip diffraction may be added in post facto in this case.) This is believed to be the first use of the GTD-MM technique in treating a truly 3-dimensional geometry.

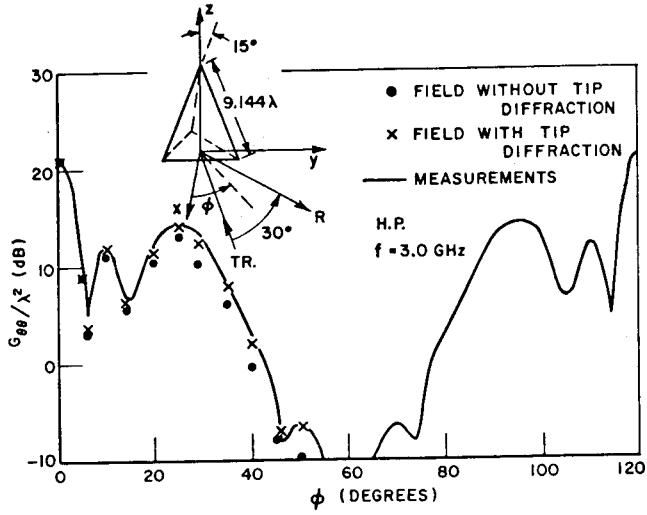

Bistatic (30°) radar cross section for ϕ polarization.

B5-8
1620

ELECTROMAGNETIC SURFACE WAVE PROPAGATION OVER A RECTANGULAR BONDED WIRE MESH

D.A. Hill, Institute for Telecommunication Sciences, Office of Telecommunications, U.S. Department of Commerce, Boulder, Colorado 80302

Wire mesh screens are often employed in electromagnetic shielding applications because they are light and inexpensive. A major difference between a wire mesh and a continuous metal sheet is the ability of the wire mesh to support a trapped surface wave. When the source and observer are located near the mesh, this surface wave is quite important. Also, the surface wave propagation constant is closely related to the shielding effectiveness. A rectangular mesh of intersecting parallel wires has been analyzed using a general Floquet expansion for the doubly periodic structure. The result is a doubly infinite set of homogeneous linear equations for the wire currents. A mode equation for the surface wave propagation constant is obtained by truncating the set of equations and setting the determinant equal to zero. The mode equation must be solved numerically, but the convergence of the process is improved by applying current and charge conditions at the wire junctions. Numerical results are generated to illustrate the dependence on the various parameters (mesh dimensions, frequency, direction of propagation, etc.). In contrast to the relatively isotropic behavior of the square mesh (D.A. Hill and J.R. Wait, IEEE Trans. Electromag. Compat., EMC-19, 2-7, 1977), the rectangular mesh is found to be highly anisotropic.

The method of averaged boundary conditions (M.I. Kontorovich, Radio Engr. Elect. Phys., 8, 1446-1454, 1963) has been used to analyze plane wave scattering by a rectangular mesh of small dimensions (M.I. Astrakhan, Telecom. Radio Engr., 23, 76-83, 1968). This analysis is extended to surface wave propagation, and the results are in good agreement with those of the general Floquet analysis. The method of averaged boundary conditions has also been used to derive an effective anisotropic surface transfer impedance representation for the mesh. This representation could be used to analyze practical mesh structures which are either non-planar or of finite extent.

B5-9
1640

MULTIPLE SCATTERING BY TWO SMALL SPHERES IN RELATIVE MOTION

Svend Berntsen and Günther Johannsen
Institute of Electronic Systems,
Aalborg University Centre, Denmark.

In a recently published paper (S. Berntsen, G. Johannsen, J.of Math.Phys., Vol. 7, No. 8, 1421-1428, 1976) the authors of the present work presented a formalism which we believe is a suitable tool in the field of relativistic, multiple scattering. We applied the formalism to a single problem only, namely to two parallel cylinders of infinite length, the incident, plane wave being polarized parallel to the cylinders. This is a (spatial) two-dimensional problem and characterized by the fact that it can be scalarized.
In the present work we are concerned with a three-dimensional configuration which cannot be scalarized, namely two small spheres which are in uniform motion relative to each other.
In the cited paper properly defined multiple scattering amplitudes of I. order are expressed as four-fold integrals in terms of scattering amplitudes of 0. order (i.e., for isolated objects) which are assumed to be known.
Starting from these expressions we show that three of the integrals can be evaluated generally by means of two δ-functions and a pole which appear in the expressions if the exiciting field is a plane wave. In the special case of two small spheres we are also able to evaluate the last integral so that the scattering amplitudes can be expressed in terms of known functions.
The scattered electrical far-field of I. order is found and some numerical results are given for the case, where the incident, plane wave propagates in the same direction as one sphere moves relative to the other.
In the limit $\beta \to 0$ (non moving objects) well-known results are obtained (W. Trinks, Ann.d.Phys., [5], 22, pp. 561-590, 1935).

Commission C Session 1

SYSTEM PERFORMANCE - PREDICTION

AND MEASUREMENT

Wednesday P.M., 11 January ECCR 0-36

Chairman: Douglass D. Crombie, Department

of Commerce, Office of Telecommunications,

ITS, Boulder, CO 80302

C1-1
1330

UNDETECTED BIT AND WORD ERROR RATES FOR STANDARD ERROR DETECTING BLOCK CODES

James C. Morakis, NASA/GSFC, Greenbelt, Maryland 20771
Hermann J. Helgert, George Washington University Washington, DC

Over the last several years, NASA's Goddard Space Flight Center has developed a Coding Standard for error control coding of data systems which use GSFC support facilities for forward or downlink data transmission. In its present form the Standard allows the use of five classes of binary linear block codes for error detection as well as several binary short and long constraint length convolutional codes for error correction together with a detailed description of the codes; it contains circuits for encoding and decoding standard ground station and spacecraft telemetry configurations and information on the guaranteed performance of these codes over the quantized additive white Gaussian noise channel. The purpose of the present paper is to make available to a wide audience this last aspect of the Standard as given by the undetected bit and word error rates over the binary symmetric channel. We restrict ourselves to the five classes of block codes, since the corresponding information for the convolutional codes contained in the standard is readily accessible in the literature.

C1-2
1355

AN APPROXIMATE METHOD FOR ESTIMATING THE DEGRADATION TO DIGITAL SYSTEMS FROM INTERFERENCE

J. R. Juroshek, U.S. Department of Commerce, Office of Telecommunication, Institute for Telecommunication Sciences, Boulder, CO 80302

The mathematical solution for the probability of error of a digital communication system in additive interference and Gaussian noise is generally complex. The resulting mathematical expressions are usually sufficiently complicated that they require a digital computer to evaluate. This talk will describe an approximate method for estimating the error rate of a variety of different types of digital systems in interference and Gaussian noise. It is anticipated that this approximate method will be useful primarily in studies that require a simple method of estimating degradation from interference, where the errors due to the looseness of estimate are acceptable.

The talk will describe the approximate method for estimating performance of both binary and M-ary coherent phase-shift keyed (CPSK) systems. The method is based on the eye diagram bound and provides an upper bound estimate of the probability of error given the signal-to-interference ratio and signal-to-noise ratio. Application of the bound is demonstrated for both constant amplitude and amplitude varying, circularly symmetric interference. The extension of the results to other types of digital systems such as noncoherent frequency-shift keyed systems (NCFSK) is also discussed.

An example of simplicity of the approximate method can be seen by considering one of the resulting expressions,

$$P_e \cong 0.5 \operatorname{erfc}\left(\frac{S}{N}\left(1 - \sqrt{\frac{I}{S}}\right)^2\right)$$

which is an estimate of the probability of error of a binary CPSK system operating in a Gaussian noise environment with signal-to-noise ratio S/N, and a single constant amplitude, circularly symmetric interference with signal-to-interference ratio S/I. For an M-ary CPSK system, the expression would be given by

$$P_M \cong \operatorname{erfc}\left(\frac{S}{N} \sin^2 \frac{\pi}{M}\left(1 - \sqrt{\frac{I}{S \sin^2 \pi/M}}\right)^2\right)$$

where P_M now denotes the probability of a symbol error.

C1-3
1420

ANALYSIS OF THE DEDICATED COMMUNICATION LINE IN A MINE TUNNEL FOR A SHUNT-LOADED TROLLEY WIRE:

J.R. Wait and D.A. Hill, Institute for Telecommunication Sciences, Office of Telecommunications, U.S. Department of Commerce, Boulder, CO 80302

Radio frequency transmission in mine tunnels is made possible by the presence of axial conductors. In fact, the trolley wire may be used effectively as a conveyor of communication signals at frequencies of the order of 100 kHz. In such cases, the rails or other conductors in the tunnel carry the return current. Both theory and experiment indicate that the attenuation rate for the unloaded trolley wire is as low as 2 dB per km of path length (D.A. Hill and J.R. Wait, IEEE Trans., EMC-18, 170-174, 1976 and R.H. Spencer, A.G. Emslie, J.D. Foulkes, R.L. Lagace, P.G. Martin, P.F. O'Brien, and P.F. Strong, Report to U.S. Bureau of Mines on Contract No. H0346045, 1977). However, the effects of shunt loads on the trolley wire will greatly increase the effective attenuation. To partially circumvent this difficulty, a separate unloaded line has been used for the purpose of carrying the radio frequency transmission (R.H. Spencer et al, 1977). The modal analysis of the performance of this dedicated line had been carried out where we assumed, for convenience, that the trolley wire loading could be simulated by an increase of continuous series resistance (D.A. Hill and J.R. Wait, IEEE Trans., COM-25, 1977). A more meaningful analysis is to consider explicitly the effect of a discrete shunt load on the trolley wire. This is the purpose of the present paper. At the same time, we re-examine some aspects of the theory that lead to simpler design concepts, particularly with regard to the effect of the ohmic loss in the tunnel walls.

First of all, we simplify the theory of transmission in a semi-circular tunnel containing two axial conductors for the case of radio frequencies by making use of quasi-static theory (J.R. Wait, IEEE Trans., AP-25, 441-443, 1977). In fact, we show that the effect of ohmic losses in the wall can be represented as series impedances per unit length in the equivalent coupled transmission line circuits. This opens the way for a systematic calculation of the mode conversion phenomena that occur when one of the axial conductors has a discrete shunt load to the ground plane. We then obtain explicit formulas for the modal conversion coefficients. We also consider the effect of a shunt load on the trolley wire on the performance of a radio frequency communication system. We confirm that the unloaded dedicated communication line provides for a low loss mode that is hardly affected by the shunt load on the adjacent trolley wire in the tunnel.

C1-4
1445 ROLE OF CONTROLLED MODE CONVERSION IN LEAKY FEEDER COMMUNICATION SYSTEMS:

James R. Wait, Consultant to ITS/OT and
David B. Seidel, C.I.R.E.S., University of Colorado/ NOAA, Boulder, CO 80309

Recently the leaky feeder concept has been utilized effectively in intra-mine communications (D.J.R. Martin, Radio and Electronic Eng., 45, 205-214, 1975; P. Delogne, Radio Science, 11, 295-304, 1976; S.F. Mahmoud and J.R. Wait, IEEE Trans., COM-24, 82-87, 1976). It had been previously found that such a system using a braided coaxial cable will propagate two low frequency transmission line modes (J.R. Wait and D.A. Hill, IEEE Trans., MTT-23, 401-405, 1975). One of these eigen modes (defined here as the monofilar mode) is readily excited from an arbitrary point within the tunnel but suffers high attenuation because the return current flows mainly in the tunnel wall. Conversely, the other eigen mode (defined here as the bifilar mode) has low attenuation because the return current flows mostly in the sheath; but it is poorly excited for an external source in the tunnel. Thus, for an efficient limited access communication system, it is desirable to convert energy from one mode to the other. Such mode conversion can be obtained through insertion of axial nonuniformities in the coaxial line or within the tunnel environment. In this paper, transmission line techniques are used to develop a theory of mode controlled conversion for a braided coaxial cable in a semi-circular tunnel. The formulation will also account for the ohmic losses of the tunnel wall as well as the spatially dispersive form of the braid transfer impedance. Various axial nonuniformities (mode converters) are considered including the use of lumped series impedances in the cable's inner conductor or braided sheath, or the introduction of a short segment of a different cable (for example, one with a different braid transfer impedance). This quasi-static theory is then used to indicate the characteristics of communication systems which use these various mode converters. The role of inadvertent mode conversion by tunnel wall non-uniformities is also considered briefly. Finally, the applicability of the technique to other types of environments such as railway right-of-ways, roadways and building corridors is discussed.

C1-5
1540 RESULTS OF A ONE YEAR TEST TO EVALUATE THE METEOR-BURST CHANNEL FOR LOW DATA RATE TELEMETRY: Dr. Daniel N. March, Electrical Engineering Department, Montana State University, Bozeman, MT 59717

A VHF meteor trail forward scatter telemetry system operated for 12 months between Bozeman, MT and Kent, WA. A basic parameter of the system was that the arrival time of the data was not critical (e.g. new data might be needed only once per 4 hours). The system was established to allow measurements of the long term (yearly cycle) occurrence statistics of reflections when using low power and low gain antennas at the remote terminal. Both the equipment and operating procedures of the system are defined.
Computers at both terminals recorded the operation of the system. The nature of the data recorded and their limitations are presented. The duty cycle parameter is not a proper measure of the remote telemetry channel. Instead the data are analyzed relative to the rate of occurrence of independent reflecting sources and the likelihood that the reflection lasts for some particular time. An algorithm was developed for the computer to determine the number of independent reflecting sources per time period. The algorithm and its computer implementation are discussed.
All data presented shows both actual operation and the number of independent reflecting sources per time period. Plots showing the daily performance of the system are presented. Histograms of hourly averages showing monthly and yearly performance are presented. Other relevant data are presented. Effects of meteor showers, auroral reflections, and sporadic E reflections are shown. The expected performance of several operational configurations of the meteor burst remote telemetry system are presented.

C1-6
1605 FIELD PREDICTION TECHNIQUE FOR DIGITAL TROPOSCATTER SYSTEM PERFORMANCE: J.A. Wick, the MITRE Corp., Box 208, Bedford MA

C1-7
1630 DIVERSITY PERFORMANCE FOR PARTIALLY CORRELATED TROPOSCATTER PATHS: J.A. Wick, the MITRE CORP., Box 208 Bedford MA

Commission F Session 4

GEOSCIENCE

Wednesday P.M., 11 January ECCR 0-30

Organized by the IEEE Group on

Geoscience Electronics

Chairman: A. Sobti, Motorola, Schaumberg,

IL 60172

* denotes invited paper

F4-1
1330 PASSIVE MICROWAVE REMOTE SENSING FOR GEOPHYSICS*

D. H. Staelin, Research Laboratory of Electronics and the Department of Electrical Engineering and Computer Science, Massachusetts Institute of Technology, Cambridge, MA 02139

Passive microwave techniques have been developed for sensing many parameters of geophysical interest; this paper reviews this progress and some prospects for the future.

Passive microwave spectrometers were carried on planetary probes beginning with Mariner II which flew past Venus in 1962. Passive microwave spectrometers have flown in polar earth orbits on Cosmos 243, Cosmos 384, Nimbus-5, Nimbus-6, Skylab and other spacecraft, and high resolution (25-km) passive microwave imaging systems have flown on Nimbus-5 and Nimbus-6. The microwave spectrometer on Nimbus-6 was also scanned so as to produce images; similar imaging spectrometers comprise the majority of passive microwave systems being prepared for future flights.

By exploiting the microwave resonances of O_2 near 60 GHz, it has been possible to map from space the global atmospheric temperature distribution with horizontal resolution of $\sim$ 150 km and vertical resolution of $\sim$ 8 km. Over ocean the resonant emission of water vapor and the non-resonant emission of liquid water are sufficiently distinctive that their abundances can be estimated individually. The accuracies of these statistical parameter estimates are sufficient to provide uniquely valuable information about global weather patterns and have warranted the inclusion of such instruments on future operational weather satellites such as Tiros-N and the Defense Meteorological Satellite Block-5D. Surface parameters such as sea ice coverage, snow cover, sea roughness, soil moisture, and sea surface temperature have also been derived from similar microwave data.

Many trace constituents of the atmosphere will be observable with improved sensors on future spacecraft. Future satellites, incorporating larger antennas and more sensitive receivers, should also have substantially improved spatial

resolution and frequency coverage. Such operational passive microwave systems in earth orbit could contribute significantly to partial fulfillment of the data requirements of a wide variety of governmental organizations.

F4-2
1355 An Analysis of Microwave Remote Sensing Data by Pattern Recognition Techniques

A. D. Fisher, S. Rotman, and D. H. Staelin,
Research Laboratory of Electronics, Massachusetts Institute of Technology, Cambridge, MA 02139

On the Nimbus-6 satellite is a scanning microwave spectrometer which continuously maps the earth's surface at two frequencies (22.235 and 31.4 GHz) and at six angles besides nadir. Cluster and principal components analyses were applied to this 14-dimensional feature vector in order to study its structure, interrelationships, and information content.

The data exhibited distinct clusters corresponding to various types of snow and ice. Such classes and subclasses as: snow-covered land (depth and moisture content subclasses), sea ice (partial ice cover and age subclasses), and polar firn (accumulation rate subclasses) appeared to be distinguishable. Characteristic SCAMS signatures produced by the various snow and ice types were also identified. These signatures could be used for evaluating theoretical microwave emission models, generating new feature vectors to facilitate automatic machine recognition and classification of snow and ice types, and developing quantitative inversion techniques for the physical parameters of the observed snow and ice.

F4-3
1420

MONOPULSE RADAR SOUNDING OF WET GLACIERS:*

Raymond D. Watts, U.S. Geological Survey
Denver, CO 80225

A monopulse radar having a center frequency of a few Megahertz has been used sucessfully to measure the thicknesses of wet glaciers. Radars of higher frequency (35 - 400 MHz) have been used previously to sound polar glaciers, but efforts to sound glaciers in temperate regions using these systems have failed. The reason is that glaciers in temperate regions are wet: their ice is at its pressure melting point, and there are water-filled voids in the ice. Scattering of radar energy (clutter) from the voids obscures the bottom echo unless the frequency is chosen so that the wavelength is long in comparison to the average size of the voids. The scattered energy is greatly reduced for long wavelengths, but the bottom echo remains strong.

The hardware for the monopulse system is exceedingly simple and reliable. Two resistively loaded dipole antennas are deployed on the glacier surface. One transmits; the other receives. Their length determines the center frequency of the system. The magnitude of the resistive loading determines the pulse duration (the number of cycles transmitted) and the sensitivity of the system. An avalanche transistor or any other high-speed, high-voltage switching device is used to feed a voltage transition to the transmitting antenna. An oscilloscope is used as a receiver. It is triggered on the air wave from the transmitter and records subsequent oscillations of the electric field. Because no rectification is used, the arrival times can be picked to about 1/10 of a center-frequency cycle, giving spatial resolution of about 1/10 wavelength.

Such a radar has been used not only to satisfy our basic interest in the bottom configuration of glaciers in Washington and Alaska, but also used as an aid in interpreting gravity surveys in ice-covered mountainous regions. In many of these areas, glaciers offer the only feasible landing sites for helicopters and, therefore, the only efficient sites for gravity measurements. The glacier's ice, however, represents an extreme mass deficit in comparision to normal surficial materials (i.e., rocks). A correction to the measured gravity values can be made successfully when the ice thickness has been measured with the monopulse sounder. Geophysicists are therefore able to evaluate the density characteristics of the rocks below the glaciers.

This method has been applied in a study of a nickel-bearing rock mass which extends under the glaciers in Glacier Bay National Monument in Alaska, where ice thicknesses as great as 1200 meters were measured using a 1.5 MHz, 270 Volt monopulse.

F4-4 1445 MICROWAVE RESPONSE OF SNOW:* Fawwaz Ulaby and Herschel Stiles, Univ. of Kansas, Lawrence, KS 66045

F4-5 1535 ELECTROMAGNETIC INDUCTION IN AN EARTH CONTAINING SURFACE CONDUCTIVITY ANOMALIES:* J.T. Weaver, Department of Physics, University of Victoria, Victoria, B.C., Canada V8W 2Y2

The electromagnetic field induced in the Earth by an external, uniform source is not easy to calculate when the Earth's conductivity varies not only with depth but also laterally. However, if the principal conductivity anomalies are locally confined to a thin surface layer, the theory can be simplified by representing the Earth mathematically as a uniformly conducting half-space covered by an infinitely thin sheet of variable integrated conductivity. This effectively eliminates variations of the conductivity with depth from the problem, and so reduces by one the number of dimensions over which the field equations must be solved numerically. Thus if the conductivity variation is limited to one horizontal direction only (normally called a two-dimensional problem) it is possible to express the electric field at the surface of the Earth as the solution of a simple one-dimensional integral equation. For quite general horizontal variations of conductivity (normally a three-dimensional problem), the horizontal electric field components are solutions of a pair of double integral equations. An outline of the theory is presented and the method of numerical solution is described. Calculations for some simple two-dimensional problems such as the "coast-effect" are also given.

F4-6
1600 WIDEBAND REMOTE INDUCTION SOUNDING OF HANNA UNDERGROUND COAL BURN II, PHASE 1: E. A. Quincy and M. L. Rhoades, Department of Electrical Engineering, University of Wyoming, Laramie, WY 82071

Experimentation with techniques of underground coal gasification has presented a need for remote delineation and characterization of these conducting burn regions from the surface. Hanna II, Phase 1 burn, located near Hanna, WY, was conducted on a 30ft thick subbituminous coal seam covered with 275ft of conducting overburden (10^{-3}mhos/m $<\sigma<$ 10^{-2}mhos/m). The maximum linear dimension of each burn lobe was estimated from chemical modeling to be on the order of 45ft.

The burn region was sounded one year after the burn was completed. A wideband loop-loop induction system employing pseudo-noise and cross-correlation techniques was used to produce the transient-time response of the burn in the field. The system was moved across the site on 4 traverses while keeping a fixed loop spacing of 120m and the loops horizontal on the earth surface. Additional signal processing in the laboratory on a Fourier Analyzer produced 3-dimensional signature maps in both time and frequency domains for each traverse. These horizontal profiling maps, corresponding to a 100Hz-50kHz passband demonstrate that significant anomalies are produced by the burn regions as the system is moved across the site. Skin depth for this system configuration and site is approximately 5kHz. Consequently frequency response at 1kHz and 5kHz were extracted from the wide-band data and plotted 2-dimensionally to provide an expanded view at these more reliable frequencies.

Collectively these inductions soundings produced strong anomalies of at least 8-to-1 at 5kHz and agree quite well with the chemical modeling estimates. However, they support the conclusion that the burn may have protruded another 5m to the West at the middle of the burn.

F4-7
1625

EFFECT OF BORE HOLE FLUIDS ON THE INDUCTION FIELDS OF AN ENCAPSULATED MAGNETIC LOOP:

A.Q. Howard, Jr., Department of Electrical Engineering, University of Arizona, Tucson, Arizona 85721; and J.A. Landt, Los Alamos Scientific Laboratory

The magnetic dipole antenna is a common probe in electromagnetic prospecting methods. Moran and Kung (Geophysics, 27, 829-858, 1962) developed expressions for induction logging techniques in bore holes as usually applied in petroleum exploration. In these investigations the loop is assumed concentric with the hole and lying in a plane perpendicular to the bore hole axis. The calculations do not include effects of an insulation cavity where the transmitter and receiver loops reside. If one is interested in measuring non-symmetrical effects such as man made or natural cracks or interfaces which intersect the bore hole, the effects of non-aligned loops and bore hole fluid need to be understood. Such effects are the subject of this paper.

In particular the modification of the induction fields of a loop antenna, as caused by the bore hole fluid above and below the cylindrical source region is treated. A simple expression is derived for the coefficients of the Fourier-Bessel series which describes the scattered fields in a cylindrical capsule. The isolation capsule contains the source and observation loops. The small electrical size of the bore hole considerably simplifies the analysis. The induction fields are shown to be succinctly described by the longitudinal component of the relevant dyad. The unknown Fourier coefficients are solved using a mode matching scheme. The problem is non-separable but it is shown that if eigenfunction expansions are employed which are orthogonal in the axial direction of the bore hole, and one assumes only inductive coupling, that a diagonal matrix equation results. The remaining problem is to evaluate a double numerical integral. To do this efficiently a special function is defined and its asymptotics are obtained. The results are of importance in the interpretation of induction logs where non-isotropic effects of the bore hole need be understood.

F4-8
1650

RADIATION OF A VERTICAL MAGNETIC DIPOLE IN THE PRESENCE OF A THREE DIMENSIONAL INHOMOGENEITY EMBEDDED IN A TWO LAYER STRATIFIED EARTH:

J.L.Martin,M.Cauterman,P.Degauque and R.Gabillard, Lille University, Elec. Dept., Bat P3, BP 36, 59650 Villeneuve d'Ascq, France

One of the prospection techniques for the remote sensing of buried inhomogeneities is based on a dipole dipole method and, in that case, it is often convenient to use a small current loop as a source. Unfortunately, the ground could not be always considered as a semi infinite medium and the presence of a conducting overburden can decrease the efficiency of this method. In order to evaluate the influence of this upper layer, we develop a theoretical model for the electromagnetic response of a vertical magnetic dipole in the presence of a two layer stratified earth and we suppose that a three dimensional inhomogeneity is situated in the lower layer.
The solution is obtained in the form of an integral equation which is solved by the moment method. Compared to the assumption of a semi infinite earth, an additional difficulty consists in the fact that the Green functions cannot be analytically expressed. They are given in an integral form and must be numerically evaluated.
We give some numerical considerations and we show on examples the influence of the conductivity and of the thickness of the first layer on the variation of the received signal in the presence of a given inhomogeneity.

Commission G Session 3

IONOSPHERIC IRREGULARITIES AND DRIFTS - II

(In Memory of Wolfgang Pfister)

Wednesday P.M., 11 January ECCR 1-42

Chairman: Dr. Kurt Toman, RADC, ETEI,

Hanscom AFB, MA 01731

G3-1
1330 E-REGION ELECTRON DENSITY IRREGULARITIES IN THE AURORAL ZONE: J.C. Ulwick, Air Force Geophysics Laboratory, Optical Physics Division, Hanscom AFB, MA 01731; K.D. Baker, Utah State University, Space Science Laboratory, Logan, UT 84322

The spatial structure of electron density irregularities in the auroral E regions has been measured by in situ probes aboard rockets launched from Poker Flat, Alaska. Auroral conditions at launch were varied including a rapidly developing breakup (IBC II+, $N_e \sim 5 \times 10^5$ cm^{-3}) a very bright auroral breakup (IBC III $N_e \sim 10^6$ cm^{-3}), a post auroral glow (IBC II, $N_e \sim 2 \times 10^5$cm^{-3}) and multiple auroral arcs. The variations of irregularity amplitude of electron density over scale sizes from 1 meter to 10 kilometers have been determined by power spectrum analysis techniques. The sections of data spectrally analyzed were detrended by removing the linear variations as given by the line of best fit and a consecutive number of these were averaged to achieve spectral smoothings. In two flights the irregularity amplitude distribution over scale sizes less than 1 km could be characterized by a power law with a spectral index only for altitudes above about 200 km. However, in the other two flights, spectral indices were obtained in the altitude region 85 to 140 km. In one case the spectral index was more or less constant while in the other it varied with rocket altitude but in both cases, a distinct increase in spectral power of almost an order of magnitude at specific scale sizes was noted in the 140 to 170 km region. The irregularity amplitude distribution with scale sizes determined from geometric and geomagnetic coordinate systems will be compared and discussed for the different auroral conditions.

G3-2
1355

DUAL COHERENT AURORAL RADAR OBSERVATIONS FROM SIPLE STATION, ANTARCTICA: W. L. Ecklund D. A. Carter, and B. B. Balsley, Aeronomy Laboratory, National Oceanic & Atmospheric Administration, Boulder, Colorado 80302

In December, 1976, a dual coherent 50 MHz auroral radar was installed at Siple Station to study backscattering from electron density irregularities in the E-region. Past studies have shown that the backscattering irregularities occur in areas where the auroral electrojet currents are being driven by the magnetospheric electric field, and that the irregularities move at nearly the same velocity as the E x B drifting electrons. Thus, spectral analysis of the Siple auroral radar signals provides information on the location and intensity of the auroral electrojet currents and the magnitude of the driving electric field. Since the electron density irregularities are aligned with the magnetic field and backscatter strongly in the perpendicular direction, the auroral radar beam must intersect the E-region nearly perpendicular to the earth's magnetic field. This perpendicularity requirement restricts most auroral radar observations to a narrow range of azimuths centered on the magnetic pole. However, at Siple the magnetic dip angle is considerably lower than for any L = 4 station in the northern hemisphere. Thus, the Siple radar beams can be pointed over a wide range of azimuths and still satisfy the perpendicularity requirement. This allows observations at Siple to be made both perpendicular and nearly parallel to the predominate east-west irregularity drift direction. The dual radar antenna beams are pointed approximately magnetic south and magnetic west. The south antenna beam covers a range from L = 5 to L = 9, and the west beam covers L = 4.5 to L = 5.5. Preliminary results show backscatter extending from 225 to 1100 km from Siple during disturbed periods. At some ranges the backscattered power is over 20 dB above the background noise level. Backscattering irregularity velocities in excess of 1000 m/s have been observed, implying driving electric fields of over 50 mV/m.

G3-3
1420

A NEW AURORAL RADAR IN ITHACA, NY: DESCRIPTION AND INITIAL OBSERVATIONS

W.E. Swartz, D.T. Farley, R.W. Reed, School of Electrical Engineering, Cornell University, Ithaca NY 14853, and B.B. Balsley, ERL, NOAA, Boulder CO 80302

An auroral radar system operating at 50 MHz with a power of $\gtrsim$10 KW and a long dipole array antenna has recently been established near Ithaca. The radar points north and can obtain echoes over a region which extends approximately from L=3.5 to L=5 and is close to magnetically conjugate to the area being probed by a similar radar operated by NOAA in Siple, Antarctica. Moreover, the Ithaca radar system is relatively portable and can be moved for special observation campaigns. The radar can be run unattended and can be automatically cycled through several modes of operation (e.g., single pulse power studies, double pulse mean velocity measurements, high PRF full spectral measurements). An inexpensive digital data processing system using a micro-processor and an electrostatic dot printer produces an on-line range-time-intensity plot of the averaged signal minus the averaged noise (thereby enhancing the effective S/N). This real time display of echoes well below the noise level has proven to be a very convenient feature of the system. The velocity and spectral data are automatically tape recorded and analyzed off line. Preliminary results will be presented.

G3-4
1445 DYNAMICS OF THE BAND OF CONTINUOUS AURORA AND AURORAL E-LAYER: J.A. Whalen and R.A. Wagner, Air Force Geophysics Laboratory, Hanscom Air Force Base, MA 01731

The continuous aurora (which is apparently the main contributor to the mantle aurora and the diffuse aurora) gives rise to the auroral E-layer (known also as night E and particle E). This aurora is a permanent feature of the night-time ionosphere forming an oval-like band which often extends across the day sector as well. Previous studies have found this band to very dynamic near midnight. The present work extends the investigation of the structure and dynamics of this band by means of an array of observation sites which span 12 hours of local time, 25° of latitude for observational durations of 12 hours. These observations include the AFGL Airborne Ionospheric Laboratory flying at constant local midnight employing ionospheric sounder and photometers; the network of ionospheric sounders in Greenland, Canada and Alaska; polarimeter measurements of total electron content using transmissions from ATS-3; keV particles measured on ATS-5; and auroral clutter measured by HF backscatter radar Polar Fox II. These measurements are supplemented by DMSP auroral photographs and ISIS-2 photometric maps and particle measurements. The band of continuous aurora undergoes large changes in latitudinal width (from 1° to 8° CGL), as well as large displacements in latitude. These displacements can be both symmetric and assymmetric about midnight, the latter implying a tilting of the night sector band as a whole. These dynamic features occur not only during substorms but also in periods of magnetic quiet. Changes in the band occur typically within 10 to 20 minutes and are simultaneous throughout the night sector and apparently at times throughout the day sector as well.

G3-5
1510

A REVIEW OF THE EVIDENCE FOR THE PREDOMINANCE OF SMALL SCALE STRUCTURES IN IONOSPHERIC DRIFT MEASUREMENTS.

J.W. Wright, Space Environment Laboratory, NOAA Environmental Research Laboratories, Boulder, CO 80302

A useful controversy continues between advocates of small- vs. large-scale structures as the cause of radio echo fading, by which drift velocities are obtained in the spaced-receiver experiment. Large-scale structures enjoy their affiliation with known modes of atmospheric gravity waves, but much radio and geophysical evidence, assembled and reviewed in the present paper, favors smaller scales.

G3-6
1535

DOPPLER-DRIFT MEASUREMENTS

Klaus Bibl and Bodo W. Reinisch, University of Lowell Center for Atmospheric Research, Lowell, Massachusetts 01854

Discrete Fourier transform of radio signals reflected at the ionospheric E-layer enables separation of simultaneously existing reflection areas. Comparing the change in time of the location of these reflection areas with the observed Doppler shifts shows significant dispersion in the motion of the E-region irregularities. The Doppler shifts imposed on the reflected signals is $d = 1/\pi\ \underline{k}\cdot\underline{v}$, where $\underline{k}$ is the wave vector and $\underline{v}$ is the velocity vector of the reflector. In the case of mid-latitude E-region reflections, the Doppler shift is predominantly determined by the motion of the small scale irregularities, since the amplitude of the large scale structure is small. Recent observations obtained with the new Digisonde 128PS will be discussed, including the effects of equatorial Es on F-region echoes. It appears that certain types of equatorial spread F are caused by or at least associated with the underlying Es-ionization.

G3-7
1600 THE INTERPRETATION OF FLUCTUATIONS IN IONOSPHERIC WAVE INTERACTION DATA: Michael P. Sulzer, Ionosphere Research Laboratory, The Pennsylvania State University, University Park, PA 16802

Possible physical causes of periodic fluctuations in data values from the wave interaction (cross-modulation) experiment are discussed. This experiment has been used for some years to measure electron densities between 55 and 90 km. and involves the use of a probe transmitter to sense electron temperature changes caused by the passage of a synchronized powerful radio wave transmitted from a second ground-based source on a different frequency.
In addition to the expected solar-induced diurnal variation in data values, other fluctuations are observed which are well above the experimental noise level and are often periodic in nature. Spectral studies show that although a purely random process may be responsible for some of the effects, a more deterministic cause must be sought for most. Analysis undertaken to recover height resolution at the expense of signal to noise ratio indicates significant correlation between periods at different heights exists in many cases. The fluctuations exhibit many of the properties attributable to the propagation of internal gravity waves, but a complete proof of this mechanism is not possible due to the single dimensionality of the data. The horizontal translation of a sequence of irregularities is also considered as a possible explanation.

G3-8
1625 SOME PROPERTIES OF INTERNAL GRAVITY WAVES AS REVEALED BY THE DISCRETE AND CONTINUOUS SPECTRA OF TRAVELING IONOSPHERIC DISTURBANCES: A. L. Hearn and K. C. Yeh, Department of Electrical Engineering, University of Illinois at Urbana-Champaign, Urbana, IL 61801.

Fluctuations of the F-region electron density in the gravity wave period range have been monitored using the Arecibo incoherent scatter radar. The radar was pointed in the vertical direction and a transmitted pulse of 50μs in length was used to provide one minute time resolution and 8.7km spatial resolution data in the altitude range of about 200km to 500km. Spectral analysis performed on the data reveals spectral peaks superposed on the background continuum. The power and phase profiles are extracted from the data corresponding to those spectral peaks that recur at nearly constant frequencies over the entire altitude range. This response in magnitude and phase was fit to an atmospheric model to yield the parameters of causative internal gravity waves. In many records the spectral continuum shows two kinds of persistent spectral dips for all heights. It will be shown that one kind of the spectral dip is caused by lack of the ionospheric response while the other is related to attenuation. In both cases the spectral dips occur in the frequency bands that are theoretically expected, based on the hypothesized excitation by gravity waves.

Commission J Session 2

INTERFEROMETRY AND APERTURE SYNTHESIS - II

Wednesday P.M., 11 January ECCR 1-40

Chairman: J.J. Wittels, Department of Earth and Planetary Sciences, Massachusetts Institute of Technology, Cambridge, MA 02193

J2-1
1330

MAPPING RADIO SOURCES WITH VLBI

J.J. Wittels, W.D. Cotton, C.C. Counselman, I.I. Shapiro, Department of Earth and Planetary Sciences, Massachusetts Institute of Technology, Cambridge, Mass. 02139
C.A. Knight, H.F. Hinteregger, A.E.E. Rogers, A.R. Whitney, Northeast Radio Observatory Corporation, Haystack Observatory, Westford, Mass. 01886
T.A. Clark, L.K. Hutton, C. Ma, Goddard Space Flight Center, Greenbelt, Md. 20771

Very long baseline interferometry (VLBI) presents additional difficulties over standard interferometry for the construction of radio brightness distributions, the primary difficulty being the lack of phase information. The use of closure phase data, obtainable using three or more antennas simultaneously, constitutes a partial solution, resulting in VLBI mapping techniques which bear a closer resemblance to conventional interferometric methods. We will briefly review the short history of VLBI mapping, from point-source models to "cleaned" maps. Common pitfalls of both the experimenters and the innocent perusers of the literature will be discussed. We will conclude with an examination of the data from sources that appear to be expanding with velocities greater than c, and what light future experiments can shed on these phenomena.

J2-2 1355 RADIO SOURCE STRUCTURES FROM LONG BASELINE INTERFEROMETRY

D.N. FORT, Herzberg Institute of Astrophysics, National Research Council of Canada, Ottawa, Canada, K1A OR6

At the present time the mapping of compact radio source structures using VLBI techniques suffers from two main problems - incomplete coverage of the transform plane of the brightness distribution and the lack of explicit phase information. A technique which utilizes the positive nature of brightness distributions and 'closure phase' measurements to help overcome these difficulties is described. The problem of ambiguous results is discussed.

J2-3 1420 MODELLING, AUTOCORRELATION, PHASELESS ITERATION, PHASE-CLOSURE, AND RELATIVE PHASE 18 CM VLB MAPPING

D. B. Shaffer, National Radio Astronomy Observatory, Green Bank, W. Va. 24944

We have analyzed a 7-station 18 cm VLBI experiment with several mapping techniques for sources of varying complexity. Sources with only a few components can be model fitted with high accuracy but require phase information to determine their orientation. CTD93 (a double) and 1611+34 (unresolved) were alternated on a 20-minute cycle, and it is possible to determine relative phase jumps in the visibility function of CTD93 by comparing the phases for the two sources. Thus, the 180° position ambiguity can be resolved.
More complex sources have been investigated by making autocorrelation maps to determine the relative position and strengths of components. The iteration technique of Fort and Yee (1976, Astronomy and Astrophysics, 50, 19), without and with closure phase has also been used. The maps that result from all these techniques are used to investigate the ease of use, reliability, and uniqueness of the various methods.

J2-4 OBSERVATIONS OF HYDROXYL MASERS WITH A VLB NETWORK:
1445 M. J. Reid, J. M. Moran, J. A. Ball, Center for Astrophysics, Cambridge, MA; A. D. Haschick, B. F. Burke, T. F. Guiffrida, A. Parrish, R. C. Walker, P. C. Crane, Dept. of Physics and Research Lab of Electronics, Massachusetts Institute of Technology, Cambridge, MA; K. J. Johnston, J. H. Spencer, E. O. Hulburt Center for Space Research, Naval Research Lab, Washington, D. C.; G. W. Swenson, Vermillion River Observatory, University of Illinois, Urbana, IL; D. C. Backer, Radio Astronomy Lab, University of California, Berkeley, CA; J. D. Romney, Owens Valley Radio Observatory, California Institute of Technology, Pasadena, CA; S. S. Hansen, University of Massachusetts, Amherst, and National Radio Astronomy Observatory, Green Bank, W. Va.; J. L. Yen, Electrical Engineering Dept., University of Toronto, Canada.

We conducted an 8-station VLB experiment at 1665 MHz in May 1976 to determine accurate positions and to study the structure of interstellar OH masers and extragalactic radio sources. We have measured over 100 pairs of delay and fringe rate from a dozen extragalactic "calibrators" in order to determine the relative locations of the stations and offsets and drift rates of the station clocks. The simultaneous solution for these station parameters using this large network substantially reduced correlations. The data, which was taken with a 2 MHz bandwidth, typically yield equatorial station coordinates accurate to $\lesssim$ 1 m, polar station coordinates to $\lesssim$ 4 m, clock offsets to $\lesssim$ 10 nSec, and clock drift rates to $\lesssim$ 5 nSec/day.
We have analyzed the fringe phase and rate data from several interferometer pairs to determine the absolute positions of the ground-state OH masers in W3(OH) and W75. The positions of these masers are accurate to $\lesssim$ 0".02. The OH masers in both of these sources are coincident with compact HII regions. Finally, we discuss the amplitude and phase calibrations needed to Fourier invert spectral-line VLB data. We intend to present high-quality Fourier inverted maps of the maser emission from W3(OH) and W75 with a synthesized beam of $\sim$ 0".01 diameter.

J2-5
1535

EVIDENCE FOR THE ZEEMAN EFFECT IN THE OH EMISSION FROM W3(OH):

J.M. Moran, M.R. Reid, C.A. Lada, Center for Astrophysics, Cambridge, MA, K.J. Johnston, J.H. Spencer, Naval Research Laboratory, Washington, D.C., and J.L. Yen, University of Toronto, Toronto, Ontario

We measured the spatial distribution of the OH maser emission at 6035 and 6031 MHz in a number of galactic H II regions with a three station very long baseline interferometer (VLBI). The maximum resolution was 0".01.
The map of W3(OH) at 6035 MHz contains about 22 components; 12 are predominantly right circularly polarized and 10 are predominantly left circularly polarized. Most of these components appear to be members of Zeeman doublets.
Each of the left circularly polarized features can be paired with a right circularly polarized feature having a velocity difference of about 0.3 km s^{-1} and offset by no more than 0".3. One of these pairs was previously suggested to be a Zeeman pair by Zuckerman et al. (Astrophy.J., 177, 59-78, 1972). The masing region has a diameter of 1".2 and is exactly coincident with a compact H II region.

J2-6 1600 AN APPRAISAL OF BROUW'S COORDINATE SYSTEM FOR APERTURE SYNTHESIS

P. C. Crane, National Radio Astronomy Observatory, Green Bank, W. Va. 24944

We consider the coordinate system presented by Brouw (Ph.D. dissertation, University of Leiden, 1971) for use in the reduction of aperture-synthesis observations. The coordinate m ($\approx \delta-\delta_o$) is redefined so that (for an east-west array) the visibility function V and a modified intensity distribution are a Fourier-transform pair. We examine the relationship between the modified and true intensity distributions. Finally, we assess the utility of Brouw's coordinate system for a non east-west array, such as the Very Large Array.

J2-7 1625 OPTIMAL STATION LOCATIONS FOR VLBI APERTURE SYNTHESIS:

G. W. Swenson, Jr., Departments of Astronomy and Electrical Engineering, University of Illinois, Urbana, IL 61801

An intensive study has been conducted of the geometrical problem of siting an additional radio telescope to improve the aperture synthesis performance of the existing network of telescopes in the USA which are suitable for very-long-baseline interferometry. The existing network suffers from the absence of intermediate-length baselines, as a result of clustering of existing observations near the east and west coasts. The assumed criteria for choosing the site of a new telescope are that it must optimize the transfer functions (U-V diagrams) and synthesized beam patterns of the network of existing telescopes, and that it must be compatible with one or more VLBI arrays of idealized geometry which might someday be built. A large number of networks has been studied by computing transfer functions and beam patterns. A method has been developed of deriving a single-number "figure of merit" for a network. This parameter is useful for comparative evaluation of networks, but does not supplant the transfer function, which is considered to be the most sensitive indicator of array quality. It is shown that locations exist which satisfy the two siting criteria given above.

J2-8
1650

THE SPATIAL FREQUENCY COVERAGE OF SATELLITE-TO-EARTH INTERFEROMETERS

Y.L. Chow and J.L. Yen, Departments of Electrical Engineering, University of Waterloo, Waterloo, Ont. N2L 3G1, and University of Toronto, Toronto, Ont., Canada

Recently it has been found that ground-based very long baseline interferometers have insufficient resolution to study certain compact radio sources. Satellite-to-earth interferometers must be used to provide the necessary resolution. We investigate the spatial frequency coverage of various satellite orbits as a guide to the design of such interferometers.

Unlike that of a ground-based interferometer, the two elements of a satellite-to-earth interferometer need not have the same rotational rate or axis. A different technique is therefore required to find the spatial frequency coverage. The technique is to consider the projected orbits of the satellite and the ground element as two line arrays on the spatial frequency plane. The boundary of correlation of the two arrays gives the spatial frequency coverage.

The general characteristics of spatial frequency coverage of typical satellite orbits, both neglecting and taking into account the effect of earth shadowing, are presented. In contrast to ground-based interferometers, the spatial frequency coverage depends not only on the declination of the source but also on its right ascension. An example for a source at 0° declination with ground element located at 45° N latitude and a polar satellite orbit is shown below. Note the presence of holes in the coverage. The avoidance of such holes will be also discussed.

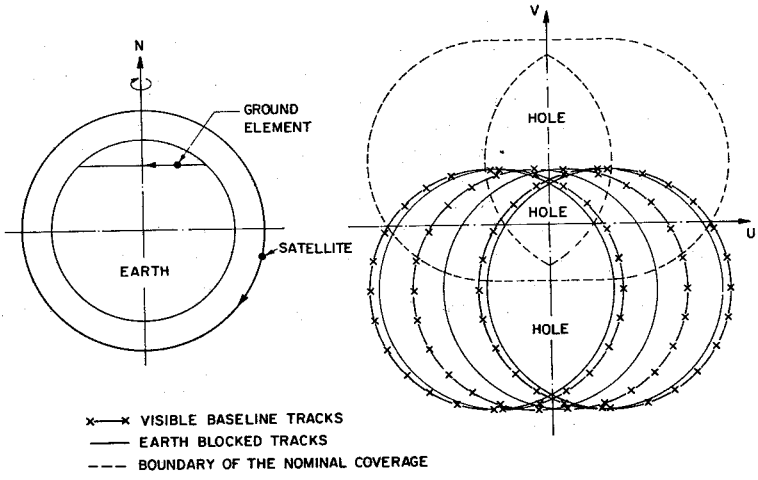

WEDNESDAY EVENING, 11 JAN., 1930-2200

Commission A Session 2 (Special)

NEAR-FIELD ANTENNA MEASUREMENTS

Wednesday Eve, 11 January UMC Forum Room

Chairman: P.F. Wacker, National Bureau of Standards, Boulder, CO 80302

A2-1 1930 COMPARISON OF NEAR-FIELD ANTENNA MEASUREMENT TECHNIQUES

C.F. Stubenrauch, National Bureau of Standards
Boulder, Colorado 80303

Near-field techniques are becoming more commonplace in measurement of antenna parameters. Several scanning geometries are compared (planar, cylindrical and spherical) on the basis of equipment and facility requirements, computational requirements including data requirements, computer resources and running times. Near-field techniques will also be compared to conventional far-field measurements.
Because the near-field formulation employs basis functions which are exact solutions of Maxwell's equations, no approximations such as small angle or Kirchoff diffraction are included. Thus, computed fields are consistent with Maxwell theory, and measurement and computation efforts can fully utilize a priori information. Because the theoretical basis is well established for these near-field measurements, various approximations and sources of error (e.g., finite scan area, truncation of an infinite set of modes, and various equipment related errors such as amplitude, phase and positional uncertainties, etc.) can be quantitively accounted for readily. Near-field measurements are typically performed in an indoor laboratory environment and thus are subject to laboratory control. Furthermore, since near-field techniques involve close coupling, errors introduced by scattering from ground or nearby objects are greatly reduced and absorber may be placed normal to the radiation so as to maximize its efficiency. Since the probe and antenna are closely coupled, signal to noise ratios can be high thus greatly reducing random errors due to noise. In contrast to far-field techniques where proximity effects are often ignored or corrected for empirically, near-field techniques provide for a full correction for proximity effects. Certain limitations also pertain to near-field scanning techniques. At low frequencies (below a few hundred megahertz) the primary problem is in the lack of suitable absorber, while in the millimeter range and beyond, measurement of phase and more stringent requirements on the probe transport mechanism

become problems. In addition to the advantages and limitations of near-field techniques, a comparison between the most common scanning geometries will be presented.

A2-2
2000

DESCRIPTIVE SURVEY OF NEAR-FIELD ANALYSIS: PLANAR, CYLINDRICAL, SPHERICAL, & EXTRAPOLATION:

Paul F. Wacker, National Bureau of Standards, Boulder, Colorado 80302

Near-field scanning on planar, circular cylindrical & spherical surfaces, like the extrapolation method for gain, is based upon a very comprehensive theory with few assumptions & idealizations & no approximations except truncation of the infinite set of exact global solutions (modes) of the differential eqn(s). (Maxwell's for the EM case). For spherical scanning the sets routinely used are mathematically complete except for supergain modes. Such solns. permit measurements to be confined to a surface and, in the EM case, to two vector components. Full correction is routinely made for the probe pattern, proximity and mismatch effects, and, in the extrapolation method, for multiple reflections. Highly efficient algorithms yield in minutes the complex coefficients of tens or hundreds of thousands of modes & the associated far field. For spherical scanning & the extrapolation method, least squares fitting is routinely used. The information routinely obtained from scanning permits one to compute (a) phase & amplitude (e.g., of the 6 EM components) as fncs. of position in the near, intermediate, & far field, (b) transducer loss, e.g., of a radiometric antenna, & (c) for a transducer pair, the complex received signal as a fnc. of separation & relative orientations, say for cosite interference. Contrary to existing literature, no assumptions are made concerning the fields (e.g., in terms of wave impedance), the magnetic pickup by the probe is not neglected, and reciprocity is not required.

Data processing consists in large part of soln. of complex simultaneous eqns., one for each separation & orientation pair & one complex unknown for each modal coefficient. Each eqn. includes the transformation of each modal coefficient under coordinate translation, rotation, and/or reflection. Such transformations are carried out for each and every measurement point -- tens or hundreds of thousands for scanning. These transformations are largely responsible for the complexity of the analysis, e.g., in the spherical case, transformation of the 3D vector modes under the three Eulerian angles and particularly radial translation.

In scanning, translation along the probe axis is carried out, leaving only the simpler transformations under the scanning operations. For measurement lattices equally spaced in each of 2 coordinates, the transformation coeffs. are orthogonal on the lattice, and data processing consists essentially of FFT's, supplemented in the spherical case by matrix multiplication.

A2-3
2030

Current Status of Near-Field Antenna Measurements

Allen C. Newell, National Bureau of Standards
Boulder, Colorado 80302

Successful implementation of near-field techniques requires a well founded theoretical basis, efficient computer programs to process the large amounts of measured data, and practical measurement systems which will measure the required data to sufficient accuracy in a reasonable amount of time. Significant progress in all of these areas for planar, cylindrical, and spherical measurement surfaces has resulted in new and powerful approaches to antenna measurements. The current status of measurement systems, recent results, and applications for each of the three types of near-field measurements are reviewed. Extensive work on planar measurements has resulted in its implementation in a number of laboratories. The mechanical probe transport is the major part of the system in terms of cost and size. A number of these have been constructed with scan areas up to 4.5m square with position accuracies on the order of ± 0.01 cm. A portable scanner has recently been built which combines a total measurement system with on-line data processing capability in a highly mobile assembly. The planar technique has been successfully applied to a wide variety of antennas including reflectors, phased arrays, shaped beam, and circularly polarized designs at frequencies from about 1 GHz to 65 GHz. Planar measurements have also been valuable in the initial testing and adjustment of complex feed arrays. Through error analyses and comparitive measurements which verify the high accuracy of the planar method have been completed.
One of the main advantages of non-planar methods is the less complicated probe transport mechanism required. A conventional rotator may be used to replace part or all of the probe motion by rotating the antenna in a "self scan" arrangement. In cylindrical measurements the probe must still be moved along a single axis which must be aligned parallel to the axis about which the antenna is rotated. Measurements made using this technique have shown it to be feasible and probably capable of high accuracy. The spherical technique offers the simplest scanning mechanism for antennas that can be rotated about two orthogonal axes. One must align the axes of the rotator so that they are orthogonal and intersect, and for efficiency of data processing it is desirable to direct the main beam of the antenna along the ϕ-axis. Criteria have been developed to specify the data point spacing and size of the scan region for a given antenna and angular region of interest. Measurements have been performed using this technique on a limited number of directive and broad beam antennas which have demonstrated the feasibility of spherical measurements and data processing schemes. As with cylindrical, considerable work needs to be done in annalyzing sources of error before this technique can be widely used.

A2-4
2100

NEAR-FIELD MEASUREMENT APPLICATIONS AND CURRENT RESEARCH AT GEORGIA TECH: E.B. Joy and W.M. Leach, Jr., School of Electrical Engineering, and D.G. Bodnar, C.F. Burns, F.L. Cain, J.L. Edwards, R.C. Johnson, and C.E. Ryan, Engineering Experiment Station, Georgia Institute of Technology, Atlanta, Ga. 30332

This paper reviews in a tutorial fashion Georgia Tech's applications and planned applications of the near field measurement technique and ongoing research to further develop the near field measurement technique. The applications include: 1) Measurement of near field scattering from cylinders and complex-shaped obstacles such as shipboard open masts located in the near field of antennas to determine the effects of such objects on the antenna patterns; 2) Measurement of the near field of antennas when excited with out-of-band frequencies; 3) Conceptual design of a portable cylindrical near field range for large NASA antennas; 4) Cylindrical near field measurement of broad beam antennas; 5) Computational efficiencies developed using band pass filtering for the calculation of near field antenna distributions; 6) Optimization of the dielectric loading of horn antennas for pattern synthesis; and 7) Development of a computational technique to reduce angular scintillation of tracking radars in the near field of complex targets.

Applications which are planned include: 1) Optimization of phased array antenna performance through near field measurement and analysis of phased array element mutual coupling; 2) Reduction of monostatic radar-crossection data requirements made from near field measurements; and 3) Further refinement of minicomputer software and hardware for processing near field data to permit quasi-real-time presentation of calculated far field patterns.

The current research areas include: 1) Development of a method for the analytic compensation of probe positioning errors for planar systems. Such compensation would simultaneously decrease the cost of probe positioning systems and increase the accuracy of the calculated far field patterns; 2) Development of a synthesis procedure for the design of optimum near field measurement probes for planar systems; 3) Derivation of a least upper bound on the far field pattern calculation error for near field measurements made on a finite portion of an infinite planar surface; and 4) Development of a focusing procedure for reflector antennas using cylindrical surface near field measurement data. This procedure will detect unfocused conditions and calculate the defocused position of the reflector feed antenna.

Commission A (Joint with D) Session 3

APPLICATIONS AND STATISTICS

Thursday A.M., 12 January ECCR 2-06

Chairman: Kenneth M. Evenson, National Bureau of Standards, Boulder, CO 80302

A3-1
0900

JOSEPHSON EFFECT MIXERS AT 130 GHz

J. H. Claassen and P. L. Richards, Dept. of Physics, University of California, Berkeley, CA 94720

Detailed quantitative measurements have been made of the properties of Nb point contact Josephson junctions operated as heterodyne system mixers at 130 GHz. The best performance observed was a single side-band conversion loss of 5.2 dB with a mixer noise temperature of 180K. These measurements, along with previous ones at 36 GHz and work done elsewhere at 115 and 300 GHz, combine to give a fairly complete experimental picture of the performance of Josephson effect mixers. In most cases the device performance is better than has been achieved with competing technologies. Our results have been compared to analog computer simulations based on the resistivity shunted junction (RSJ) model. These calculations have been considerably extended, to include the effects of strong microwave coupling, non-thermal noise sources (shot noise or photon fluctuation noise), and saturation effects. The observed noise in our junctions is usually within a factor 2 of the prediction assuming thermal driving noise. Uncertainties about the matching cirucit used in the experiments make it more difficult to compare the observed conversion loss with the calculations, but rough estimates imply agreement again within a factor 2. There is some evidence, however, that junctions whose resistance exceeds ~60 ohms are not well described by the RSJ model. Definitive comparisons with predictions of strongcoupling effects could not

be made due to limitations of the rf matching circuit. It was found that the rf coupling bandwidth must be limited to avoid saturation even with a room temperature source, in agreement with the modelpredictions. Estimates of the improvement in performance that can be expected with stronger rf coupling and more nearly ideal junctions will be made.

A3-2
0930

CHARACTERISTICS OF HIGHER-ORDER DFB LASERS

D. L. Jaggard, California Institute of Technology
Pasadena, California 91125
G. A. Evans, University of Washington
Seattle, Washington

We consider the threshold lasing characteristics of distributed feedback (DFB) lasers at higher Bragg orders through the use of the extended coupled waves (ECW) theory. The ECW equations allow the phase mismatch and the coupling coefficient to be calculated at all Bragg orders for any longitudinal periodic perturbation of the index or gain. Explicit expressions are given here for the coupling coefficient, phase mismatch, threshold gain and longitudinal mode spectra at the first three Bragg orders. Typical singly-periodic and multiply-periodic structures are considered. The analysis reduces to the well-known results of Kogelnik and Shank (J. Appl. Phys. 43, 2327, 1972) at the first Bragg order.

The results indicate that the mode spectrum is shifted away from the exact Bragg resonance for higher Bragg orders and that the threshold gain in the low-gain approximation is dependent upon Bragg order and coupling type. In particular, the use of both index and gain coupling can reduce the threshold gain in certain cases and can also remove mode degeneracy. The use of multiply-periodic structures significantly reduces the threshold gain at certain higher Bragg orders as shown in the example below.

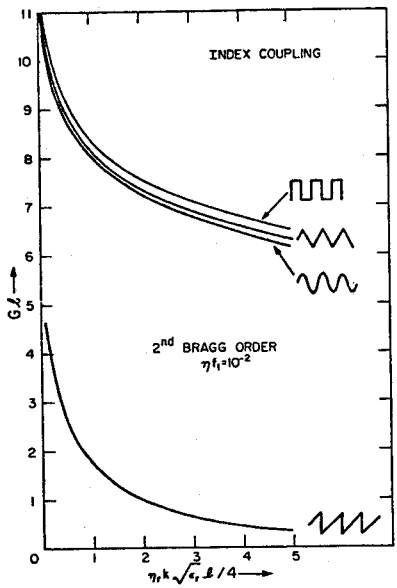

Threshold gain ($G\ell$) as a function of normalized length ($\eta_r k\sqrt{\epsilon_r}\,\ell/4$) for several profiles at the second Bragg order with index coupling and a perturbation $\eta f_1 = 10^{-2}$. Note the lowered threshold gain of the sawtooth profile over that of the sinusoidal, triangular or square-wave profile. This is due to the finite Fourier component of the sawtooth profile at the second Bragg order.

A3-3 1000 CURRENT VERSIONS OF LARGE (10^5-10^6 CHANNEL) MCSA'S FOR SETI APPLICATIONS: J.C. Tarter, J.N. Cuzzi, D.C.Black, M.A. Stull, NASA-Ames Research Center, T.A. Clark, NASA-Goddard Space Flight Center, and F.D. Drake, Cornell University

This paper describes the adaptation of two pre-existing technologies to produce multi-channel spectrum analysers (MCSA's) which achieve frequency resolution of 1 to 5 Hz over bandwidths of several MHz. These MCSA's are intended specifically for use in a limited high sensitivity Search for Extra-terrestrial Intelligence currently being conducted at several NASA centers. Both techniques depend on the use of high speed tape recorders at radio observatories to collect and save raw data for subsequent non-real-time analyses. Observations recorded at Arecibo, Puerto Rico with a modified Ampex VR7500 were Fourier transformed using an Optical Spectrum Analyser at the Environmental Research Institute of Michigan. The resulting power spectra for 23 objects have frequency resolution of 1 Hz over a bandwidth of 4 MHz centered on 1666.4804 MHz (rest frequency at the sources) and achieved a 12σ sensitivity to narrowband signals of $\sim$1.E-25 W/sq m in 15 minutes of telescope integration time. One-bit sampled digital data was recorded at a rate of 720,000 bps onto computer compatible tape using a Mark-I VLBI* recorder at the 300 ft antenna of NRAO, and these data were then transformed by software implementation of an FFT algorithm on the CDC 7600 computer at Ames Research Center. The resulting power spectra for several hundred objects have a frequency resolution of 5 Hz over an effective bandwidth of 1 MHz constructed from four nearly contiguous bandpass filters between 1665 and 1667 MHz (rest frequency at the sources) and achieved a 12σ sensitivity to narrowband signals of $\sim$1.E-23 W/ sq m in 4 seconds of telescope integration time. To date the spectra have revealed no reproducible evidence of ETI signals although several instances of RFI were encountered.

* very long baseline interferometry

A3-4
1030 MINIMUM MEAN SQUARE ERROR BAYESIAN ESTIMATION OF DUAL INDUCTION MODEL PARAMETERS: M. L. Rhoades and E. A. Quincy, Department of Electrical Engineering, University of Wyoming, Laramie, WY 82071

Bayesian parameter estimators are formulated for one or two parameter linearized responses. A quadratic cost function is used to guarantee a minimum mean square error estimate. The estimator is derived as a closed form expression where gaussian statistics were employed to represent the a priori knowledge about the parameters and the additive noise was assumed gaussian. In order to evaluate performance closed form expressions for the variance and mean square error are derived. The estimators are shown to be unbiased. To initially investigate the estimators, their asymptotic behavior for sample size and "signal-to-noise" ratio is studied. To further investigate the estimators and to show examples of their application, model response of underground coal burns sensed by remote electromagnetic induction techniques (E. A. Quincy and D. F. Moore, IEEE Trans. Geosc. Electron, GE-14,4, 236-243, 1976) are subjected to the estimation algorithms. The single parameter estimator is applied to estimate the radius of the conducting infinite length cylinder from noisy induction responses. The dual parameter estimator is applied to estimate the length and width of a buried conducting box of known thickness. Induction responses for the box were obtained from computer calculations on a simulated model employing a wire grid (J. H. Richmond, Ohio State University, Annual Report 4491-3, May 1977.
The responses are first linearized and then the linear response is used to reduce the variables present that influence error. In this manner, the actual estimator errors are more easily observed. The estimator is tested using accurate and inaccurate a priori estimates. Resulting estimates are obtained at a variety of sample sizes and "signal-to-noise" ratios. Bias, mean square error (MSE) and variance are evaluated to show three-dimensionally the performance of the estimator at the different sample sizes and "signal-to-noise" ratios. From the performance, observations are made about the speed and accuracy of the estimator. Causes of error in the estimators are discussed.

A3-5 1100 A COMPARISON OF SEVERAL ESTIMATES OF PROBABILITY DENSITY FUNCTIONS: R. F. Kubichek and E. A. Quincy
Department of Electrical Engineering, University of Wyoming, Laramie, WY 82071

Five estimates of probability density functions are described and compared using intergral square error criteria. An accurate approximation is important to the solution of problems such as pattern recognition and parameter estimation. Two of the estimates involve finding coefficients of an expansion of basis functions. Simulations are run using random numbers from normal, Rayleigh, and lognormal distributions to provide various degrees of skewness. It is shown that an averaging technique provides faster convergence and a better fit than a method using potential functions although performance drops off for the more highly skew cases. It is also shown that, as expected, including more terms of the expansion reduces the estimate error.

The three remaining methods give point estimates. The Parzen estimate is simulated and graphs are presented which show estimate error versus the number of samples used and error versus various values of the "smoothing parameter". These results demonstrate that the Parzen estimate provides an excellent idea of the shape of the parent distribution but has the drawback that selection of the proper smoothing parameter is not straightforward. A similar error analysis was performed using the "nearest neighbor" technique. The simulations indicate that the selection of the number of nearest neighbors determines the noisiness or smoothness of the estimate. A smaller number of nearest neighbors results in an estimate with a much larger variance while a larger number of nearest neighbors gives smaller variance but a poor fit at the tails of the density function. A substantially larger number of samples is required for the nearest neighbor estimator than for the Parzen estimator in order to achieve a comparable approximation.

Finally, a histogram with variable cell size is examined and performance is checked against a fixed cell histogram. Examples show that more detail is often provided by the variable cell histogram for the same number of cells than is given by the fixed cell histogram. The flexibility of this approach is given by its ability to adjust the number and size of the cells to characteristics of the data. Examination of estimate error however, indicates that the accuracy of the histogram is highly sensitive to the selection of the parameters determining cell growth.

Each technique is extended to the multivariate case and a two-dimensional example is given.

Commission B Session 6

GROUND EFFECTS

Thursday A.M., 12 January ECCR 2-28

Chairman: Prof. A.Q. Howard, Department of Electrical Engineering, University of Arizona, Tucson, AZ 85721

B6-1
0830 ANALYSIS OF BURIED INSULATED THIN SHIELD COAXIAL CABLE FOR USE IN AN EXTREMELY LOW FREQUENCY TRANSMITTING ANTENNA: Ruey-Shi Chu and Ronald V. Row, Communication Systems Division, GTE Sylvania Inc., Needham, MA 02194

In the SEAFARER ELF communication system, an insulated thin shield coaxial cable buried in the ground is one candidate being considered for antenna cable of the transmitting system. It is anticipated that such a circumferential shield will provide a significant level of protection of the main insulation system against lightning damage. In order to limit the current induced on the shield by normal system operation, the shield must be broken (segmented) at appropriate intervals. The influences of the shield segment length and end shield grounding impedances on performance of such an antenna cable are analyzed here. We first set up the EM field equations and solve the rigorous boundary-value problem to obtain the principal modes of propagation when this cable is buried in the ground. Two principal modes of propagation, γ_1 and γ_2, have been found. The propagation constant γ_1 is associated with the mode that the main current flows in the central core and the return current is principally through the shield. The propagation constant γ_2 is associated with the mode that main current flows in the combination of the shield plus the central core and the return current is only through the ground. When the shield thickness τ approaches to zero the propagation constant γ_1 reduces to γ_0, the propagation constant for the buried insulated wire solution, and the propagation constant γ_2 approaches to infinity, this means there will be no field quantities for mode γ_2. By applying the terminal conditions at z = o, the excitation end, and at z = 1, the load end, we determine the current and potential distribution induced on the shield by normal system operation. Comparison between the theoretical predictions and some experimental measurements on short lengths has been made and demonstrates the practical engineering utility of the theory.

B6-2
0850 SCATTERING AND DIFFRACTION BY A DIELECTRIC COVERED SLOT IN AN INFINITE PLANAR SCREEN:

R. D. Nevels and C. M. Butler, Department of Electrical Engineering, University of Mississippi, University, MS 38677

The problem considered here is that of an infinite slot in a conducting screen immersed in a dielectric slab of infinite extent and finite thickness. The electrical characteristics of the homogeneous dielectric slab are arbitrary. The slot is excited by an incident plane wave TE/TM to its axis. Integral equations are first formulated for the electric field in the aperture for the general case of the aperture in the screen situated at $z = 0$ and centered in a slab of width $2h$. Integral equations are next obtained for the two limiting cases where the dielectric thickness is allowed to recede to zero, first on one side of the screen (i.e. $z < 0$) and then on the other side (i.e. $z > 0$). The integral equations are solved numerically with particular attention paid to singularities of the resulting Sommerfeld integral kernel. Results are presented for selected cases of interest.

B6-3
0910

RADIATION AND MUTUAL COUPLING BY VERTICAL MONOPOLES OVER A COATED PERFECT CONDUCTOR.

N.K.Uzunoglu,J.G.Fikioris and N.G.Alexopoulos,Department of Electrical Engineering,National Technical University of Athens, Athens 147,Greece.

Radiation from an array of vertical monopoles, fitted on a dielectric sheet of thickness B which is mounted on a perfect conductor surface is considered.
In order to determine the field produced by assumed sinusoidal current distributions on these antennas we determine first the Green's function $G(\underline{r},\underline{r}')$ for a unit excitation vertical dipole.The evaluation of $G(\underline{r},\underline{r}')$ is based on Sommerfeld's method. Boundary conditions on the perfect conductor and on the dielectric-air surfaces are satisfied.The computation of $G(\underline{r},\underline{r}')$ involves integrals of the form

$$\int_0^\infty du\ f(u)\ J_0(ur) \qquad (1)$$

where f(u) is a function of electrical and geometrical quantities.The direct evaluation of these integrals by numerical methods is rather costly. By using superposition principle it is possible to determine the electric field $\underline{E}(\underline{r})$ at any point. For $|\underline{r}|\to\infty$ the far field behaviour of the radiation field is obtained by using the "stationary phase integration" approach for points $z \gg z'$.For an element of the array the radiation field is obtained in the form

$$E_\theta = \frac{\exp(ikR)}{R} f'(\theta) \qquad (2)$$

Finally in order to determine the self and mutual coupling impedances we employ the EMF method.This requires precise computation of the integrals similar to those of eq.(1).In order to do this we employ complex contour integration by taking into account the surface modes and the u =k branch cut contributions.

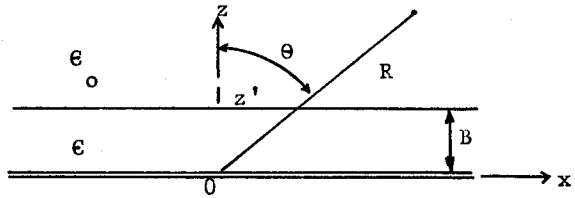

B6-4
0930

A NEW SERIES SOLUTION FOR SOMMERFELD INTEGRALS IN A TWO MEDIA PROBLEM*:

J. N. Brittingham and J. T. Okada, Lawrence Livermore Laboratory, University of California, Livermore, CA 94550

In a recent paper [A New Series Solution for a Hertzian Dipole on an Interface, J. N. Brittingham and E. E. Alexander, IEEE-APS, International Symposium, Stanford, California, June 1977] a series representation was developed for the Sommerfeld integral when the field-point and source-point were on the interface. This paper extends this series development to the case where the field-point and the source-point are above the interface. The series is developed by introducing a parameter (the difference in the branch-points of the integrand) into the integrands, then expanding the integrand in a Taylor's series in the new parameter. The infinite series and the integration are interchanged to give a new infinite set of integrals. The series can be shown to be absolutely convergent for a large range of electrical parameters irrespective of the spatial coordinates. The new integrals can be further reduced to make the numerical evaluation of the series possible.

The numerical evaluation of this series has been developed and is compared to the values obtained by integrating the Sommerfeld integrals numerically. Although the numerical implementation of this series makes it inappropriate for evaluating these integrals at all points above the interface, it is an appropriate procedure when the field-point and source-point are both very close to each other and the interface. This is the region that must be evaluated efficiently before the effects of finite length ground screens on antennas can be studied numerically.

B6-5 1020 PARAMETRIC EVALUATION OF ANTENNAS NEAR GROUND*:

J. N. Brittingham, E. K. Miller and J. T. Okada, Lawrence Livermore Laboratory, University of California, Livermore, CA 94550

A method was recently developed by the authors [A Bi-variate Interpolation Approach for Efficiently and Accurately Modeling Near a Half-Space, J. N. Brittingham, E. K. Miller and J. T. Okada, IEEE-APS, International Symposium, Stanford, California, June 1977] for improving the efficiency of computer modeling antennas located near ground. This approach can greatly reduce the computer time associated with the rigorous analysis of such problems by using an interpolation procedure to obtain the required Sommerfeld-integral values. Because the interpolation grid which is employed is independent of antenna geometry, it can be set up once and used for repeated parametric evaluations.

In this paper we exploit this capability, coupled with an integral-equation approach, to parametrically analyze several antenna types. We first employ the procedure to model the simpler problems represented by vertical and horizontal electric dipoles, varying parameters such as their height above the ground. Next, we model more interesting antennas like the vertical half rhombic and slanted Vee, which are frequently employed in communication systems. Finally, we demonstrate the procedures utility for the ground-screen problem, by explicitly including in the antenna model the wires in the ground screen, a radial system for example. The advantages of the approach in this case include a straightforward way to include the screen's finite extent upon both the antenna's current distribution and radiated fields.

B6-6
1040

A NUMERICALLY EFFICIENT SCHEME FOR COMPUTING THE TRANSIENT RESPONSE OF AN ELECTRIC DIPOLE OVER A LOSSY GROUND:

H.A. Haddad and D.C. Chang, Electromagnetics Laboratory, Department of Electrical Engineering, University of Colorado, Boulder, CO 80309

In this paper, the problem concerning the propagation of an electromagnetic pulse, as emitted from an electric Hertzian dipole located on a lossy ground will be presented. For a lossless dielectric half-space, the exact solution of a delta-function source can be given analytically in closed form in terms of waves arriving from direct path in air, through the dielectric space and in a form of lateral waves along the interface (B. Van der Pol, IRE, AP-4, #3, 288-293, 1956). However, only approximate solutions are known when one extends the problem to include the losses in the half-space, and even then, only for a highly conducting earth with no explicit error estimate (J.R. Wait, IEEE-GAP, AP-13, #6, 904-918, 1965; D.C. Chang, tech. Rept. 8, EE., U. Colo., 1973). It turns out that in order to compute the response accurately one needs first to evaluate the so-called Sommerfeld integral numerically which is of the following form:

$$\int_{-\infty}^{\infty} [k_o^2(\alpha^2-k_1^2)^{\frac{1}{2}} + k_1^2(\alpha^2-k_o^2)^{\frac{1}{2}}]^{-1} \, H_o^{(1)}(\alpha\rho)\alpha d\alpha$$

where $k_o = \omega/c_o$, $k_1 = [\omega(\omega+i2\Delta)]^{\frac{1}{2}}/c_1$

c_o is the speed of light in free space

c_1, Δ are respectively the speed of light and relaxation parameter of the lossy half-space

for a given frequency, and then integrates over the entire frequency spectrum. Thus, the numerical computation involving double infinite integrals can indeed be prohibitive. In this paper, it is shown how the Sommerfeld integrals can be changed into terms that correspond to arrival time between $\rho/c_o < t < \rho/c_1$, where ρ is the distance between the source and observation point, and terms that arrive after $t = \rho/c_1$. With the use of the time causality principle, these terms can be readily reduced to double finite integrals, instead of infinite ones, with integration limits related to the arrival times as well as the relaxation parameter. Our result actually reduces to the closed form expression of Van der Pol's in the case of lossless dielectric half-space. It also agrees with our earlier expression for the highly conducting case. Numerical results corresponding to a dissipative earth will be presented.

B6-7
1100

LOADED HORIZONTAL ANTENNA OVER AN IMPERFECT GROUND

Y. Rahmat-Samii, P. Parhami, and R. Mittra
Electromagnetics Laboratory, University of Illinois
Urbana, Illinois 61801

Loaded wire antennas often find applications in EMP simulators, particularly open simulators. The basic design requirement of an EMP simulator is the generation of a temporal signal matching the waveform of an exoatmospheric burst. Such waveforms are typically characterized by the rise and fall times that are on the order of tens and hundreds of nsecs, respectively. One of the fundamental limitations on the use of wire simulators is imposed by the undesired reflections off the ends of the antenna. The adverse effects of these reflections on the radiated pulse shape are predominantly felt during the early time period. The transient response of the antenna during this time period is governed by its high frequency response.

One possible scheme for minimizing the end reflections is to load the antenna with nonuniform resistive loading. Many different loading functions have been proposed and investigated (Liu. et. al. S.S. Notes, Note 178, Feb. 1973; Tesche S.S. Notes, Note 177, May 1973) for antennas in free space. These authors have shown that a desirable loading function takes the form: $\Lambda(x) = \Lambda_0 (1 - |x|/L)$, where x is measured along the antenna and 2L is its length.

In this paper we investigate a more realistic model of an open simulator, viz., a wire antenna over a lossy imperfect ground, and analyze the effect of continuous, resistive loading of the antenna with the loading function $\Lambda(x)$ of the form given above. We show that there exists an optimum choice for the parameter Λ_0 and devise a novel technique for determining this constant. We employ the Fresnel reflection coefficient approach in conjunction with the E-integral equation for the loaded wire problem and solve for the current distribution on the antenna as a function of the parameter Λ_0. Since, for critical loading, the phase distribution of the current is known to be almost linear, we take advantage of this fact to determine Λ_0 in the following manner. As a first step, we numerically interpolate the phase curve and obtain the best-fit straight line. We then minimize the deviation between the phase curve and the best-fit straight line in the least square sense by varying the parameter Λ_0. The resultant phase curve for the optimum choice of Λ_0 is found to be very nearly linear with the exception of the neighborhoods of the feed and the end-points of the antenna, indicating an almost reflectionless current distribution on the wire. Extensive results are given in the paper for the antenna current, input impedance, radiation pattern, etc., for the critical loading case with the antenna dimensions and ground parameters as parameters.

B6-8 SCATTERING BY A BURIED SPHERE

1120 S.K. Chang, Science Applicatons, Inc., Berkeley, CA 94701; K.K. Mei, Department of Electrical Engineering and Computer Sciences, University of California, Berkeley, CA 94720

Classical solutions of a sphere in free space are solved by using the expansions of the conventional spherical vector waves. These types of expansions are not suitable for a buried sphere, because the planar boundary is not a natural surface for the spherical vector waves.

This paper presents a Multipole Expansion Technique (MET) which solves the scattering by a buried sphere. The solutions are expanded in terms of the spherical multipoles in the cylindrical vector waves. The secondary fields are derived from the generalized Sommerfeld's integrals of the multipoles. Numerical results of both a buried dielectric sphere and a buried perfectly conducting sphere will be presented.

Using the MET, it is possible to calculate the near and far fields scattered by a buried sphere with a diameter up to several wavelengths. Buried objects of other shapes or with inhomogeneities can also be solved by using the MET in conjunction with the uni-moment method.

Commission C Session 2 (Invited)

COMPUTER COMMUNICATION NETWORKS:

DESIGN AND OPERATION

Thursday A.M., 12 January ECCR 0-36

Co-Chairmen: Dr. Ivan T. Frisch, Network Analysis Corporation; and Prof. Robert R. Boorstyn, Polytechnic Institute of New York (on leave at Bell Laboratories)

C2-1
0830 PROTOCOL ISSUES AND DATAPAC: Peter Cashin, Manager, DMS Control System Development, Department No. 7020, Bell Northern Research, P.O. Box 3511, Station C, Ottowa, Canada K1Y4H7

The evolution of packet-switched networks for computer communications has involved the development of a wide range of communication protocols. The definition of these protocols and how they should fit together and be standardized has been the subject of considerable debate. These issues are discussed in terms of the development of the protocols for the TransCanada Telephone System's Datapac public packet-switched data communications network. This network illustrates how several layers of protocols are used to support the various interfaces by the subscriber terminals and host computers.

C2-2
0855

RESOURCE MANAGEMENT IN SNA-LIKE NETWORKS

Martin Reiser, Thomas J. Watson Research Center, IBM
Yorktown Heights, New York 10598

In the first part, the structure and history of SNA (Systems Network Architecture) will be outlined. The layered architecture, routing strategy and evaluation from centralized trees to full meshed networks will be described. In the second part, problems of meshed networks will be described in some generality and research done at the Thomas J. Watson Research Center will be described.

1. Routing
2. Flow control, and
3. Network management and reconfiguration.

It is argued that flow control is among the most urgent problems in an environment where networks can be expected to be driven into saturation. This is so because uncontrolled networks have a tendency to break down in this regime (they may even exhibit total deadlock). It will be shown how deadlock can be avoided by suitable management of store-and-forward buffers and how degradation can be prevented by controlling entering messages.
A simple window scheme will be described and its analytical solution outlined. Connection between buffer management and flow control will be highlighted. Routing, a function to which most attention has been paid so far, will be shown to be a secondary resource management function, which performs best in a suitable flow controlled subnetwork.

C2-3 CONTROL STRATEGIES FOR COMPUTER NETWORKS

0920 Roy Rosner, DCEC, Attn. Code R310, 1860 Wiehle Ave., Reston, Virginia 22090, 703-437-2261

The United States Department of Defense, having successfully supported the development of packet switching for computer networking in the ARPANET, is presently engaged in the development of AUTODIN II, as an operational military computer and data communications network. Major differences exist between the message and transaction handling, the flow control, information security, priority structure, and overall system control of the ARPANET and AUTODIN II. This presentation will focus on the control philosophies and techniques employed in these two networks. The issue of control in packet networks is a broad issue since the nature of packet switching as a computer networking technique inherently distributes many of the traditional control functions throughout the network and imbeds them in the basic functional protocols used to assure traffic flow. Examples of this are routing control and flow (network/traffic) control. Simultaneously, prudent management calls for system overview to be provided by a high-level interface for a network control center (NCC). The role of NCC as an active "controller" or a passive "observer" to network function is a design choice which depends upon such variables as the homogeneity of the community of subscribers, the potential threat environment (from the viewpoint of security and computer crime) and reliability/survivability issues. This presentation will attempt to provide insight into these issues using the ARPANET technqiues as representative of the functionally homogeneous (e.g., all users members of the R&D community) benign environment, and AUTODIN II as representative of the functionally disjoint community of users operating under a variety of threats to security and network integrity. The AUTODIN II environment is not unlike that seen by a broad based carrier network serving the general public, while the more benign environment of the ARPANET would be characteristic of a more localized or limited network, serving the interest, for example, of a single corporation or agency.

C2-4 A COMPARISON OF TECHNOLOGIES FOR LOCAL ACCESS:
0945 Ivan T. Frisch, Network Analysis Corporation
130 Steamboat Road, Great Neck, New York 11024

For local transmission of signals from a nationwide interconnecting network, the user's technical problems are significant because many of the techniques are in the experimental stage. Often the problem is not just one of configuring facilities, but actually designing the channel. The classical technique of using multidrop lines with polling concentrators is available and in many cases the best strategy. But new techniques such as the use of rings or random-access multiplexing, such as in packet radio, offer better prospects in many cases. However, neither of these are standard techniques and hence protocols and hardware are in a developmental stage. Furthermore, new physical links are becoming available. Among the most promising of these is the coaxial cable of existing CATV systems.

In this paper, we illustrate the tradeoffs in selecting among several local access strategies: conventional techniques using concentrators, multiplexers and polling; ring networks; packet radio networks; cable television distribution systems; optical fiber systems; and satellite systems with local antennas.

Since local access costs are often the dominant component of system costs, these tradeoffs are critical in arriving at an optimal system design.

C2-5
1040

PERFORMANCE OF DISTRIBUTED MULTI-ACCESS COMPUTER-COMMUNICATION SYSTEMS

Leonard Kleinrock
School of Engineering and Applied Science,
University of California
Los Angeles, California 90049

We consider an environment of geographically distributed message sources which communicate with each other over a "common" broadcast channel of fixed total capacity. This geographic dispersion along with the random generation times for messages creates a difficult channel resource-sharing problem. In this presentation, we discuss the performance degradation resulting from this problem, present known results for various multi-access schemes, define a measure of the "effective" number of users, demonstrate that "mixing" of access schemes cannot provide an improvement, introduce and analyze a very effective dynamic reservation control access method, and finally present graphs showing the delay-throughput performance profiles in a fashion which displays the effect of the key system parameters.

C2-6
1105

MODELS FOR DATA COMMUNICATION

Alan Konheim, IBM Research
Yorktown Heights, New York 10598

In this talk we will consider the applicability of a class of discrete queuing models to the study of data communication systems. A data communication system is a service system in which the service operation (transmission) is made available to a class of customers (messages). The problem is to understand the relationship between the demands made upon the system, the service protocol, and the grade of service as measured by queuing delays and system utilization. We will review a number of simple models and develop techniques for modeling these phenomena.

C2-7
1130

BOUNDS ON THE NUMBER OF POSSIBLE DISTINCT NETWORKS:

Martin Nesenbergs, U.S. Department of Commerce, Office of Telecommunications, Institute for Telecommunication Sciences, Boulder, CO 80302

This study is concerned with the number of all distinct networks, also called connected graphs, or Cayley, or linear graphs that are possible for n given nodes. For any practical number of nodes, such as n=100, an explicit enumeration seems difficult if not impossible. It appears that the original work on the number N(n) of all possible distinct networks with labeled nodes was that of Riddell (R.J. Riddell, Jr., Contributions to the Theory of Condensation, Ph.D. Dissertation, University of Michigan, Ann Arbor, 1951). Riddell and other graph theorists showed that the number of disjoint graphs form an increasingly more insignificant fraction as n increases, and that asymptotically $N(n) \sim 2^{n(n-1)/2}$ for large n.
Here we offer improved bounds that enable tight approximation for n reasonably large. In particular, we review

$$(1-E_n)2^{n(n-1)/2} < N(n) < 2^{n(n-1)/2},$$

where E_n assumes several new and interesting forms. The tighter bounds show a relative error less than 10^{-26} for a network of hundred nodes, and less than 10^{-294} for thousand nodes.

Commission F Session 5

RADIO METEROLOGY

Thursday A.M., 12 January ECCR 0-30

Chairman: J. Goldhirsch, Applied Physics Lab, Johns Hopkins University, Laurel, MD 20810

F5-1
0830 MULTIPLE SCATTERING IN PROPAGATION THROUGH RAIN: D. V. Rogers, COMSAT Laboratories, Clarksburg, MD. 20734, and R. L. Olsen, Communications Research Centre, Ottawa, Canada K2H 8S2

For wave propagation through a sparsely populated, uniformly random medium of discrete scatterers, the expression for the coherent transmitted field is generally derived by explicitly or implicitly applying the single scattering approximation to successive thin layers of the scattering medium. It is often subsequently assumed that no multiple scattering effects are included in the resulting expression for the coherent transmitted field, and that this apparent neglect of multiple scattering is perhaps responsible for certain disagreements between theory and experiment for rain attenuation. In this paper, scattering quantities for the rain medium are analyzed, with particular attention given to an interpretation of the scattering processes involved. It is shown that the so-called "single scattering theory" actually accounts for all multiple scattering interactions that involve purely forward scattering processes. Numerical calculations, based on Twersky's "free-space" scattering formalism, are then presented to show that all other multiple scattering processes are negligible in the rain medium for frequencies up to at least 1000 GHz. It is therefore concluded that the classical formulation for calculating rain attenuation and phase rotation is quite accurate for the rain medium.

F5-2
0855 SIMPLE TECHNIQUES FOR THE PREDICTION OF RAIN DEPOLARIZATION STATISTICS: R.L. Olsen and W.L. Nowland, Department of Communications, Communications Research Centre, Ottawa, Canada, K2H 8S2

With the advent of satellite and terrestrial communications systems utilizing orthogonal polarizations to increase capacity, the need has arisen to determine the statistics of rain depolarization. Various workers have made calculations relating the differential attenuation and phase shift along the raindrop axes to rainrate, but because of the number of variables involved it has been difficult to present these calculations in a form which can be readily used to predict rain depolarization statistics. In this paper, the theoretical basis for simplifying the problem is discussed, and approximate, but accurate, prediction equations are presented. These equations allow statistics of cross-polarization discrimination (XPD) for earth-space paths to be calculated directly from rainrate statistics, or from attenuation or XPD statistics available for a different frequency, polarization, and elevation angle. For terrestrial paths both attenuation and rainrate statistics are normally required. The parameters in the equations were obtained for frequencies between 4 and 50 GHz from Oguchi's scattering amplitudes for both spheroidal and Pruppacher-Pitter form raindrops. Also, several negative-exponential dropsize distributions were employed in addition to the Laws and Parsons distribution. Suggestions are given regarding the application of these results, and some comparisons are made with experimental measurements.

F5-3
0920 MEASUREMENT OF THE INCOHERENT COMPONENT IN TRANSMISSION THROUGH RAIN

G.C. McCormick and A. Hendry, Division of Electrical Engineering, National Research Council of Canada, Ottawa, Ontario, Canada.

The two channels of a polarization diversity system permit the direct measurement of the coherency matrix. Such a system at 16.5 GHz has been used in an attempt to measure the incoherent component in transmissions over a link of 0.85 km length between high gain antennas during periods of very heavy rain. Previous attempts using circular polarization were negative. The experiment here described was performed using linear vertical polarization with the level in the cross-polarization channel initially set to as low a value as possible. In this way, cross-polarization levels of 35 - 50 dB were possible during rain with specific attenuations up to 15 dB/km. The incoherent component was found still to be at a barely detectable level. It was, typically, 50 dB below the coherent component for an integration time of 0.3 s and 60 dB down for an integration time of 22 ms. There were, however, some observations at the longer integration time when the incoherent level was apparently more than 55 dB below the coherent signal.

F5-4 RAIN ATTENUATION AT 74 GHz:
0945 M.M. Kharadly, J.D. McNicol and J.B. Peters
Department of Electrical Engineering, University of British Columbia, Vancouver, B.C., Canada V6T 1W5

This paper describes some attenuation measurements on an experimental transmission link at the University of British Columbia. The radar-type transmission path is almost horizontal and is 2 x 0.9 km long. The transmitted cw signal is horizontally polarized, the transmitting and receiving antennas are similar parabolic dish antennas and the reflector is 1 m square flat surface. A narrow-band phase-locked receiver is used and a clear-weather fade margin of about 40 db is obtainable. The instrumentation for weather parameters includes five tipping-bucket rain gauges of 0.05 mm tip size, a propeller type anemometer for measuring three components of wind velocity and a temperature transducer. The latter two instruments are placed at the transmitter-receiver location.
The level of the microwave signal and the outputs of the weather sensors are transmitted to a central station where thirty-two channels of data are recorded at one second intervals by a dedicated NOVA minicomputer data acquisition system, on ½ in. 9 track magnetic tape. Subsequently, data are further processed and analysed on an IBM 370.
Attenuation results obtained so far indicate reasonable agreement with values predicted from theory using well-known drop-size distributions for some storms, while for others, siginificant deviation is observed. Presently, a real-time rain drop size measuring apparatus is being constructed.

F5-5
1035

RADIOMETRIC DETERMINATION OF RAIN ATTENUATION AT MILLIMETER WAVELENGTHS:

Akira Ishimaru and Rudolf Cheung
Department of Electrical Engineering, University of Washington, Seattle, Washington 98195

Below 30GHz, the multiple scattering effect on radiometric measurement of rain attenuation is negligible compared with absorption and the total rain attenuation can be adequately determined from the temperature measurement using simple formula. At frequencies higher than 30GHz, however, the multiple scattering effect can not be ignored. This paper describes the calculations of the observed temperatures at the ground both for vertical and horizontal polarizations and for various rain drop temperatures, precipitation rates, ground temperatures, ground albedos, and frequencies ranging from 30 GHz to 120 GHz. The calculations are based on the equation of transfer taking into account the polarizations and the Stokes parameters. The cross sections of rain droplets are calculated using the Mie solution with the Laws and Parsons drop size distribution, and Saxton's formula for refractive index of water. For example, at 30 GHz, for the rain temperature of 273°K, the precipitation rate of 12.5mm/hr, the ground temperature of 283°K, and the rain layer thickness of 2km, the calculated temperature for vertical and horizontal components are found to range from 171°K to 260°K and 171°K to 257°K respectively as the observed direction varies from vertical to horizontal. But at 120 GHz, the observed temperatures for vertical and horizontal polarizations very from 248°K to 266°K and 248°K to 263°K respectively. Based on these calculations, the differences between the true rain attenuation and the attenuation calculated from the temperature measurements and the assumed rain temperatures are calculated showing the effects of various parameters.

F5-6 1100 EVIDENCE FOR THE QUADRATIC DEPENDENCE ON WATER VAPOR OF THE MICROWAVE ABSORPTION COEFFICIENT OF MOIST AIR.

E. R. Westwater and D. C. Hogg, NOAA/ERL/Wave Propagation Laboratory, Boulder, CO 80302

Excess attenuation in the wings of the 22 GHz water vapor line was first observed by Becker and Autler (Phys. Rev., 70, 300-307, 1946). Ad hoc multiplication of the nonresonant absorption contribution by a factor of ~5, and using conventional line broadening equations, accounts for some, but not all, of this excess. The parameters of the 22 GHz line have been measured by Liebe and Dillon (J. Chem. Phys. 50, 727-732, 1969). If the absorption from the 22 GHz line, calculated from Liebe and Dillon's measurements, is subtracted from the Becker and Autler data, the residual attenuation exhibits a strong quadratic dependence on absolute humidity. The coefficient and frequency dependence of the quadratic term are derived, and the resulting predicted absorption compared with measurements of Liebe (Office of Telecommunications, Report 75-65, 1975) and Hogg (presented at this meeting).
The implication of these results in radiometric remote sensing of water vapor are discussed.

F5-7 1125 MEASUREMENTS OF 70 and 80 GHZ ATTENUATION BY WATER VAPOR ON A TERRESTRIAL PATH: D.C. Hogg, NOAA/ERL/Wave Propagation Lab., Boulder, CO 80302

Knowledge of the behavior of attenuation by water vapor at millimeter wavelengths is of importance in communications, radio astronomy, and especially in remote sensing of the atmosphere. It has been accepted by many for years (see for example, D.E. Kerr "Propagation of Short Radio Waves," MIT Rad. Lab. Series, No. 13, McGraw-Hill, 1951, p. 661) that the attenuation bears a linear relationship to the amount of water-vapor in the air. But there is increasing evidence that the relationship has a significant square-law term. Attenuation measurements made in two-way transmission over a 1.5 km path using a calibrated dual-reflector method at 70 and 80 GHz are discussed. The measurements at both frequencies, taken over a range of water-vapor content 2 to 20 gm/m^3 strongly support the evidence of a square-law dependence.
Acknowledgement: The measurements were made in collaboration with R.H. Turrin of Bell Labs and the best-fit curves to the data were obtained by E.R. Westwater of WPL/ERL/NOAA.

F5-8
1130

CURRENT RESULTS OF 11, 19 and 28 GHz SATELLITE PATH ATTENUATION AND DEPOLARIZATION MEASUREMENTS:

C.W. Bostian, W.L. Stutzman, E.A. Manus, P.H. Wiley, R.E. Marshall, S.R. Kauffman, W.P. Overstreet, and R.R. Persinger,
Electrical Engineering Department,
Virginia Polytechnic Institute and State University, Blacksburg, Virginia 24061

This paper summarizes the results of attenuation, depolarization, and phase shift measurements made in the summer and fall of 1977 on the CTS and COMSTAR D2 spacecraft downlinks. The CTS beacon is right-hand circularly polarized at 11.7 GHz and COMSTAR carries two switched orthogonal linearly polarized beacons at 19.04 GHz and a single linearly polarized beacon at 28.56 GHz. The propagation measurements are supported by a rain gauge network, wind sensors, and a weather radar. The paper discusses signal behavior during individual rain storms and presents statistical data on attenuation and polarization isolation at the three wavelengths. The statistical relationships between attenuation and rainrate and the resulting information on effective path lengths are examined. The frequency dependence of rain attenuation and depolarization is discussed and the problem of ice depolarization is explored. Implications of the data for future satellite systems planning are discussed.

Commission J Session 3

MILLIMETER WAVELENGTH TECHNIQUES

Thursday A.M., 12 January ECCR 1-40

Chairman: S. Weinreb, National Radio Astronomy Observatory, Charlottesville, VA, on leave at Radio Astronomy Lab, University of California, Berkeley, CA 94720

J3-1
0830 A NEW MEASUREMENT OF THE COSMIC BACKGROUND RADIATION AT NEAR MILLIMETER WAVELENGTHS: D.P. Woody, N.L. Nishioka, P.L. Richards, Department of Physics, University of California and Materials and Molecular Research Division, Lawrence Berkeley Laboratory, Berkeley, California 94720

We have used a balloon borne liquid helium cooled spectrophotometer operating in the frequency range from 2 to 40 cm^{-1} to measure the night sky emission spectrum at an altitude of 43 km. The apparatus features a ^3He cooled bolometeric detector, a Fourier transform spectrometer, a well characterized cooled antenna, and several blackbody sources for absolute calibration. The detector is a composite bolometer operated at 0.36 K. It has an electrical noise equivalent power of 6×10^{-16} Watts/$\sqrt{Hz}$ and an optical absorption efficiency of 50% throughout the far-infrared and millimeter frequency range. The spectrometer is a Martin-Puplett interferometer, which uses a wire grid polarizer as a beam splitter. The interferometer has an efficiency larger than 90% throughout the frequency range of interest and a spectral resolution of 0.1 cm^{-1}. The instrument has a 6° wide field of view which is defined by a Winston light concentrator. Both the Winston cone and the interferometer are immersed in superfluid helium to reduce the amount of radiation emitted by the instrument itself. The diffraction sidelobes were reduced by adding an apodizing horn and a large ground plane to the antenna system. The antenna response was measured out to 70° off axis where it was less than -60 db. The results agree with theoretical calculations based upon the geometrical theory of diffraction. The instrument has produced excellent measurements of the emission spectra of the night sky in the frequency range from 2 to 40 cm^{-1}. Below 12 cm^{-1} the spectrum is dominated by the ≈3K cosmic background radiation (CBR) which is interpreted as a remnant from the primordial fireball in the "Big Bang" theory of the universe, while at higher frequencies the molecular line emission from H_2O, O_3, and O_2 in the atmosphere dominates the spectrum. We have developed a simple model for the molecular emission which accurately reproduces the atmospheric con-

tributions to our observed spectrum. After removing this atmospheric contribution, we are left with the spectrum of the CBR. An earlier flight produced the first measurement of the CBR which clearly shows that the spectrum does peak at ≈ 6 cm^{-1} and follows the Planck spectrum for a 2.9 K blackbody out to 17 cm^{-1} (D. Woody, J. Mather, N. Nishioka, and P. Richards, Phys. Rev. Lett., 34, 1036 (1975)). Greatly improved data were obtained on a recent flight. These new data should yield a significantly improved measurement of the CBR which will be sensitive to deviations from an ideal blackbody at the level of several percent. The results from analyzing this data will be reported.

J3-2
0855 INSTRUMENTATION USING QUASI-OPTICAL TECHNIQUES AT THE NRAO 11-M RADIO TELESCOPE, J. M. Payne, R. W. Freund, B. L. Ulich, National Radio Astronomy Observatory, 2010 N. Forbes Blvd., Suite 100, Tucson, AZ 85705

This paper describes various quasi-optical millimeter wave devices that are used on the N.R.A.O. 11-m radio telescope in Tucson. A quasi-optical polarizer for use at 100 GHz is described. The device consists of quarter wave plates positioned in front of the receiver feed assembly. Rotation of one plate between two selected angles results in the receiver being alternatively sensitive to right hand circular and left hand circular polarization. A second, fixed plate is required for linear polarization work. Continuum observations at the 11-m telescope are usually made with the aid of the switching subreflector. The maximum switching angle of the subreflector is 8 arc minutes which is insufficient for measurements on extended sources. A new method of beam switching is described which overcomes this problem. A quasi-optical local oscillator injection system for the 130-170 GHz band is described. This system is very suitable for cooled mixer systems in that all the components, with the exception of the mixer, are mounted outside the evacuated dewar. The performance of a Fabry Perot image rejection filter (P. G. Wannier et al., Review of Scientific Instruments, 47, 56-58, 1976) when used on the antenna is reviewed.

J3-3
0920

LOW NOISE MILLIMETER WAVE PARAMETRIC DOWN-CONVERTERS

S. Weinreb, National Radio Astronomy Observatory
Charlottesville, Virginia, on leave at Radio Astronomy Lab., U. of California, Berkeley, CA 94720

Reverse biased Schottky diodes, operated in a non-linear capacitor mode at 4°K have the potential of providing very low-noise millimeter wave receivers when used with a low-noise high-frequency I.F. amplifier, such as a maser. The practicality of this configuration has been greatly enhanced by the development of reliable closed-cycle 4°K refrigerators and very low noise, high-frequency (∿22 GHz) masers at Jet Propulsion Laboratory. The very low noise aspect of a maser I.F. amplifier can be used to great advantage with a cooled varactor mixer because these devices, when pumped and biased to avoid forward current, have only thermal noise sources whereas cooled diode mixers have fairly large non-thermal noise sources even when cooled. The high-frequency aspect of the maser I.F. amplifier is advantageous because, in their most stable mode of operation, all non-linear reactances have conversion loss inversely proportional to the output frequency as dictated by the Manley-Rowe relations.
The theoretical receiver noise temperature for cryogenically-cooled varactor converters combined with maser IF amplifiers will be presented. Limitations due to varactor loss and local oscillator heating will be discussed. Experimental results concerning a 115 GHz reciever with 275°K single-sideband receiver noise temperature will be described. This receiver combines a quasi-optical local oscillator diplexer, a reverse-biased Schottky diode used in a non-linear capacitor (varactor) mode, a 20-25 GHz tunable maser, and a 4°K closed cycle refrigeration system.

J3-4 A RECYCLABLE JOSEPHSON JUNCTION MIXER AT 115 GHz
0945 Y. Taur and A.R. Kerr
NASA - Institute for Space Studies
New York, New York 10025

Josephson effect mixers suitable for practical applications have been tested at 115 GHz. The junctions are recyclable niobium point contacts fabricated in a structure compensated for thermal expansion. The mixer is followed by a calibrated 1.4 GHz IF system which enables us to measure the output mismatch and noise temperature. The Josephson junction is mounted across a reduced height waveguide (0.096"x0.013"), and operated at pumped liquid helium temperature. A backshort can be adjusted from outside the dewar to maximize the input coupling. Filters are used in all bias leads and input and output lines to prevent the junction from saturation by external noise.

The signal is supplied by a calibrated gas-discharge noise tube. After the LO is applied, the junction is biased at about 20μA and 120μV and a Y-factor measurement is performed to determine the mixer conversion loss and noise temperature. After corrections for input and output transmission line losses are made, preliminary numbers for the single sideband conversion loss and mixer noise temperature are 3 dB and 150K. The LO power required is a few nanowatts. The output impedance of the mixer is close to 50 ohms for most of the junctions.

The mixer performance represents a significant improvement over existing Schottky diode mixers. It is believed that further reduction in the mixer noise temperature is possible by the use of better junctions and modifications of the mixer mount configuration. Efforts toward the realization of such a receiver on a millimeter-wave telescope are now in progress. Major work includes using a compact liquid helium dewar, eliminating the large input attenuation, and using a cooled IF amplifier with a noise temperature less than 30K. Such a receiver should have an overall noise temperature of 200-300K.

J3-5 DEVELOPMENT OF A FIELD-USABLE 300 GHZ
1035 JOSEPHSON MIXER SYSTEM

J. Edrich, Denver Research Institute
University of Denver
Denver, Colorado 80208

Extensive laboratory studies have shown that Josephson mixer receivers with batch cooling and adjustable point contacts can achieve a relatively low noise temperature of 1500K and a wide tuning range of more than 100 GHz (J. Edrich et al., IEEE Trans. MTT, 25, 476-479, 1977). Recently, rugged and permanent point contact junctions have been developed and successfully tested in a 4K closed cycle refrigerator. Based on these devices a telescope receiver for the 220 to 325 GHz frequency range is presently being developed. Long term cooling is provided by a reliable 4K closed cycle refrigerator. A lens corrected scalar horn serves as signal input followed by an LO coupler which is fed by a cooled varactor multiplier driven by a source oscillator below 100 GHz. The Josephson mixer is followed by a 130 MHz wide C-band maser and an uncooled paramp. Important system components and features including the tunable Josephson mixer, LO coupler, cooled multiplier, junction biasing, filtering and shielding are described. DC tests of the Josephson junctions together with preliminary rf system performance data are presented.

J3-6 1100

SPECTRAL LINE SEARCH AND OBSERVATION AROUND 110 GHZ USING A COMPACT CRYOGENIC MIXER RECEIVER WITHOUT LO FILTER

J. Edrich, University of Denver, Denver, Colo. 80208
W.L. Shuter, W.H. McCutcheon and P.C. Gregory,
University of Brit. Columbia,
Vancouver, B.C., Canada

A 20K cooled mixer receiver for spectral line observations in the 80 to 115 GHz range is described. In contrast to previously reported cooled mixer receivers a special broadband LO coupler with high directivity is used; this eliminates the need for narrow-band LO injection filtering and therefore reduces system complexity, and improves tuning characteristics and system gain stability. The Schottky barrier junction* used in the mixer is packaged in a miniaturized Sharpless wafer exhibiting wide rf and if bandwidths, good mechanical stability, excellent cooling characteristics and ease of field replacement. A servo-controlled, multiple $\lambda/4$ section short is mounted in fifth-height waveguide; it provides a reproducible match of high quality for the signal and minimizes LO leakage out of the input horn. All of the pump, LO, servo and bias circuits are integrated in a relatively small 1 cubic foot package on the back of the dewar; this light-weight and compact design makes it possible to use the receiver even on relatively small millimeter wave telescopes with limited space in the apex area.
The instantaneous if bandwidth of the system is defined by the cooled C-band paramps to 500 MHz. The measured double sideband noise temperature is 370K for the entire receiver. This receiver has recently been installed on the U.B.C. 15 ft. millimeter telescope in Vancouver. Preliminary observations and a line search around 110 GHz are described.

*2μ GaAs-Pt junctions developed by R. Mattauch, Univ. of Virginia.

J3-7 MEASURING THE SHAPE OF REFLECTOR ANTENNAS
1125 J. W. Findlay and J. M. Payne, National Radio Astronomy Observatory, Green Bank, W. Va. 24944

A very brief review of all known methods by which the shape of the surface of a reflector antenna can be measured will be given, under the headings: range-angle methods, angle-only methods, range-only methods, holographic methods, and other methods. A short summary of published work with references will be made available for distribution.
The most recent method developed and tested at NRAO for measuring the shape of a millimeter-wave radio telescope will be described. An inclinometer which can measure tilt angles with respect to the gravity vertical, to an accuracy of an arc second over a range of $\pm$ 14.5 degrees, is used. It is mounted at the center of a rigid bar, about 65 cm long; the length of the bar is defined by having it rest on two hard steel spheres near its ends, these in turn rest in small concave seats on the antenna surface. The method thus measures the angle of inclination of the bar between two well-defined points and, since the length between the steel spheres is also precisely known, the hole separation is known. The bar is stepped along a radial line of holes, and the inclination angles measured and recorded on a small computer. The surface profile along the radius is easily derived.
The method has been tested by measurements on the NRAO 42.7 meter telescope and on a 12.5 meter long test track. Under good conditions it is able to measure the surface shape to about 40 microns for a 25 meter diameter telescope.

J3-8 TELESCOPE STANDING WAVES: THEIR CAUSES
1150 AND CURES: B. L. Ulich, National Radio Astronomy Observatory, Tucson, AZ 85705

Mismatches in radio telescopes produce standing waves which appear as frequency-dependent sinusoidal modulations of the received signals. Imperfect cancellation of these sinusoidal components results in spectrometer baseline ripple which in some cases may ultimately limit the spectrometer sensitivity, especially for line widths on the order of the standing wave period. Serveral sources of standing waves are discussed, and measurements with the NRAO 11-m telescope on Kitt Peak are presented. In addition, several schemes are suggested for reducing the amplitude of the standing wave and for producing a second reflection of the same amplitude but of opposite phase. Thus the net standing wave amplitude can be made negligibly small, and the troublesome baseline ripple will be eliminated.

Commission B Session 7

ELECTROMAGNETIC THEORY

Thursday P.M., 12 January ECCR 2-28

Chairman: Dr. R.J. Pogorzelski,

TRW, Redondo Beach, CA 90278

B7-1
1330

Reciprocity Test for Asymptotic Solutions

M. Tew and R. Mittra, Electromagnetics Laboratory,
University of Illinois, Urbana, Illinois 61801

Solutions based on ray techniques are widely used for analysis of problems involving radiation and scattering from electrically large perfectly conducting bodies. These asymptotic solutions are quite versatile and straightforward in application; however, they unfortunately do not lend themselves to a convenient check of their accuracy. This paper proposes a test based on the application of Lorentz Reciprocity which may be used to evaluate the accuracy of an asymptotic solution. Specifically, test sources are introduced and Generalized Reciprocity is applied, resulting in an equation of the form

$$\iint \bar{E}^{ASYM} \times \bar{H}^{TST} \cdot d\bar{s} = \iint \bar{E}^{TST} \times \bar{H}^{ASYM} \cdot d\bar{s} + \bar{H}^{ASYM}\big|_{TST} - \bar{H}^{TST}\big|_{ASYM}.$$

The surface integration is performed on the perfectly conducting surface, where the tangential E-fields must vanish. Thus, the exact solution would result in the left hand term being equal to zero. This constitutes the reciprocity test - - checking to see how well the right hand side satisfies the zero condition. The right hand side is checked instead of the left, because H on the surface is usually given by the asymptotic solution, while the corresponding surface E-field may be difficult to obtain. The test fields are those of the test dipoles radiating in free space (from Generalized Reciprocity); and the reciprocity volume is enclosed by another surface at infinity whose contribution is zero, for bounded sources. The Reciprocity Test, then, is straightforward in application and conducive to tests of solutions for a wide variety of problems. It is not limited to one particular class of problems, for it may be adapted to planar, cylindrical, and conical geometries. It fills an important need by providing a numerical check on the accuracy of an asymptotic solution. Such a check has not been heretofore available. An added benefit of the reciprocity test is that

it is readily manipulated into an iterative equation, raising the possibility of improvement of any asymptotic solution.
This paper presents results from application of the Reciprocity Test and Iterative Equation to three asymptotic solutions to the problem of a magnetic dipole radiating on an infinite, perfectly conducting circular cylinder.

B7-2
1350 COMPLETE DYADIC FORMULATION OF APERTURE COUPLING INTO A RECTANGULAR CAVITY:

W. A. Johnson and D. G. Dudley, Department of Electrical Engineering, University of Arizona, Tucson, Arizona 85721

The exterior to interior coupling problem for a rectangular cavity with N - apertures and M - obstacles is formulated by use of vector Green's identities and dyadic Green's functions. The dyadic Green's functions are expanded in terms of the $\overline{L}$, $\overline{M}$, and $\overline{N}$ vector wave functions (Tai and Rosenfeld, IEE. Trans. on Microwave Theory, 9, 597-601, 1976); completeness and orthogonality of the vector wave functions are shown. Consideration is given to the singularities of the Green's functions and aperture fields. Numerical difficulties encountered in obtaining a numerical solution, such as the evaluation of triply infinite sums in the Green's function's expansion, are discussed.

B7-3
1410

APPROXIMATE SOLUTIONS FOR NARROW STRIPS AND SLOTS SUBJECT TO TE AND TM EXCITATION:

C. M. Butler and D. R. Wilton, Electrical Engineering Department, University of Mississippi, University, Mississippi 38677

Approximate integral equations are presented for the problem of a narrow conducting strip of infinite length, subject to TE and TM (to strip axis) illumination, or for the dual problem of a narrow slot of infinite length in a planar conducting screen. These equations are exact in the limit, $w/\lambda \to 0$, where w is the slot or strip width and where λ represents wavelength. Approximate analytic solutions of these equations are given and are shown to be exact in the above limit. These solutions are compared with results obtained by numerical methods for various values for w/λ. It is shown that the above approximations can be extended to the case of a slot in a screen separating half spaces filled with different dielectrics (C. M. Butler and K. R. Umashankar, Radio Science, 11, 611-619, 1976).

Approximations are presented for fields scattered from the strip. Also, data for penetration through the slot are given for the same dielectric material on both sides of the screen as well as for different material.

B7-4
1430

WAVE PENETRATION THROUGH A SMALL APERTURE ON A MULTICONDUCTOR TRANSMISSION LINE:

Darko Kajfez, Department of Electrical Engineering, University of Mississippi, University, MS 38677

Multiconductor transmission line (MTL) filled with inhomogeneous dielectric is located above an infinite perfectly conducting plane which contains a small aperture. An electromagnetic plane wave in the form of a pulse is incident from below the plane. Some energy of the wave passes through the aperture and induces the outgoing waves on the MTL. The object of this investigation is to evaluate the voltages on the extremities of the MTL which are terminated in arbitrary resistances. The mechanism of coupling from the plane wave to the MTL has been modeled by the Bethe's theory of small apertures, making use of an electric and a magnetic current moment. The wave propagation on the MTL is modeled with the aid of quasi-TEM modes, each of them propagating with a different velocity. The voltages at the terminals are evaluated in the frequency domain and in the time domain. The early time-domain response is then computed from the time-table of multiple reflections on the terminated MTL. The first-order equivalent circuit of the MTL section containing the aperture consists of the self inductances and mutual inductances in series, and self (negative) capacitances and mutual (negative) capacitances in parallel. For small apertures, the elements of the equivalent circuit are so small that they do not influence the wave propagation on the MTL in any appreciable way.

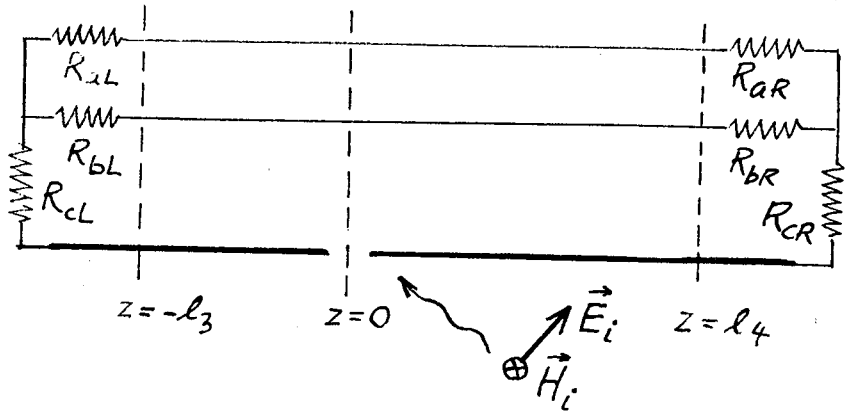

B7-5
1520

ELECTROMAGNETIC COUPLING TO AN INFINITE CABLE PLACED BEHIND A SLOT PERFORATED SCREEN:

K.R. Umashankar and J.R. Wait, Cooperative Institute for Research in Environmental Sciences, University of Colorado/NOAA, Boulder, CO 80309

In electromagnetic interference studies, one often needs to assess the response of protected objects behind perforated metallic screens. Also, in related scattering problems, the distribution of the electric field in the aperture determines the radiation mechanism which has a direct bearing on the electromagnetic coupling to nearby objects. As shown by Butler and Umashankar (C.M. Butler and K.R. Umashankar, IEEE Trans. AP, AP-24, 456-462, 1976), the fields in the aperture are affected by the presence of nearby scatterers. They considered the boundary value problem of a finite thin wire behind a slotted conducting screen and derived a coupled set of integro-differential equations where the distribution of the electric field in the narrow slot and the induced current on the finite thin wire were unknown. Such formulations (C.M. Butler and K.R. Umashankar, IEEE Trans. AP, AP-24, 456-462, 1976; Radio Science, 11, 611-619, 1976; K.R. Umashankar and C.M. Butler, EMP Interaction Notes, July 1974) are only tractable at relatively low frequencies because of the excessive computing needed. Also, this method would not be viable when dealing with very long cables or bundles of cables located behind such aperture perforated screens. However, as we shall show, one may formulate the basic integro-differential equations for such situations in a form more convenient for calculation. In this paper, an integro-differential equation for the case of an infinitely long cable placed behind a narrow finite rectangular slot in a conducting screen and an efficient approach to calculate the current response of the cable with complete account of slot coupling is indicated. The method is similar to that used by Hill and Wait (Radio Science, 12, 231-238, 1977) who were concerned with the response of coaxial cables to dipolar fields. The transfer admittance function so obtained, is in a form very convenient to estimate the electric current on the infinite cable. Results of the slot electric field distribution and the current induced on the infinite cable are given for a few typical cases. Not surprisingly, the axial distribution of induced voltage on the slot is markedly affected by the presence of the cable.

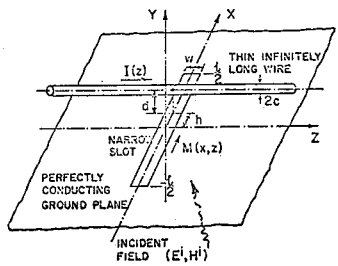

B7-6 1540 STATIC FIELD COMPUTATIONS BY THE METHOD OF OPTIMIZED IMAGES: Y.L. Chow, Dept. of Electrical Engineering, C. Charalambous, Systems Design, University of Waterloo, Waterloo, Ontario, N2L 3G1 Canada.

Static field computations can be simple and fast if the method of images can be used. However, except for some simple geometries, such as planes and spheres, one normally cannot determine the locations and strength of the images. This paper overcomes this difficulty and makes the required determinations by an optimization technique.

In the technique a nonlinear differentiable objective function is created, which is proportional to the mean square error in the boundary condition and is a function of the locations and strength of the images. Since the function to be minimized is differentiable very efficient gradient techniques may be used. For the examples in this paper, Fletcher's optimization technique (Comp. J. 13, 317-322, 1970) is used. This algorithm is currently one of the most powerful for unconstrainted optimizations. Two examples are used to demonstrate the rapid convergence of this optimized method. The first is the capacitance between two conducting spheres separated by a distance of three radii, centre to centre. The known solution by the normal image method (Smythe, Static and Dynamic Electricity, McGraw-Hill, 3rd Ed., 1968, pp. 128-129) requires 8 point charge images in each of the two spheres, while the solution by the optimized point images requires only two. The possible error in either solution is 10^{-3}%. The second example is the capacitance between two crossing wires of which no known solution is available. The two wires are approximated by two prolate spheroids of major to minor axis ratio of 9 and crossing each other at a distance of 1.5 times the minor axis, centre to centre. Even at such large axis ratio, only three line charge images are required in each spheroid to give a possible error of 2%. With a wire radius of 1 cm, the capacitance is found to be 6.9 pf.

B7-7
1600

ISOPERIMETRIC INEQUALITIES IN ELECTROMAGNETIC THEORY

D. L. Jaggard, California Institute of Technology
Pasadena, California 91125

We consider the solution of boundary value problems in electromagnetic theory by the use of isoperimetric inequalities (Pólya and Szegö, Isoperimetric Inequalities in Mathamatical Physics, Princeton University Press, Princeton, 1951). These problems are usually solved by separation of variables or a numeric technique. However, as a preferable alternative, one can reformulate the boundary-value problem so that one seeks a set of upper and lower bounds to the true solution rather than the true solution itself. One approach, using the variational method, has been successfully used in the past (see e.g. Borgnis and Papas, Randwartprobleme der Mikrowellenphysik, Springer-Verlag, Berlin, 1955). However, if there are topological changes in the boundaries, the variational approach becomes cumbersome and certain isoperimetric inequalities may be more useful. These inequalities typically involve simple geometric quantities of the boundary such as the perimeter, area or volume and hence provide a simple and economical means for sandwiching the true value between upper and lower bounds. It is the purpose of this paper to introduce some of these inequalities into the solution of various problems in electromagnetic theory and to make assertions about the bounds on quantities of physical interest.

As an example, Pólya and Szegö have asserted that the capacitance of a conducting plate of arbitrary shape and of area A and perimeter P is bounded by the capacitance of a circular plate with inner and outer radii $r_{in} = \sqrt{A/\pi}$ and $r_{out} = P/2\pi$. The values for these radii are shown in the figure below for the case of a square and an equilateral triangle. In an analagous way, we conjecture that the inner and outer radii can be used in the calculation of polarizabilities, aperture transmission coefficients and scattering cross-sections. Other isoperimetric inequalities may be used to approximate cut-off frequencies of waveguides with arbitrary cross-sections. It is anticipated that isopermetric inequalities will play a role in such diverse areas as optical fiber characteristics and EM leakage problems.

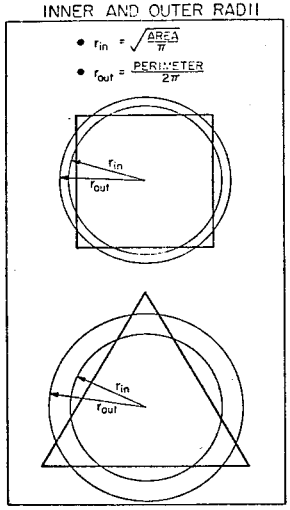

B7-8
1620

ELECTROMAGNETICS: ENTITIES-PROPERTIES-UNITS

J. B. Smyth, J. A. Durment, and D. C. Smyth, Smyth Research Associates, San Diego, CA 92123

Maxwell' s equations represent a single relationship amalgamating electricity and magnetism. These equations identify the electrical conduction current as the sole "thing-like", entity, characterized by its electromagnetic field. The multiplicity of phenomena occurring under different conditions specified by electromagnetic properties of physical media are witness to the efficaciousness of the entity. All evidence indicates that the elements of physical theory contained in Maxwell' s equations are necessary and sufficient to account for all the elements of physical reality exhibited in phenomena described by electromagnetic field theory. The acceptance of this premise requires that no additional entity, characteristic or property be allowed in electromagnetic field theory.

The removal of superfluous conceptions such as poles and dipoles eliminates much of the confusion, especially in phenomena which appear characteristically magnetic;for example, the long standing question concerning which field quantity to use in computing the moment of a bar magnet is resolved uniquely.

Commission C (Joint with B) Session 3

ANTENNA ARRAYS AND FEEDS

Thursday P.M., 12 January ECCR 0-36

Chairman: Dr. Mark Ma, Office of

Telecommunications, ITS, Boulder, CO 80302

C3-1 1330 RANDOM GAIN AND PHASE ERRORS EFFECTS IN OPTIMAL ARRAY STRUCTURES

C.W. Jim, L.J. Griffiths
Department of Electrical Engineering, University of Colorado, Boulder, CO 80309

This paper summerizes a quantitative analysis of the effects of random gain and phase errors and angular variations on the performance of a class of Least-Mean-Square (LMS) optimal array processor. The structure, depicted in Figure 1, was a generalized side-lobe cancelling array. It employed a conventional beamformer, Wc, as an integral part and a simple spatial hardware preprocessor, Ws, was used to implement a linear constraint. Model for the effects of random input errors were presented and formulated. Briefly, each spatially propagated signal incident on the array was modelled as having been transmitted to the array by a random channel. The characteristics of this channel then determine the nature of the phase and gain errors observed at the element outputs.

Sensitivity comparisons of the optimal array processor and a conventional beamformer to random gain and phase errors were performed. Major findings indicated that the optimal array processors were more sensitive to input errors than the conventional processor, but nevertheless offered significant interference rejection improvements over conventional beamforming methods. It was also shown that degradations due to random gain and phase errors could be restored to some extent by increasing the number of temporal/spatial degrees-of-freedom.

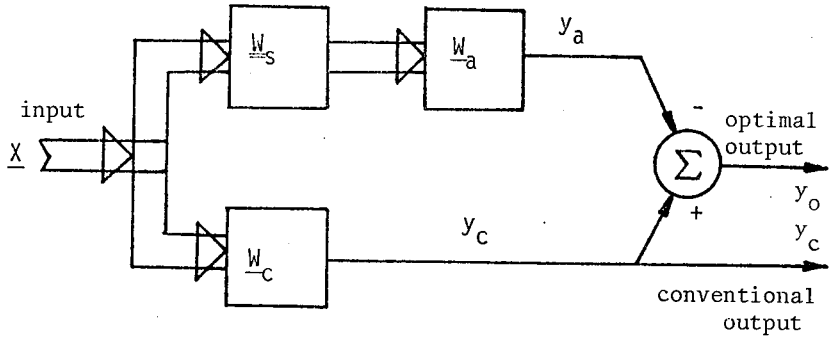

Fig. 1 Hardware constrained noise-cancelling optimal array structure.

C3-2
1400

ARRAY DISPERSION EFFECTS ON MATCHED FILTER OUTPUT FOR A LINEAR FM SIGNAL

M. R. Patel, Center for Applied Research in Electronics, Indian Institute of Technology Delhi, Hauz Khas, New Delhi 110029, India, and Rajendra K. Arora, U.S. Department of Commerce, National Oceanic and Atmospheric Administration, Environmental Research Laboratories, Boulder, CO 80302

The response of a matched filter to a linear FM radar pulse transmitted and received through a linear phased array after return from a stationary target is studied with the matched filter assumed to be matched to the undistorted pulse. The investigation is carried out for three different feed arrangements: the corporate feed, the series end-feed, and the series center-feed.

Numerical results are presented for the three configurations assuming the feed to be of the TEM type. It is observed that the output pulse is symmetrical in time for corporate and series end-feeds; however, the pulse is asymmetrical in the case of series center-feed and there is a lateral displacement of the pulse. Other distortions observed are: reduction in peak amplitude resulting in a fall in signal-to-noise ratio; pulse widening, leading to loss of resolution; and reduction in level of range sidelobes (a desirable effect). The results are presented in a general manner so as to apply to an arbitrary linear array.

It is noted that the degradation of the signal is appreciable for large time-bandwidth product signals which are normally encountered in pulse-compression systems. As expected, the distortions are more in the case of two-way transmission than in the case of one-way transmission studied earlier (K. Arora and R. K. Arora, IEEE Trans. Aerospace and Electronic Systems, AES-12, 73-77, January 1976). However, the general nature of the distortions is similar.

C3-3 1430 THE DETERMINATION OF THE DIRECTIONAL OF ARRIVAL OF THE COMPONENTS OF A MULTIMODE FIELD: Hang H. Lai and John D. Dyson, Department of Electrical Engineering, University of Illinois, Urbana, IL 61801

The problem of resolving the complex interference field at a receiving site, that is caused by multimode propagation at high frequencies, into the individual plane wave components and determining the direction of arrival of these components is considered. The method developed is based on Prony's algorithm. Effects of noise level on the solution are discussed and examples are illustrated. A first-order linearized model of a statistical study of a single two planewave problem for this conventional Prony's method is presented. Problems and discussions pertinent to this conventional algorithm are also presented. In this approach it is assumed that the interference field will be sampled by observing the amplitude and phase of the signals from two uniform linear arrays. The solution of the set of non-linear equations representing the information from one array yields the included angle between the wave normal and the axis of the array, a conical angle. Information from two arrays is necessary in order to solve for the two coordinate angles in a spherical coordinate system.

A modification of Prony's technique, an eigenvalue approach has also been applied to this problem. It is shown that this approach not only allows one to analytically determine the number of waves in the problem, but also offers a way to pair the conical angles to insure proper identification of the waves. It is also shown that this latter approach is less susceptible to the effect of noise. Comparisons and statistical tests of this method with the conventional method using simulated data are presented.

Data obtained from a controlled experiment when a signal from a distant source was repeated and retransmitted at a different location, verify that the system as well as the algorithm is capable of resolving waves coming from different directions. Experimental evidence related to multimode as well as single mode propagation coming from the same source has been obtained.

C3-4 ON THE GRATING LOBES OF ARRAYS OF LARGE SUBAPERTURES
1530 Curt A. Levis, ElectroScience Laboratory, The Ohio State University, Columbus, Ohio

The number of elements in a large filled aperture may become excessive if the usual spacing criteria for grating-lobe prevention are observed. For example, a 10 meter by 10 meter array at 30 GHz with half-wavelength spacing would contain four million elements.

Conceptually there is a way to avoid this problem while still reducing the number of terminals to be connected to the system. It is based on approximating a continuous distribution with piecewise-continuous polynomials. For the zero-order (staircase) approximation it is found that the grating lobes become degenerate when there is no gap between the subaperture since the element pattern of the uniform subapertures has nulls precisely at the grating-lobe angles of the array pattern. The first-order (piecewise linear) term is shown to have the proper form for further reducing the degenerate grating lobes, but not for reducing the grating lobes arising from gaps between the subaperture elements. The effect of gap size on grating lobe level has been calculated for cosine-on-a-pedestal distributions.

In the case of scanned arrays, another potential source of grating lobes is the phase jumps which occur when the phase slopes of the subapertures contain a random error: i.e., when they are not scanned each to precisely the correct direction. Calculated estimates of this effect will also be presented; in general it is found that the dispersion of the phase slopes must be much smaller than unity for acceptable grating-lobe performance.

C3-5
1600

FEEDS FOR SHAPED BEAM SATELLITE ANTENNAS

H. Frijters, M.E.J. Jeuken and V.J. Vokurka
Department of Electrical Engineering, Eindhoven
University of Technology, Eindhoven.
The Netherlands

Great technological progress has been made in satellite communications over the past decade finding expression, among other things in the improved design of satellite-borne antennas. For some future missions, however, the radiation pattern of these last-named antennas should be optimized so that some area on the earth will be illuminated as uniformly as possible. Outside the above-mentioned area the radiated power should be minimized. The shape of the area to be illuminated could be circular or have some other general cross-sections. In this paper we restrict ourselves to the special case of a circular area.

Microwave antennas with a sector-shaped beam can be designed, at least approximately, if there is phase reversal over the aperture. Such an aperture distribution can be realised with two systems at least. The first system employs a parabolic reflector antenna which is illuminated with a coaxial corrugated waveguide radiator having a symmetrical power radiation pattern. In this case the central part of the reflector is illuminated by the main lobe of the feed pattern, whereas the first side lobe (with a phase reversal of 180°) illuminates the outer part of the reflector. Good results were obtained with this system.

A second solution to the above-mentioned problem is to illuminate a reflector with a corrugated circular waveguide radiator operating in two modes, viz. the HE_{11} mode and the HE_{12} mode. Applying the appropriate excitation between these two modes gives rise to a high first side lobe in the feed pattern. This side lobe plays the same part as in the system already discussed above. Promissing results were obtained in this case too. Finally, we have investigated the second system in an off-set configuration, because blocking of the feed in a front-fed reflector is found to disturb the original design considerably. With the use of an off-set configuration this disadvantage can be overcome.

Commission F Session 6

OPTICAL AND RADIO SENSING OF

ATMOSPHERIC PARAMETERS

Thursday P.M., 12 January ECCR 0-30

Chairman: D. Hodge, Ohio State University,

Columbus, OH 43212

F6-1
1330 METEOROLOGICAL RADAR CALIBRATION BY MEANS OF RADIOMETRY:*

D. B. Hodge
ElectroScience Laboratory, The Ohio State University, Columbus, Ohio 43212

The accuracy of quantitative remote rainfall measurement has been limited in the past by the difficulty encountered in establishing a precise radar calibration. Traditional techniques such as calibration against ground level rain gauges or theoretical determination of antenna gain and waveguide losses introduce significant uncertainties in the resulting rain rate measurements.

Methods of meteorological radar calibration directly in terms of radiometry will be described. These methods offer the advantage that the calibration is in terms of an independent measurement of the medium throughout the same region "seen" by the radar. These methods are simple and permit continuous calibration of operating radar systems at either attenuating or non-attenuating wavelengths.

As a subsidiary result, a bound on the integrated radar return is established for the case of radars operating at attenuating wavelengths. This bound may be used to establish radar calibration without the use of radiometric information. Alternatively, once the radar has been calibrated, this bound may be used to determine in real time whether the radar has become saturated, i.e., "blind", to targets located behind an attenuating region.

F6-2 1355 REMOTE SOUNDING OF ATMOSPHERIC PARAMETERS USING 100-183 GHz

A. L. Cassel, P. W. Rosenkranz, and D. H. Staelin, Research Laboratory of Electronics and the Department of Electrical Engineering and Computer Science, Massachusetts Institute of Technology, Cambridge, MA 02139

Atmospheric temperature profiles may be estimated from microwave radiometric measurements made from an orbiting satellite. A number of different frequencies are used on the edge of an absorption band (e.g., the O_2 absorption bands at 60 and 118 GHz). The opacity of the atmosphere varies within these bands, enabling one to obtain weighted averages of the temperatures at varying levels of the atmosphere. Using radiosonde data and theoretical models to calculate these weighted averages, linear regression techniques can be applied to retrieve estimates of the actual atmospheric temperatures.

Satellites employing frequencies below 60 GHz for sounding atmospheric temperatures have performed well in space; this work explores the possible use of the 100-183 GHz region for the same purpose. It has been found that, over ocean in cloud-free model atmospheres, a set of 13 channels based on the 118 GHz oxygen absorption line can retrieve actual atmospheric temperatures better than can a set of 9 channels based on the 60 GHz absorption line, and additionally give better geographical resolution. (The latter channel set is similar to that soon to be launched on the operational Tiros-N sounder, but includes more channels.) There is little difference in the accuracy of temperature retrievals between these two channel sets in the presence of several different types of clouds.

Integrated water vapor and liquid water may also be estimated by means of linear regression. The augmented Tiros-N set yields better retrievals for water vapor over ocean and comparable retrievals for liquid water when compared with a system consisting of 12 channels around 118 GHz plus 6 channels near the 183 GHz resonance of water vapor. Temperatures and altitudes of cloud tops have been estimated with reasonable accuracy for various cloud models by using a combination of 20, 60, 100 and 118 GHz channels.

F6-3
1420 OPTICAL PATH-AVERAGED MEASUREMENT OF RAINDROP SIZE DISTRIBUTION: R. S. Lawrence, T-i. Wang, and K. B. Earnshaw, NOAA Research Laboratories, Boulder, CO 80302

The path-averaged terminal velocity distribution of raindrops falling through a laser beam can be measured by observing the cross-correlation function of their scintillation patterns as they move across a vertically spaced pair of horizontal line detectors. Drop-size distribution results directly from the terminal-velocity information because of the known monotonic relationship between drop size and terminal velocity. Once drop sizes have been determined, the rain rate can be deduced. The large capture area of an expanded laser beam permits accurate drop-size distributions and rain-rate measurements to be obtained at less than one-minute intervals. We have demonstrated the method with a 200 m path using a 20 cm collimated beam and two horizontal line detectors 20 cm in length separated vertically by 3 cm, and will show the result of analyzing data from a 3-hour storm at 42-second intervals. Since the measurement of drop-size distribution requires a collimated beam, path lengths greater than about 200 m are probably impractical unless a servo-controlled pointing mechanism is provided to eliminate beam wander.

F6-4
1445

PULSED COHERENT INFRARED LIDAR SYSTEM FOR GLOBAL WIND MEASUREMENTS

P. A. Mandics and R. M. Huffaker, Wave Propagation Laboratory, Environmental Research Laboratories, National Oceanic and Atmospheric Administration, Boulder, CO 80302

Coherent lidar techniques have been developed to measure atmospheric winds (R. M. Huffaker, D. W. Beran, and C. G. Little, Preprints of the Seventh Conf. on Aerospace and Aeronautical Meteor. and Symp. on Remote Sensing from Satellites, 1976, Melbourne, Florida). Preliminary studies conducted at NOAA/WPL indicate the feasibility of measuring winds to ranges of 20 km using ground-based state-of-the-art pulsed coherent CO_2 lidar technology. NOAA/WPL is currently evaluating the capabilities of coherent infrared lidar technology to measure global winds from a space platform. System performance for two wavelength regions (3.9 and 10.6 μm) is assessed in terms of the coherently detected returned signal-to-noise ratio (SNR). The effects of atmospheric attenuation (caused by molecular absorption, rain, fog, and clouds), turbulence, and aerosol scattering on the SNR are evaluated and their global characteristics are ascertained. Similarly, system parameters such as optics size, focussing, scan geometry, transmitted power, and pulse duration are assessed. Platform characteristics including spacecraft motions affecting pointing accuracy, weight limitations, and power availability are also evaluated for space shuttle payloads. Computer programs that include models of the sensor system components (optics, laser, and signal processor), atmospheric wind fields, and the above-mentioned parameters are used to simulate and predict overall system performance.

F6-5
1535

RADAR-DERIVED WIND PATTERNS IN THE URBAN BOUNDARY LAYER:

R. A. Kropfli, NOAA/ERL/Wave Propagation Laboratory, Boulder CO 80302

The dual-Doppler radar system developed at the Wave Propagation Laboratory has been used to observe the boundary layer wind field at St. Louis during July and August 1975 as part of METROMEX. The data was taken by coordinated scanning of two X-band, Doppler radars through a cloud of chaff released from an airplane and, on one occasion, from the ground. Coplane scanning was used so that the radars simultaneously scanned within planes tilted slightly with respect to the horizon. Motions normal to these planes were computed through an integration of the equation of continuity in cylindrical coordinates.

Mid-afternoon data from seven clear days has revealed many interesting aspects of the boundary layer wind field perturbed by a large city. A summary of results includes: 1) verification of the dual-Doppler technique in the P.B.L. since the vertical integration of the continuity equation generally produced very small vertical velocity components near the capping inversion, and 2) direct observation of persistent horizontal rolls that seem to be very efficient in mixing the boundary layer. Time histories of the three-dimensional wind field for as long as one hour revealed wave-like features traveling at about 1 m/s relative to the mean flow, features moving with the mean flow, and updrafts that are fixed to the surface. Representative samples of boundary layer wind fields will be compared and discussed.

F6-6
1600 MEASUREMENTS TOWARD A C_n^2 CLIMATOLOGY IN THE BOUNDARY LAYER:

R. B. Chadwick, K. P. Moran, and G. E. Morrison, NOAA/ERL/Wave Propagation Laboratory, Boulder CO 80302

The capability of an FM-CW radar to make real time wind measurements in the clear air has been established (Chadwick et al., Radio Science, vol. 11, 795-802, 1976). The advantage of the FM-CW technique is that measurements can be made very close to the radar, and in turn, due to the range dependence of return signal power, a relatively inexpensive radar can make clear air wind measurements in the boundary layer. Since a large, high power radar is not needed, operational uses of clear-air radar in the boundary layer become more attractive. Two possible uses are detection of hazardous wind shear in the vicinity of airports and measurement of low level winds for short term, local weather prediction. However, before such operational uses can evolve, some knowledge of the statistics of return signal power are necessary.

A one-year program to characterize the strength of boundary layer refractive-index fluctuations (or equivalently return signal power) was undertaken in late 1976 and is nearing completion. An FM-CW clear-air Doppler radar has been in almost continuous operation in the Boulder, Colorado, area since February 1977, and takes data from nine range cells to a height of 1500 m. The returns are electronically averaged for one minute and then recorded on magnetic tape for off-line analysis. Hourly histograms of measured structure constant (C_n^2) values are then calculated for each range cell and are presented as a function of time. These histograms can be reduced to daily, monthly, or seasonal histograms to determine a preliminary climatology of C_n^2. These histograms and conclusions will be presented.

F6-7
1625 OBSERVATIONS OF ENHANCED CLEAR AIR REFLECTIVITY ASSOCIATED WITH CONVECTIVE CLOUDS: J.L. Green, R.H. Winkler, J.M. Warnock, W.L. Clark, K.S. Gage, and T.E. VanZandt, Aeronomy Laboratory, National Oceanic and Atmospheric Administration, Boulder, CO 80302

Enhancements of radar reflectivity associated with, but outside of, visible convective clouds have been observed by the 7.4m Sunset Radar, located in the Rocky Mountains 15km west of Boulder, CO. At this wavelength, the contribution of hydrometeors to the total reflectivity is quite negligible. Convective clouds are very frequent over the station during summer daylight hours. Comparison of the radar observations with triangulated photographs shows that enhancements of reflectivity begin well before the cloud intersects the radar beam, and that the enhancement extends several kilometers above the cloud-top level, to as high as 19km, in the lower stratospphere. In most of these events no significant vertical velocity (also measureable with this radar) was observed above 10km. Since the radar reflectivity is proportional to the turbulence structure constant for radio refractive index fluctuations, these observations imply that the turbulence associated with convective clouds extends well outside the visible cloud.

F6-8
1650

DUAL-DOPPLER MEASUREMENT OF CLEAR AIR TURBULENCE

R.J. Doviak, T. O'Bannon, and M. Berger,
National Severe Storms Lab., Norman, OK 73069

Flow in a clear, dry convective boundary layer has been mapped with the National Severe Storms Laboratory's dual-Doppler weather radar system. The radars, 41 km apart, measure the three-dimensional vector wind over large areas without chaff. We report on the turbulent wind over an area 25 x 25 km^2 on 27 April 1977, show its spatial spectra, and determine the correlation of wind fields measured approximately 3 minutes apart. Spatial spectra show that the -5/3 power law is dominant to scales of the order of few kilometers and that wavelengths about 6 km have the most energy on this day of moderate wind shear. In addition, eddy dissipation rates of about 4 cm^2/sec^3 have been deduced from the spatial spectra. Comparison of Doppler synthesized winds with those obtained from a tall (444 m) instrumented tower shows good agreement. Although echo signal strengths were mostly below receiver noise, estimation produced by minimum variance processing techniques and high sample spatial density produces velocity estimates with standard error of a few tenths of a meter per second.

The correlation between reflectivity fields, measured independently at the two radars, is about 0.8. Noise in velocity and echo intensity estimates is calculated to determine the quality of the synthesized wind and reflectivity fields. Reflectivity and velocity structure suggest alignment of waves parallel to the shear direction--a result expected when waves relate to convective instabilities. We also compare two reflectivity estimation techniques, coherent and incoherent.

Commission C Session 4 (Invited)

SIGNAL PROCESSING IN ADAPTIVE ARRAYS

Friday A.M., 13 January ECCR 0-36

Chairman: A.E. Zeger, Zeger and Abrams, Inc.

C4-1 0830 ADAPTIVE ARRAY PERFORMANCE USING AN ESTIMATE OF THE DESIRED SIGNAL DIRECTION DELAY VECTOR

T. W. Miller, Staff Engineer, Electronics Laboratory
Hughes Aircraft Company, Fullerton, CA 92634

Maximization of the signal to interference plus noise ratio (S_o) at the output of an adaptive array requires knowledge of the desired signal direction-delay vector $\underline{R}_{xs}$. In many applications, however, $\underline{R}_{xs}$ is unknown due to a lack of a priori angle of arrival information or due to an inability to accurately characterize the antenna array. An example is an airborne communication system in which the desired signal source may be located anywhere within the hemispheric field-of-view. This paper describes the achievable steady-state performance of an adaptive array when $\underline{R}_{xs}$ is estimated from measurements of the input signals. The estimate is obtained by averaging the product of the desired signal and each antenna signal over a finite interval of time. The estimation technique is applicable if the desired signal is known to within an arbitrary (but constant) amplitude and phase error (e.g., during the preamble portion of a communications signal) and if the desired signal is uncorrelated with interfering signals.

The estimate of $\underline{R}_{xs}$, denoted $\hat{\underline{R}}_{xs}$, is used to direct the weighting coefficients toward the steady-state solution $\hat{\underline{W}}_{ss} = \underline{R}_{xx}^{-1} \hat{\underline{R}}_{xs}$, where R_{xx} represents the covariance matrix of the input (antenna array) signals. It is well known that this solution leads to optimization of the output signal to interference ratio ($\hat{S}_o = S_{o\,opt}$) when $\hat{\underline{R}}_{xs} = \underline{R}_{xs}$, and that $S_o < S_{o\,opt}$ when the estimate $\hat{\underline{R}}_{xs}$ is in error. An expression for the average value of S_o, normalized to $S_{o\,opt}$, is determined as a function of averaging time used in the estimate of $\underline{R}_{xs}$. The expression applies for an m-element antenna array of arbitrary geometry and for any number of directional interference sources. The results show that the estimate of $\underline{R}_{xs}$ is sufficiently accurate to obtain an average S_o within 3 dB of optimum in less than $m/2(S_{o\,opt} B)^{-1}$ seconds, where B is the input signal bandwidth, and R_{xx} is the covariance matrix of noise plus interference. However, a longer averaging time is required when R_{xx} includes desired signal terms, since any error in the $\underline{R}_{xx}$ estimate causes the adaptive array to treat the desired signal as an interferer.

C4-2 0900 EIGENVECTOR DECOMPOSITION ALGORITHMS FOR ADAPTIVE ARRAYS: A. F. Culmone, Massachusetts Institute of Technology/Lincoln Laboratory, Lexington, Massachusetts 02173

Optimum adaption to a desired source in a field of interferers usually requires knowledge of the source location. This knowledge is provided explicitly when the spatial coordinates of the source are known, or implicitly when known characteristics of the source signal are exploited to estimate source direction. In some applications of adaptive arrays, source locations are unknown and it is not practical to derive location estimates from known signal characteristics. In such cases, a matrix eigenvector decomposition algorithm may be used to obtain a level of adaption that is "close" to optimum -- without prior knowledge of interferer or desired source locations. The essential requirement for a successful decomposition process is that interferers exhibit greater power levels than desired sources. When interferers are substantially stronger than desired sources the decomposition process can be shown to yield the following information: 1) the mathematical subspace (of antenna array output vectors) in which the interferers reside, 2) the complementary mathematical vector subspace from which the weight vector can be arbitrarily chosen and still null the interferers -- this complementary subspace is the one in which it is possible to exploit "unused" degrees freedom for array pattern shaping, and 3) the eigenvector (array weighting vector) that "almost" optimizes the desired source power-to-interference power ratio.

A variational description of the eigenvalues of a matrix (the Courant-Fischer Min-Max theorem) is interpreted in light of the adaptive nulling problem. It is claimed, by way of this Theorem, that the eigenvalues of the correlation matrix are descriptors for the eigenvectors and vector subspaces possessing the properties described above.

Examples are included to demonstrate the performance of the decomposition algorithm.

C4-3
0930

A GENERALIZED TECHNIQUE FOR ADAPTIVE ARRAY REFERENCE FUNCTION GENERATION

Dr. G. Patrick Martin
Harris Electronic Systems Division
Communication Systems Department
Melbourne, Florida 32901

This paper details a generalized practical technique for obtaining a "desired signal reference function" as required for optimal performance of a temporal reference S/N maximizing adaptive array. Specifically, waveforms containing the desired signal, noise and interference are subjected to an operator function, referred to here as a "signal recognizer", which yields precisely, in the context of the algorithm's average value adaptation transient and optimum solution, an ideal desired signal reference function. A signal recognizer requires an a priori discriminant which uniquely identifies the desired signal. Specifically, a desired signal must be composed of products, a suitable term of which must be known. (Thus the technique can apply to any modulated carrier.) This requirement is contrasted to the classical formulation which requires that the entire signal be known.
A prime example is a desired signal, s(t), where

$$s(t) = Ad(t)c(t)\cos(\omega_c t)$$

In the above, A is unknown amplitude, d(t) is unknown data, c(t) is an a priori known spreading function (the unique discriminant), and ω_c is the carrier frequency, which may be doppler shifted by an unknown and arbitrary amount. Specific examples of the signal recognizer, conceptually the same for all signals, are given for ordinary AM, FSK, PSK, and for the spread spectrum signal just mentioned.

C4-4
1030

PERFORMANCE OF A POWER INVERSION ADAPTIVE ARRAY:

J.A. Graniero, C.J. Luvera, Rome Air Development Center, Griffiss Air Force Base, NY 13441

The power inversion type of adaptive array adapts to minimize its total output power under the constraint that one of the array weights is held fixed at a value of unity. The performance of this type of adaptive array has been analyzed in many experiments at Rome Air Development Center (RADC) using an experimental model developed for RADC in 1973 by the General Atronics Corporation. The experimental model, called the Interference Cancellation System (ICS), operates at a frequency of 300 MHz. Its functional block diagram is shown in Figure 1.

The ICS differs from adaptive arrays using the LMS (least mean square) algorithm for adaptive control. The two main differences which can be seen from Figure 1 are: 1) there is one unweighted antenna in the ICS; and 2) the ICS uses power level as a discriminant between an interference and a desired signal. In the ICS, the array output signal is the feedback error signal applied to the error signal side of the correlators in the adaptive control circuit. The ICS adaptive control utilizes a fixed threshold level P_t. The ICS does not attenuate (null) input signals when they are below the fixed threshold level P_t. As the input power is increased above P_t, the output decreases in a reciprocal suppresion manner. The effect of using a power threshold as a discriminant between desired and interfering signals has been evaluated for various types of signal modulations including both narrowband and wideband (spread spectrum) modulation. The nulling performance of this processor has been determined in an anechoic chamber and on an antenna range for various antenna element configurations. Testing was conducted on short ground planes and on a large aircraft structure. The ICS has also been used as an IF adaptive antenna processor at the IF output of a 4.5 GHz phased array.

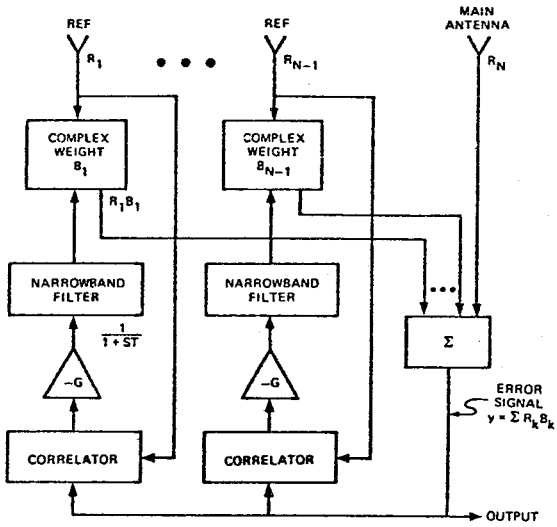

Figure 1.

ICS Functional Block Diagram

C4-5 1100 TRANSIENT BEHAVIOR OF AN ADAPTIVE ARRAY: Edwin D. Banta, AEL Industries, Inc., Richardson Rd., Colmar PA

Although applications for adaptive arrays are becoming more common there is still little understanding of the transient behavior of these adaptive arrays using different control algorithms. A new analytic tool--the Root Trajectory Method--which allows the entire adaptive array transient behavior to be shown in one diagram, will be described. Several examples will be presented showing unusual and unexpected behavior or an adaptive array using a gradient search algorithm.

A new and novel control algorithm will be described, and its performance will be illustrated using the Root Trajectory Method. This algorithm employs direct control of the null locations rather than indirect control through the complex array weights. A peculiar property of this algorithm illustrates the dangers in working with average values of weights in the control equations rather than treating them as stochastic systems.

This last point is illustrated further by the exact solution of a simple adaptive system using one control loop. The average values of the exact solutions will be compared to the values obtained from the same control algorithm using average weights. In particular, it will be seen that for certain values of the control parameters the exact solution can have a bounded average value while its variance diverges with increasing time.

C4-6 1130 AN L-BAND ADAPTIVE ANTENNA ARRAY

S.J. Rosasco, General Atronics Corporation, a subsidiary of Magnavox G&I Electronics Co., Philadelphia, Pennsylvania 19118

A four-element adaptive antenna array is being developed to provide jammer suppression for a broadband data communication system which operates at a nominal RF of 1700 MHz. The beamformer for the array is implemented at RF in order to ease the problem of achieving cancellation for jamming signals occupying the greater than 100 MHz instantaneous bandwidth of the data signal. Control of the beamformer complex weights is achieved by an analog implementation of least-mean-square (LMS) control loops in order to provide rapid nulling. A unique feature of these control loops is that energy from CW jammers is removed to prevent the control loops from reacting to CW jamming signals which can be suppressed in the data receiver by frequency domain techniques. The available array degrees of freedom are thus preserved to null wideband jamming signals.

Commission F Session 7

SCATTERING: ROUGH, TURBULENT,

AND COHERENT

Friday A.M., 13 January ECCR 0-30

Chairman: C.W. Bostian, Virginia Polytechnic

Institute, Blacksburg, VA 24060

F7-1
0830 EFFECTS OF SURFACE ROUGHNESS ON CORRELATION LENGTHS OF SCATTERED FIELDS FROM BARE GROUND:
H.N. Kritikos, Department of Electrical Engineering and Science, University of Pennsylvania, Philadelphia, PA 19174

Radar scattering data from bare ground having a range of surface roughness from 1.1 to 4.1 cm rms and a range of soil moisture from .1 to .34 gm/cc were analyzed. The statistics of the scattered fields were determined on an equivalent aperture lying just above the scattering surface. It was found that the correlating distance of the scattered field along the effective aperature offered the means for differentiating the surface roughness from the soil moisture effects. The representation of the data in a Nadir scattering crossection and correlation length diagram resulted in distinct regions (one standard deviation) of constant soil moisture. This technique enables one to determine the soil moisture through the frequency range of 1.1 to 7.25 6HZ. See figure below.

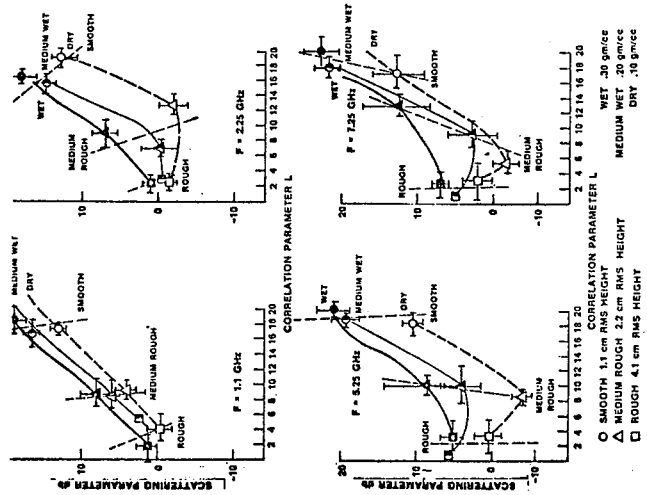

F7-2
0855 SOME RESULTS IN ELECTROMAGNETIC SCATTERING FROM PERIODIC ROUGH SURFACES: Rayner K. Rosich, U. S. Department of Commerce, Institute for Telecommunication Sciences, 325 Broadway, Boulder, CO 80302

An interest in establishing the validity and the convergence (or not) of the perturbation treatments of electromagnetic scattering from rough surfaces given by Rayleigh (Proc. Roy. Soc., A79, 399-416, 1907), Rice (in Theory of EM Waves, ed. by M. Kline, Interscience Pub., 351-378, 1951), Barrick (Radio Science, 6, 517-533, 1971), and Wait (Radio Science, 6, 387-391, 1971) led to the analysis reported in Rosich (Ph.D. dissertation, Univ. Colo., 1977) and Rosich and Wait (Radio Science, 12, to be pub., 1977). In this analysis a numerical model was developed which was found to agree well with the work of Rayleigh, Rice, Barrick, and Wait. Also by using a perturbation approach, a general expression was obtained for the amplitudes of the scattered waves which is valid for all spectral orders (modes) and for all perturbation orders. This expression is also consistent with the earlier results of the workers cited above. In addition it permits one to discern some important properties of the amplitudes for a purely sinusoidal surface. Among other things, all odd perturbation orders have zero amplitude for all even order modes, and vice versa for odd order modes. This permits one to explain the rather spectacular success of the earlier perturbation treatments which only went through second order.

An overview of some of the results obtained in this analysis will be given. In particular, the following topics will be briefly discussed: (1) the numerical and the perturbation analyses, (2) some results of these analyses, (3) some of the shortcomings of this model, (4) the Rayleigh hypothesis and some of its possible causes and cures, and (5) some suggestions of possible directions for future work.

F7-3
0920

MEASUREMENTS OF THE DEPOLARIZATION OF MICROWAVE BACKSCATTER FROM ROUGH SURFACES

J.W. Rouse, Jr., Remote Sensing Center, Texas A&M University, College Station, Texas, 77843
A.J. Blanchard*, Continental Oil Company, Ponca City, Oklahoma, 74601

Recent theoretical and experimental results suggest that depolarization of electromagnetic backscatter from rough surfaces is primarily caused by subsurface volumetric scattering. This hypothesis has been confirmed in tests with laser light incident on inhomogeneous media. However, most published measurements in the microwave region do not agree with this contention. This discussion presents a new treatment of a depolarization model and supportive experimental data which show that microwave measurements are consistent with previous laser measurements. That is, the depolarization is due to volumetric scatter; is independent of surface roughness; and is relatively insensitive to angle of incidence. These results suggest that the contradictory published radar data are in error.

*Formerly with the Remote Sensing Center, Texas A&M University.

F7-4 0945 ON THE CORRELATION FUNCTION IN RADAR SCATTERING: THEORY: A.K. Fung and R.K. Moore, The University of Kansas, Center for Research, 2291 Irving Hill Drive, Lawrence, KS 66045

Application of the physical-optics approach to scattering from rough surfaces has led to controversy over the proper form for the correlation function of surface height (A.K. Fung and H.L. Chan, Proc. IEEE, 59, 1280-1281, 1971 and D.E. Barrick, Radio Science, 5, 647-654, 1970). For assumed isotropic roughness, the two most popular correlation functions have been a quadratic-form (usually expressed as a Gaussian) that leads to equivalence between physical optics and geometric optics and a form having linear decay near the original (sometimes expressed as an exponential and sometimes as a Taylor-series expansion about the peak of the integrand). Some authors (D.E. Barrick, Radio Science, 5, 647-654, 1970) have expressed the view that the latter form cannot be correct because the exponential has a discontinuous slope at the origin. Here we show two forms that behave like the exponential form over the dominant region for integration, but do have zero slope and finite second derivatives at the origin:

$$P_1(\xi) = e^{-\xi^2/\sqrt{\ell^4 + L^2\xi^2}}$$

and

$$P_2(\xi) = e^{a - \sqrt{a^2 + (b\xi)^2}}$$

Values of the parameters are indicated where the calculated scattering integral behaves as if the Gaussian form had been used and others where it behaves as if an exponential form had been used. Although real correlation functions may actually be different from these forms, the results given here indicate that one is not constrained to use the quadratic form in the scattering integral, that an exponential is often a better approximation than a Gaussian. The implication is that a similar "regularization" technique might be used to satisfy the conditions at the origin if the approximate correlation function takes on other forms that, like the exponential, are discontinuous at the origin.

F7-5
1035

RADAR SCATTERING MEASUREMENTS OF SEA ICE:

R.K. Moore, R. Onstott, The University of Kansas*, Lawrence, KS 66045 and W.L. Weeks, U.S. Army Cold Regions Research and Engineering Lab, Hanover, NH 03755

Measurements have been made of the radar backscatter from ice in the following categories: thick first-year ice, multi-year ice, a pressure ridge, lake ice frozen to the bottom, lake ice with water beneath. These measurements were made at frequencies in the 1-2 GHz and 8-18 GHz bands using a wide-band frequency-modulated portable radar spectrometer mounted on the ice over an angle-of-incidence range from 10° to 70°. Concurrent measurements were made of the physical properties of the ice. In most cases results are similar to those reported by (Parashar et. al, Proc. Ninth Symposium on Remote Sensing, Ann Arbor, Michigan, April 1974) for airborne measurements, with the angular dependence lying between Parashar's experimental and theoretical curves.

F7-6
1100

LUNAR RADAR MAP AT 7.5 METER WAVELENGTH:

T.W. Thompson, Planetary Science Institute, Science Applications, Inc. 283 S. Lake Ave., Suite 218, Pasadena, CA 91101

A high-resolution map of lunar radar reflectivity has been obtained using delay-Doppler interferometry techniques and the 7.5 meter (40 Mhz) radar at the Arecibo Observatory in Arecibo, Puerto Rico. This new mapping, an extension of an earlier experiment, demonstrated an improvement of surface resolution to 20-40 kilometers. The new map shows scattering behavior similar to previous maps at 3.8 and 70 cm wavelengths. The maria backscatter less power than the terrae by factors of one-half to one-fourth. A few terrae areas have the same low backscatter as the mare. The large young rayed craters like Tycho have backscatter enhancement (over the environs) by about 1.5:1, a much smaller difference than that observed at centimeter wavelengths. In addition, the mean scattering behavior of the Moon was measured for a range of angles from 10^{o} to 67^{o}. The new scattering law measurements differ little from previous measurements at 6 meter wavelength. These data have three effects: (1) Average radar backscatter at 7.5 meter wavelength for the large angles of incidence differs little from scatter at meter wavelengths. (2) The maria and highland have very similar scattering behavior although maria backscatter less power by factors of one-half to one-quarter. (3) The large rayed craters have relatively small enhancements compared with enhancements at meter and centimeter wavelengths. These effects are explicable if one assumes that the backscatter at higher angles of incidence are due to diffuse scattering from surface and subsurface rocks with sizes of several meters.

F7-7
1125 PARTIAL REFLECTION OF VHF RADAR SIGNALS FROM THE TROPOSPHERE: J. Röttger and R. Rüster, Max-Planck Institut für Aeronomie, 3411 Katlenburg-Lindau 3, F.R.G. and C. H. Liu, Department of Electrical Engineering, University of Illinois at Urbana-Champaign, Urbana, IL. 61801

Partial reflections of VHF radar signals from strong gradients of the refractive index in the troposphere are investigated. Theoretical estimates indicate that under rather realistic atmospheric conditions, partial reflection may contribute significantly to the received echo power of the VHF radar. Observational data from the SOUSY VHF radar at Lindau, Germany are used to study possible cases of partial reflections from the troposphere. The 53.5 MHz radar was operated both in the vertical and 12.5^0 off-zenith positions. The peak power was 220 kw and the height resolution was 150m. Examples will be shown in which echoes from the vertical radar position have long correlation times of many seconds indicating almost coherent reflections from thin layers. Height intensity profiles for both the vertical and oblique cases will be compared. It is often observed that at the same height the intensity is higher for the vertical case. This implies again the contributions from partial reflections. Implications of these results on VHF radar probing of the atmosphere will be discussed.

F7-8
1150 EVIDENCE FOR SPECULAR REFLECTION FROM MONOSTATIC VHF RADAR OBSERVATIONS OF THE STRATOSPHERE:

K.S. Gage and J.L. Green, Aeronomy Laboratory, National Oceanic and Atmospheric Administration, Boulder, CO 80302

The relative contribution of turbulent scatter and partial reflection in clear air atmospheric echoes observed at 10 cm was considered by Saxton et al. (Proc. IEE, III, 875-283, 1964). They concluded that turbulent scatter is primarily responsible for the observed echoes, but that specular reflection may be important at longer wavelengths. Evidence of specular reflection at tropopause altitudes was shown by Gage et al. (J. Appl. Met., 12, 1205-1212, 1973) from bistatic radar observations that were sensitive to refractivity structure with a length scale of a few meters. Recently, several monostatic radars have been used to probe neutral atmospheric structure at wavelengths from 6 to 7.4 m. The first such radar to be dedicated solely to atmospheric research is the 40 MHz Sunset Radar located near Boulder, CO, and operated by NOAA's Aeronomy Laboratory.

The received S/N obtained on the vertical antenna of the Sunset Radar often reveals an order of magnitude enhancement over the received S/N obtained nearly simultaneously on an antenna pointed 30° from the zenith. The enhancement is most pronounced in regions of the atmosphere that are very stable and where active turbulence is suppressed. Profiles of received S/N obtained from the vertically pointing antenna have been compared with profiles of the square of the gradient of potential index of refraction obtained from routine Denver radiosonde observations. These profiles are well correlated, especially above the tropopause.

These observations confirm the existence of partially reflecting horizontal layers in the stable atmosphere. These layers are certainly important in over-the-horizon radio propagation and they may enable radar probing of the neutral atmosphere to higher altitudes than previously thought possible. Because of their excellent time and space resolution, the new VHF Doppler radars are ideal for studying the morphology of the partially reflecting layers.

Commission J Session 4

SOLAR SYSTEM AND GALATIC

RADIO ASTRONOMY

Friday A.M., 13 January ECCR 1-40

Chairman: B. Balick, Astronomy Department,

FM-20, University of Washington,

Seattle, WA 98195

J4-1
0830 HIGH RESOLUTION OBSERVATIONS OF THE SUN AT CENTIMETER WAVELENGTHS

Kenneth R. Lang, Department of Physics, Tufts University, Medford, MA 02155

Interferometric observations of the quiet Sun at centimeter wavelengths show that the entire solar chromosphere is covered with small-scale features. Structures with angular sizes of about 30" are arranged in a pattern with a characteristic spacing of 6' between the intense structures. These features emit more radiation at the lower wavelengths. Ubiquitous chromospheric features with angular sizes of about 3" exhibit intrinsic fluctuations with time scales of minutes whereas the 30" features do not seem to vary. It is tempting to identify the 3" and 30" features, respectively, with the granules and supergranules seen at optical wavelengths in the underlying photosphere. When sunspots are present on the solar surface the solar emission at centimeter wavelengths is dominated by second-of-arc features within the sunspots. These small-scale features have angular sizes, intensities and degrees of circular polarization which remain constant for days. Synthesis maps of one sunspot region show four intense features smaller than 5" in angular size. These features are up to 60% circularly polarized with different senses of polarization in different features.

J4-2 0900 SECOND HARMONIC RADIATION IN TYPE III SOLAR RADIO BURSTS: D. F. Smith, High Altitude Observatory, NCAR , P. O. Box 3000, Boulder, CO 80307

Observations of type III radiobursts and their accompanying plasma waves near 0.45 A.U. are analyzed and shown to provide no definitive support for coherent parametric processes in these bursts. The incoherent weak turbulence process of induced scattering on the polarization clouds of ions is sufficient to produce a quasi-isotropic spectrum of plasma waves. These waves lead to emission near the second harmonic of the plasma frequency which is almost three orders of magnitude larger than observed for the burst of 31 March 1976, 18:10 UT. This radiation level is compared with the radiation from collapsing solitons recently derived by Reiter and shown to be higher for the observed plasma wave level of $W_p/nKT_e = 1.4 \times 10^{-5}$. However, the comparison is only pedagogic because plasma waves are unlikely to collapse for this value of W_p.

J4-3 0930 STUDIES OF SATURN'S RINGS BY RADIO INTERFEROMETRY:

F.P. SCHLOERB, D.O. MUHLEMAN, G.L. BERGE, Division of Geological and Planetary Sciences, California Institute of Technology, Pasadena, CA 91125

Aperture synthesis and model fitting techniques are used to analyze interferometric observations of the Saturn system at wavelengths of 3.71 and 1.30 cm. The 3.71 cm observations were obtained at the Owens Valley Radio Observatory during May-June 1976 and the 1.30 cm observations were made at the Hat Creek Radio Observatory during November 1976. The rather complete sampling of the U-V plane by each of the experiments allows aperture synthesis maps of Saturn and the rings to be made. The maps are used to determine which parts of the Saturn system contribute significantly to the observed radiation. Model fitting is then used to estimate the brightness temperature of each component. The rings are found to have a very low brightness temperature relative to that of the planet. It is, therefore, necessary to accurately remove the contribution of the planet from the aperture synthesis maps in order to study the radiation from the rings. This removal is made difficult by small errors (1/4 arcsec) in the geocentric position of the planet. The errors are likely to be due to errors in the AENA geocentric ephemeris, but they are also on the order of the uncertainties in the positions of the phase calibrators. Future aperture synthesis studies of Saturn and the other planets must make use of an improved geocentric ephemeris if they are to detect the kinds of features which are presently interesting. The maps of the Saturn system with the planet removed show the rings to be significant features. The visible A and B rings and the inner C ring all have nearly the same brightness temperature and this brightness temperature is a few percent of that of the planet. The area of the planet that is blocked by the rings indicates that they attenuate the emission from the planet significantly. The optical depths inferred from this attenuation are quite close to those measured at visible wavelengths. The low radio brightness temperature and significant radio optical depth are consistant with models of the rings in which the ring particles are good scatterers and poor emitters. In these models, the majority of the radio radiation received from the rings is planetary emission that is scattered to the earth by the ring particles. The similarity between the visible and radio optical depths probably indicates that the particles are large compared to the radio wavelengths and, therefore, must be composed of either a very low-loss material or a highly reflecting one. The most likely candidate is water ice.

J4-4 CO AND HCO^+ IN THE DIRECTION OF CAS A
1030 T.H. Troland and C. Heiles
Dept. of Astronomy
University of California, Berkeley, CA 94720

We report on observations of the 115 GHz CO line and the 89 GHz HCO^+ line in the direction of Cas A. We have mapped CO emission across the face of Cas A and at selected positions up to 30' off source. At nearly every position the CO emission consists of components corresponding to the local and Perseus arm HI absorption features. Typical line temperatures are 1 to 4°K, angular structure exists on a scale of 1' or less. We compare the CO data for Cas A with HI optical depth in front of the source, with the optical filaments, and with 5 GHz H_2CO absorption on and off source. For the HCO^+ transition in the direction of Cas A, we find that the line temperature is less than 0.2°K.

J4-5 PROGRESS REPORT ON ZEEMAN STUDIES IN HI EMISSION.
1100 C. Heiles and T.H. Troland
Dept. of Astronomy
Univ. of California, Berkeley, CA 94720

We are continuing our attempts to detect Zeeman splitting in the 21-cm line seen in emission. All previous results reported at meetings are incorrect, having resulted from polarized sidelobes of the antenna pattern. We have employed two techniques to eliminate and reduce these sidelobes, and have made their effects negligible. We currently have no positive results; because fields are very weak, we are sensitivity limited. We will soon begin using a dual-channel system, a digital correlator, and a noiseless polarization switching arrangement which will increase our sensitivity by nearly a factor of two.

J4-6
1130

HIGH RESOLUTION, LOW FREQUENCY RADIO ASTRONOMY BY MEANS OF CHEMICAL DEPLETION OF THE F-LAYER

Paul A. Bernhardt, Readiscience Laboratory, Stanford University, Stanford, California 94305

Observation of the radio sky at the lower end of the radio frequency spectrum is limited by 1) reflection of waves from the topside ionosphere and by 2) the large size of antenna apertures necessary for the realization of narrow beamwidths. Both of these limitations may be overcome through chemical modification of the F-layer ionosphere.
The O^+ ion which constitutes the F2-layer is highly reactive with such gases as H_2O, CO_2, H_2 and NO_2. Consider the chemical reaction with H_2O

$$H_2O + O^+ \rightarrow H_2O^+ + O \quad \text{rate: } 2.3 \times 10^{-9} \text{ cm}^3/\text{sec}$$

$$H_2O^+ + e^- \rightarrow OH + H \quad \text{rate: } 3.0 \times 10^{-7} \text{ cm}^3/\text{sec}$$

as compared with the naturally occuring reaction with N_2

$$N_2 + O^+ \rightarrow NO^+ + N \quad \text{rate: } 1.3 \times 10^{-12} \text{ cm}^3/\text{sec}$$

$$NO^+ + e^- \rightarrow N + O \quad \text{rate: } 4.1 \times 10^{-7} \text{ cm}^3/\text{sec}$$

The reaction rate between H_2O and O^+ is three orders of magnitude larger than the rate between N_2 and O^+ and, consequently, a relatively small quantity of water vapor (or similar reactive substances) released into the ionosphere will cause a substantial reduction in ion and electron concentration.
The release of reactive vapors into the F-layer will reduce the peak ionospheric plasma concentration and allow the penetration of lower-frequency extraterrestrial radio waves (M.D. Papagiannis and M. Mendillo, Nature, 255 (5503), 42-43, 1975). Also, the opening in the ionosphere created by a chemical release may act as a convergent lens for focusing radio astronomical signals in the 1-10 MHz frequency range (P.A. Bernhardt and A.V. daRosa, Radio Science, 12, 327-336, 1977). Numerical simulations of radio propagation through the modified ionosphere indicate that the hope created by the release of 100 kg of H_2 into the mid-latitude F-layer may be used as a refractor at 7 MHz with a beamwidth of less than .2 degree.

INDEX

FUTURE MEETINGS SPONSORED BY USNC/URSI:

Spring Meeting - Washington, DC, 15-19 May, 1978 to be held jointly with AP-S/IEEE (contact Dr. G. Hyde - Mgr., Propagation Studies Dept., Comsat Laboratories, P.O. Box 115, Clarksburg, MD 20734).

National Radio Science Meeting - Boulder, CO, 5-10 November 1978 in cooperation with various groups and societies of the IEEE (contact Prof. S.W. Maley - Electrical Engrg. Dept., University of Colorado, Boulder, CO 80309).*

National Radio Science Meeting - Seattle, WA, 18-21 June 1979 to be held jointly with AP/S IEEE (contact Prof. A. Ishimaru-Dept. of Electrical Engrg., FT-10, University of Washington Seattle, WA 98195).

Canadian/American Radio Science Meeting - Quebec City, 2-6 June 1980 to be co-sponsored by CNC/URSI and held jointly with AP-S/IEEE (contact J.A. Cummins - Université Laval, Departement de Genie Electrique, Faculté des Sciences et de Génie, Cité Universitaire, Québec G1K 7P4, Canada).

The USNC/URSI will also be sending a delegation to the URSI General Assembly to be held in Helsinki, Finland from 31 July to 10 August 1978. With the exception of business sessions, this will be an open meeting (contact C.M. Minnis - Secretary-General of URSI, Rue de Nieuwenhove 81, B-1180 Brussels, Belgium).

*First Call for Papers is available at Registration Desk

1978

IN

WASHINGTON, D. C.

IEEE APS/URSI
INTERNATIONAL SYMPOSIUM

15 - 19 MAY 1978
at the
UNIVERSITY of MARYLAND
COLLEGE PARK, MARYLAND

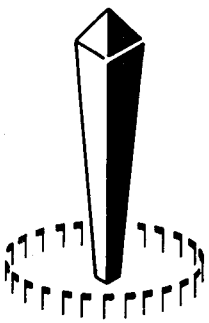

FOR INFORMATION WRITE TO

DR. GEOFFREY HYDE
COMSAT Laboratories
22300 COMSAT DRIVE
CLARKSBURG, MD. 20734

Wednesday, 11 January continued

0830-1200		
G-2	Ionospheric Irregularities and Drifts - I	ECCR 1-42
J-1	Interferometry and Aperture Synthesis - I	ECCR 1-40
1330-1700		
B-4	Antennas	ECCR 2-26
B-5	Scattering: Inverse and Direct	ECCR 2-28
C-1	System Performance--Prediction and Measurement	ECCR 0-36
F-4	Geoscience	ECCR 0-30
G-3	Ionospheric Irregularities and Drifts - II	ECCR 1-42
J-2	Interferometry and Aperture Synthesis - II	ECCR 1-40
1715		
Commission A Business Meeting		ECCR 2-06
Commission B Business Meeting		ECCR 2-28
Commission H Business Meeting		ECCR 1-46
1930-2200		
A-2	Near-Field Anetenna Measurements	UMC Forum Room
2000-2200		
IEEE AP-S AdCom Meeting		Broker Inn

THURSDAY, 12 JANUARY

0830-1200		
A-3,D	Applications and Statistics	ECCR 2-06
B-6	Ground Effects	ECCR 2-28
C-2	Computer Communication Networks: Design and Operation	ECCR 0-36
F-5	Radio Meteorology	ECCR 0-30
J-3	Millimeter Wave Length Techniques	ECCR 1-40
1330-1700		
B-7	Electromagnetic Theory	ECCR 2-28
C-3,B	Antenna Arrays and Feeds	ECCR 0-36
F-6	Optical and Radio Sensing of Atmospheric Parameters	ECCR 0-30
1400		
Commission J Business Meeting		ECCR 1-40
1645		
Commission C Business Meeting		ECCR 0-36
2000		
USNC/URSI Executive Committee Meeting		Broker Inn

FRIDAY, 13 JANUARY

0830-1200		
C-4	Signal Processing in Adaptive Arrays	ECCR 0-36
J-4	Solar Systems and Galactic Radio Astronomy	ECCR 1-40